Summer 2013

The Effects of Conformation and Aggregation on the Pharmaceutical Chemistry Properties of Lipopeptide (Daptomycin)

Jiang Qiu
University of Iowa

THE EFFECTS OF CONFORMATION AND AGGREGATION ON THE PHARMACEUTICAL CHEMISTRY PROPERTIES OF LIPOPEPTIDE (DAPTOMYCIN)

by

Jiang Qiu

A thesis submitted in partial fulfillment
of the requirements for the Doctor of
Philosophy degree in Pharmacy
in the Graduate College of
The University of Iowa

August 2013

Thesis Supervisor: Professor Lee E. Kirsch

Graduate College
The University of Iowa
Iowa City, Iowa

CERTIFICATE OF APPROVAL

_____

PH.D. THESIS

_____

This is to certify that the Ph.D. thesis of

Jiang Qiu

has been approved by the Examining Committee
for the thesis requirement for the Doctor of Philosophy
degree in Pharmacy at the August 2013 graduation.

Thesis Committee: _____

Lee E. Kirsch, Thesis Supervisor

_____

Douglas R. Flanagan

_____

Mickey L. Wells

_____

Liping Yu

_____

Jennifer Fiegel

To my family members:
Parents Peijie Liu and Jinxue Qiu
Parents-in-Law Feijing Zhang and Lanshao Bo
Wife Wei Bo
Daughter Qiong Qiu
For their unconditional support and love

ACKNOWLEDGEMENTS

I would like to express my gratitude to those who supported me to go through the particular journey in my life.

First, I own my sincere gratitude to my advisor, Dr. Lee E. Kirsch, for his valuable guidance, inspiration, and patience, which made it possible for me to come to the goal.

I am also very grateful to Dr. Douglas R. Flanagan, Dr. Liping Yu, Dr. Mickey L. Wells, and Dr. Jennifer Fiegel for serving as members on my thesis defense committee. A special thanks to Dr. Aliasger K. Salem for serving my comprehensive examination.

I would like to acknowledge Dr. Liping Yu, Dr. William R. Kearney, and Margaret Allaman for their assistance, discussion, and contributions on the NMR experiments; Dr. John Wiencek and Cynthia Hoppe for their comments and supports on light scattering experiments.

My special thanks go also to my college mates who help me pass through the ups and downs during the past years, Salil, Zhixin, Yi, Hefei, Dong, Nui, Fon, Radaduen, Hoa, and Chenming.

I am deeply indebted to my wife Wei and daughter Qiong for all their encouragement and support.

TABLE OF CONTENTS

LIST OF TABLES

LIST OF FIGURES

CHAPTER I INTRODUCTION

Peptide/Protein Aggregation

The rapid advances in peptide synthesis and recombinant DNA technology have provided an increasing number of peptide and protein therapeutic agents. Proteins and peptides are biopolymers composed of amino acid residues interlinked by amide bonds. They have heterogeneous, complicated, and high-order structures. The three-dimensional structure of peptide proteins are susceptible to environmental factors, such as medium conditions (temperature, pH, concentration, ionic strength), and stresses from freezing, exposing to air, and shear-stress, which may cause the loss of the functional activity. Peptide and protein conformational and aggregation changes may occur in purification, formulation, shipping, and storage processes. The aggregation of peptide/proteins is associated with degradation, stability, immunogenicity, and therapeutic activity. Thus, the physical instability of peptides and proteins including conformational changes, aggregation, and adsorption is an essential consideration in developing stable and efficacious formulations or delivery systems. Peptide/protein aggregation is regarded as one of major degradation pathways along with deamidation and oxidation.

Aggregates of proteins may arise from several mechanisms[1] and may be classified in numerous ways including soluble/insoluble, covalent/noncovalent, reversible/irreversible.

Daptomycin

Daptomycin is an acidic lipopeptide antibiotic derived from the fermentation of *Streptomyces roseosporus*.[2,3] It is the first cyclic anionic lipopeptide antibiotic approved for the treatment of complicated skin (soft tissue) infections, bacteraemia, and right-side endocarditis caused by multi-resistant Gram-positive bacteria, including vancomycin-resistant *enterococci*, vancomycin-resistant *Staphylococcus aureus*, methicillin-resistant

Staphylococcus aureus, penicillin-resistant *Streptococci*, and coagulase-negative *Staphylococci*.[4,5]

Daptomycin is a cyclic lipopeptide composed of 13 amino acid residues (Figure I-1). The 10-membered ring in daptomycin is linked via an ester bond between threonine (Thr-4) hydroxyl group and the C-terminal carboxyl groups of kynurenine (Kyn-13). The N-terminal residue tryptophan (Trp-1) is acylated with a decanoyl aliphatic chain. Without terminal amine and carboxyl groups, daptomycin contains six side-chain ionizable groups: four carboxyl residues (three aspartic acids, Asp-3, Asp-7, and Asp-9, one methyl-glutamic acid, mGlu-12) and two amines (aliphatic amine in ornithine Orn-6 and aromatic amine in Kyn-13).

Most currently available antibiotics target enzymes responsible for formation and maintenance of cell wall structure or inhibition of protein synthesis, nucleic acid synthesis, or metabolic pathway.[6] Hypothetical mechanism of action of daptomycin is proposed in Figure I-2. The mechanism of action involves in direct binding to the Gram-positive cell membrane by its lipid tail, followed by calcium-dependent insertion and oligomerization. Daptomycin oligomers form ion channels, disrupting the functional integrity of the membrane, and trigger a release of intracellular ions. Daptomycin aggregation induced by calcium ions is an essential step for therapeutic activity to disrupt the bacterial membrane through the formation of trans-membrane channels. [7-9] Details of daptomycin's mechanism of action have not been yet fully elucidated, i.e., how the rapid bactericidal activity of daptomycin is related to its dynamic nature and its interaction with the cytoplasmic membrane and whether oligomerization in the membrane is crucial.[10-12]

Daptomycin's three-dimensional structure and its biologically-active conformation have been investigated in a number of recent NMR studies, but with the different findings.[11-15]

The aqueous conformation of daptomycin has been reported by Rotondi et al.[15] to be qualitatively similar to the Ca^{2+}-bound structure reported by Jung et al.[14] A preferred

aqueous conformation for daptomycin proposed by Jung et al.[14] and Ball et al.[13] differs from that from Rotondi et al.[15] primarily by the presence or absence of a cluster of the hydrophobic side chains of a decanoyl lipoidal tail, Trp-1, and Kyn-13 (Figure I-3).

Jung et al.[14] in Figure I-4 showed that daptomycin undergoes significant calcium-dependent conformational changes upon association with model lipid membranes. In contrast, Ball et al.[13] in Figure I-5 demonstrated that the binding of calcium ions does not result in major conformational changes, but does induce aggregation. The subsequent studies results from Scott et al.[12] suggested that daptomycin undergoes only a minor conformational rearrangement upon binding with 1,2-dihexanoyl-sn-glycero-3-phosphocholine (DHPC) in the presence of calcium ions.

Investigations of daptomycin aggregation at different pH values in aqueous solution would be helpful for reconciling the different findings regarding daptomycin conformation and understanding the effects of conformation and aggregation on its pharmaceutical properties.

The objective of this research is to evaluate the conformation and aggregation of daptomycin in aqueous solutions and effects of conformation and aggregation on pharmaceutical and chemistry properties with the complementary techniques, fluorescence, static and dynamic light scattering, and NMR spectroscopy.

Research Objectives

The primary research objectives are to evaluate the conformational transition and aggregation behavior of daptomycin in different pH aqueous solutions, and to elucidate the effects of conformation and aggregation on the pharmaceutical chemistry properties of daptomycin.

The specific objectives of this project are the following:

- Assign and estimate the sequence-specific ionization constants (pK_a values) of daptomycin

- Develop daptomycin aggregation detection methods and evaluate the external factors on daptomycin aggregation
- Explicate the different findings of daptomycin conformational structures of NMR study
- Elucidate the interaction mechanism of daptomycin with polyamidoamine (PAMAM) dendrimers

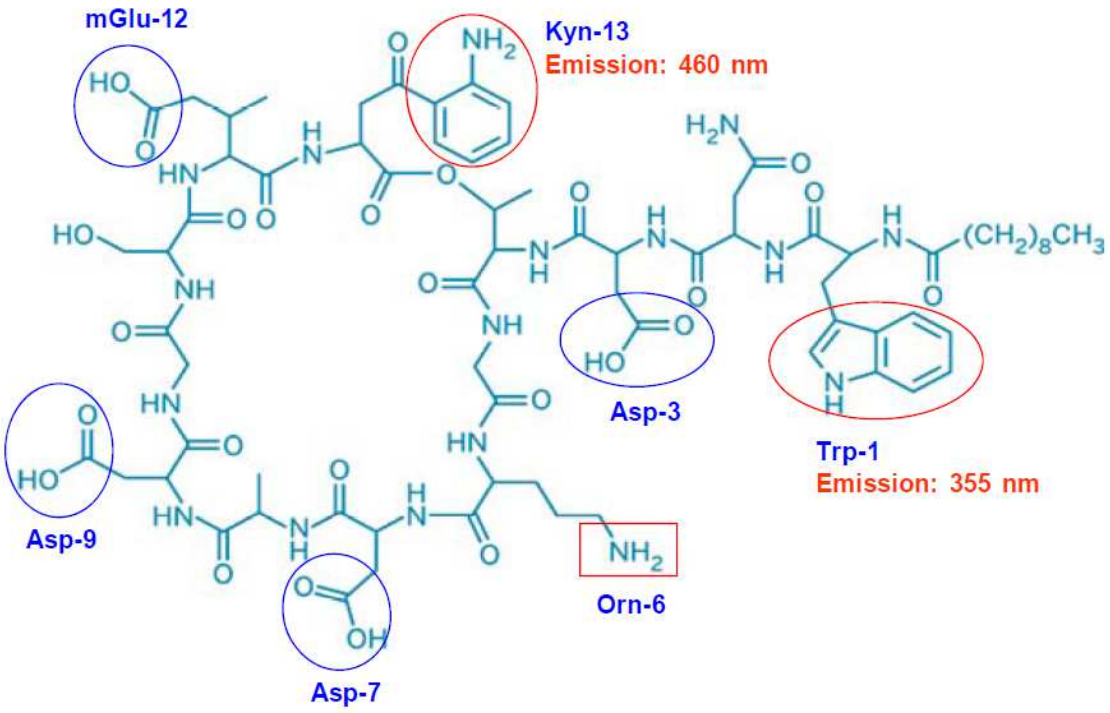

Figure I-1. Daptomycin molecular structure and fluorescence properties. The residues with ionizing groups and/or exhibiting fluorescence properties are labeled. The maximum emission wavelengths of donor Trp-1 and acceptor Kyn-13 in the fluorescence resonance energy transfer are also labeled.

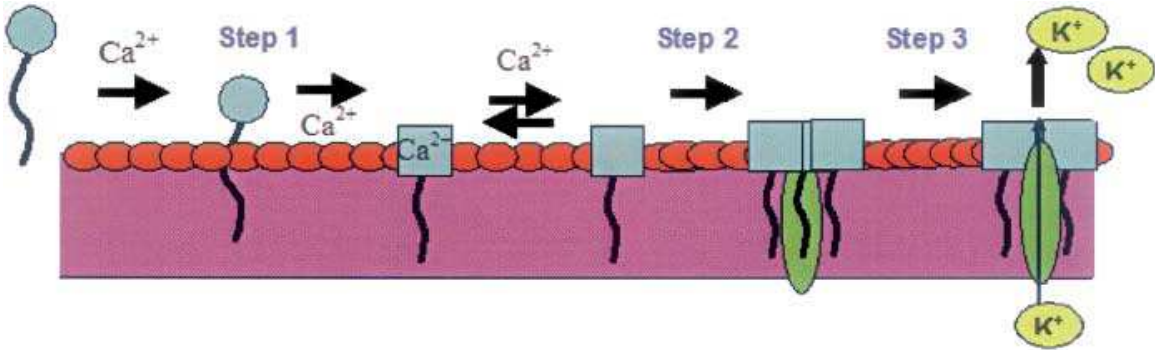

Figure I-2. Proposed mechanism of action of daptomycin. Hypothetical steps: step 1, daptomycin binds to the cytoplasmic membrane in a calcium-dependent manner; step 2, daptomycin oligomerizes, disrupting the membrane; step 3, the release of intracellular ions and rapid cell death.[8]

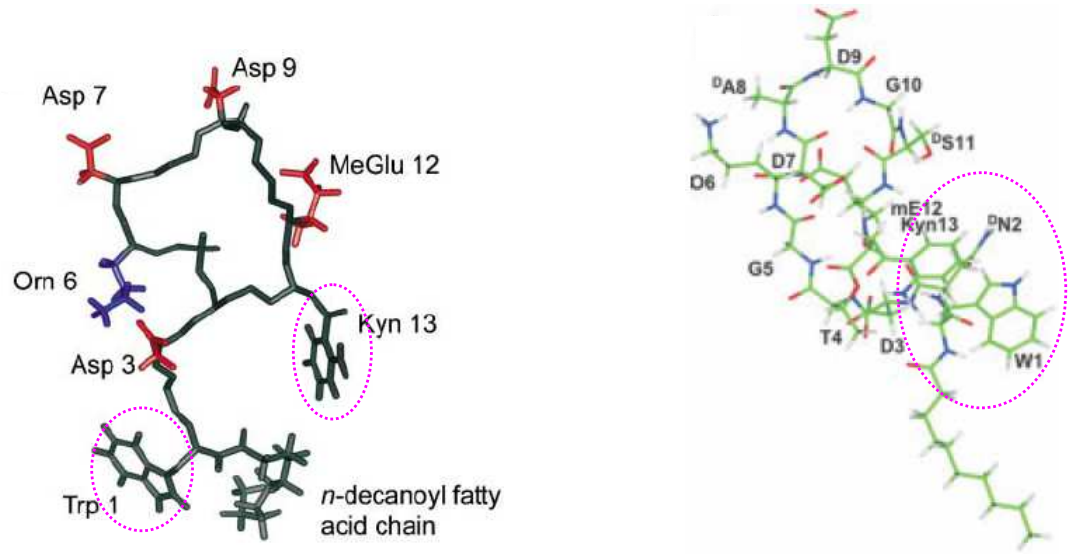

Figure I-3. The NMR structures of daptomycin. No clustering of the hydrophobic side chains of amino acid residues near the N-terminus (left, negatively charged side chains colored red and positively charged side chains colored blue),[14] and a cluster of the hydrophobic moieties of a N-decanoyl, Trp-1, and Kyn-13 side chains (right).[15] The aromatic groups of Trp-1 and Kyn-13 are circled.

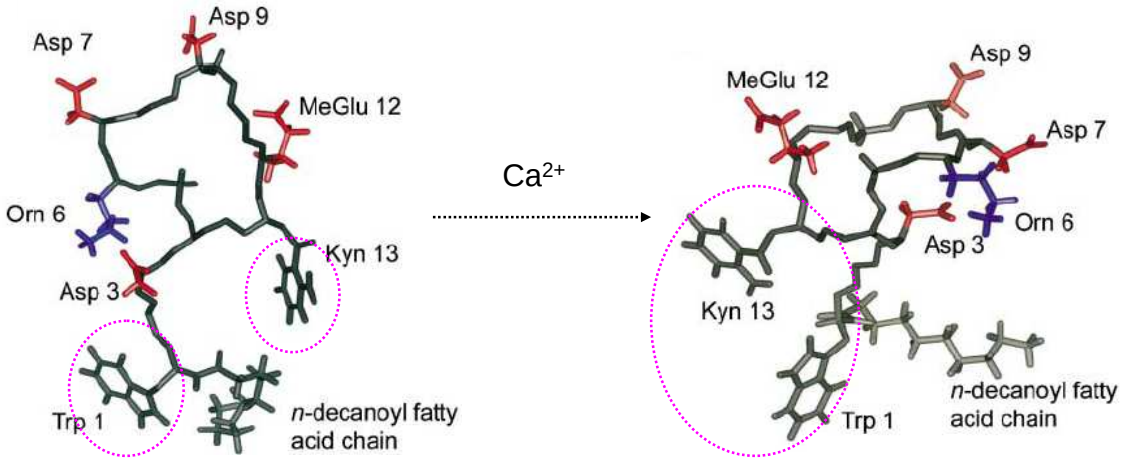

Figure I-4. Structures of daptomycin (left) and Ca^{2+}-conjugated daptomycin (right) (negatively charged side chains colored red and positively charged side chains colored blue).[14] The aromatic groups of Trp-1 and Kyn-13 are circled.

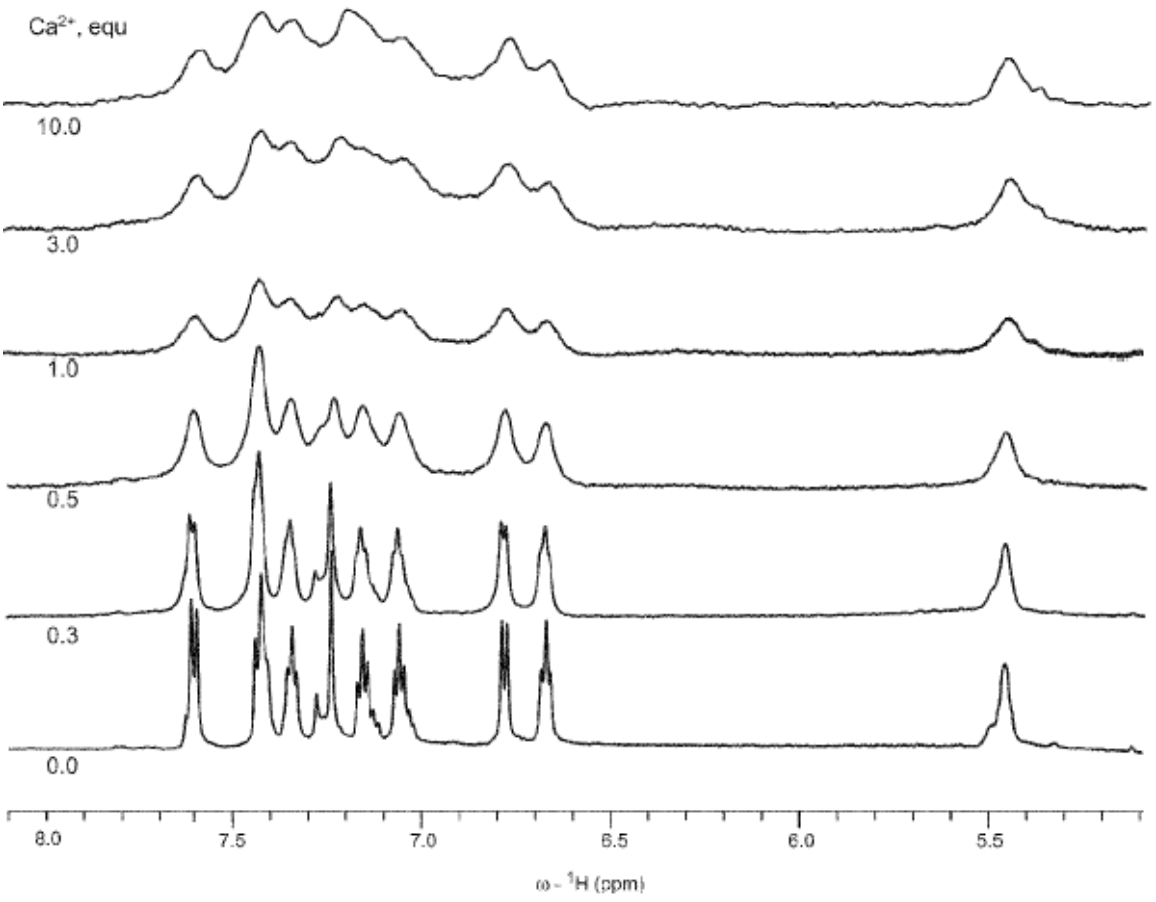

Figure I-5. ^{1}H-NMR spectra of daptomycin (0.8 mM) with increasing molar equivalents of Ca^{2+} in D_2O at pH 5.0.[13]

CHAPTER II DETERMINATION OF COMPLEX IONIZATION BEHAVIOR OF DAPTOMYCIN

Introduction

The ionizable peptide side-chains frequently play important roles in establishing peptide conformations, stability, and function. Electrostatic interactions between charged groups may help stabilize the native conformation of a protein, as well as define the specificity and affinity of ligand or substrate binding. The ionization constants (pK_a values) are key fundamental physicochemical properties of daptomycin. Compared with smaller molecules, the pK_a determination is more complicated because of multiple overlapping ionizable groups and conformational aggregational dependencies.[13] While the pK_a values of small molecules can be accurately measured with potentiometric and spectroscopic methods, the ionization constants of macromolecules due to the multiple dependent factors such as concentration and local environments, may only be estimated to be close to the "true" values. The pK_a values are influenced by neighboring peptide bonds, charge-charge interactions, and/or the burial of the ionizable groups.[16,17] Hence, pK_a perturbations from their normal values for ionizable groups in a peptide/protein serve as a sensitive probe of local environments.

Daptomycin has six residues with ionizable side chains, including three aspartic acids (Asp-3, Asp-7, and Asp-9), one methyl-glutamic acid (mGlu-12), one aliphatic amine ornithine (Orn-6), and one aromatic amine kynurenine (Kyn-13). The pK_a values of these four carboxylic groups in daptomycin have been estimated previously by potentiometric titration using non-linear curve-fitting.[18] One carboxylic acid group is reported to dissociate around pH 3.0, while the other three groups have overlapping pK_a values around 5.3. From the previous study using UV spectrophotometry and potentiometric method,[19] the pK_a values of the primary aromatic amine of Kyn-13 and primary aliphatic amine of Orn-6 were reported to be 0.8 and 10.7, respectively.

NMR chemical shifts are sensitive to the electronic environment around the nucleus of an atom. The sequence-specific assignments of daptomycin for the ^{1}H NMR resonances have been reported previously.[13,14] The effort has been made previously to determine the pK_a values of the acidic residues by performing NMR pH titration of daptomycin over the pH range of 8 to 2.[13] Small changes in chemical shifts of the resonances for these residues were observed on decreasing the solution pH from 8 to 4. However, further decrease in pH resulted in considerable line broadening of these resonances due to intermolecular aggregation, thus preventing pK_a estimation. Up to now, the individual ionization constants of these acidic residues have not been determined.

NMR relies on the excitation of magnetic nuclei (nuclear spins) in a static external magnetic field by radiofrequency (RF) pulses, after which the excited nuclei return to the ground state re-emitting at resonant frequencies. The emitted resonant frequencies depend on the type of nucleus (e,g.,^{1}H proton) and local atomic environment. The nucleus is surrounded by electrons which may be viewed as moving electrical charges with associated magnetic fields. These electrons act as a source of magnetic shielding for the nucleus. The resonant frequency is shifted by the effect of neighboring atoms and in particular the extent of magnetic shielding from local electrons. The variation in precise resonant frequency is referred to as the “chemical shift, δ”, the resonant frequency of a nucleus relative to a standard. The intensity of these resonance peaks corresponds to the number of atoms or nuclei in the compound with identical chemical shifts. The width of these peaks corresponds to the speed of the local and global tumbling motions of the molecule, with faster moving atoms or molecules having narrower peaks. Many peaks also have a fine structure (splitting), which represents a coupling or direct linkage between two or more protons. This splitting is called spin-spin coupling, scalar coupling, or J-coupling. The spin-spin coupling interactions between the protons are mediated through the intervening covalent bonds.

The excited nuclei return to the ground state via one of several relaxation mechanisms. The spin-lattice relaxation time T_1 reflects return to the ground state by exchange of energy with the surroundings (longitudinal relaxation), while spin-spin relaxation time T_2 is a measure of the efficiency of exchange energy with other nuclei (transverse relaxation). For large molecules, transverse relaxation is predominant. And since T_2 is proportional to the reciprocal to the line width of a resonance signal, the peaks in NMR spectra become broader with increasing molecule size.

Conventional (one-dimensional) NMR spectra are plots of intensity vs. frequency. In one-dimensional pulsed Fourier Transform NMR, the signal is recorded as a function of a single time variable and then transformed to give a spectrum which is a function of a single frequency variable. In two-dimensional NMR the signal is recorded as a function of two time variables, evolution t_1 and detection t_2, and the resulting data is transformed twice to yield a spectrum which is a function of two frequency variables.[20]

The general sequence for two-dimensional NMR consists of the preparation and mixing periods. Each period may be as simple as a single pulse, or a much more complex arrangement of pulses and delays. In the preparation time, the sample is excited by one or more pulses. The coherence generated evolves for time t_1, but there is no detection during this time. Then the mixing time period follows, which consists of a further pulse or pulses. After the mixing period, the signal is recorded as a function of the second time variable, t_2. This sequence of events is called a pulse sequence, and the exact nature of the preparation and mixing periods determines the information found in the spectrum.[20]

The general pulse sequence for Total Correlation Spectroscopy (TOCSY) is shown in Figure II-1.[21] The pulse sequence of a TOCSY consists of a 90° excitation pulse, followed by an incremented delay t_1, then a mixing sequence known as a spin-lock (SL) or isotropic mixing for time, τ_m. The coherence transfer period of the TOCSY sequence occurs during a multiple-pulse spin-lock period. The length of the spin-lock period determines how far the spin coupling network will be probed. In practice, isotropic

mixing is achieved by the use of a specially designed multiple pulse sequence (Figure II-2).[20,21]

TOCSY not only provides homonuclear proton correlation spectra based on scalar couplings, but it can also establish correlations between protons that are within the same spin system, regardless of whether they are themselves coupled to one another. In other words, there is a continuous chain of spin-spin coupled protons. In TOCSY the cross-peaks between spins are also observed which are connected by an unbroken chain of couplings. So, for example, if spin A is coupled to spin B, and spin B is coupled to spin C, then in a TOCSY spectrum a cross-peak between A and C can be observed even though there is no direct coupling between these two spins.[20] Thus, 2D NMR TOCSY[21] is a powerful NMR technique for identifying proton coupling networks and molecular connectivity through bond correlations via spin-spin coupling. It not only yields homonuclear proton correlations between geminal or vicinal protons but also is able to establish correlations between distant protons as long as there are couplings between intervening protons.

The objective of this chapter is to present various approaches to determining the pK_a values of daptomycin and the perturbations of pK_a values of daptomycin due to the intermolecular aggregation.

The sequence-specific pK_a values of daptomycin residues were determined in a monomeric state at low concentrations. In addition, the effects of concentration-dependent aggregation on ionization were observed and will be discussed. These studies were conducted by pH titration with potentiometric and spectroscopic methods including 2D ^{1}H TOCSY NMR, UV, and fluorescence spectroscopy.

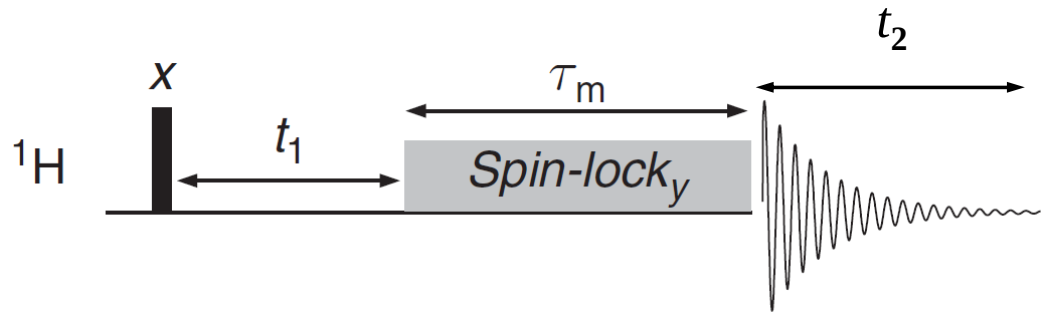

Figure II-1. The pulse sequence for TOCSY. The t_1, τ_m, and t_2 are the evolution time, spin-lock mixing time, and detection time, respectively.[21]

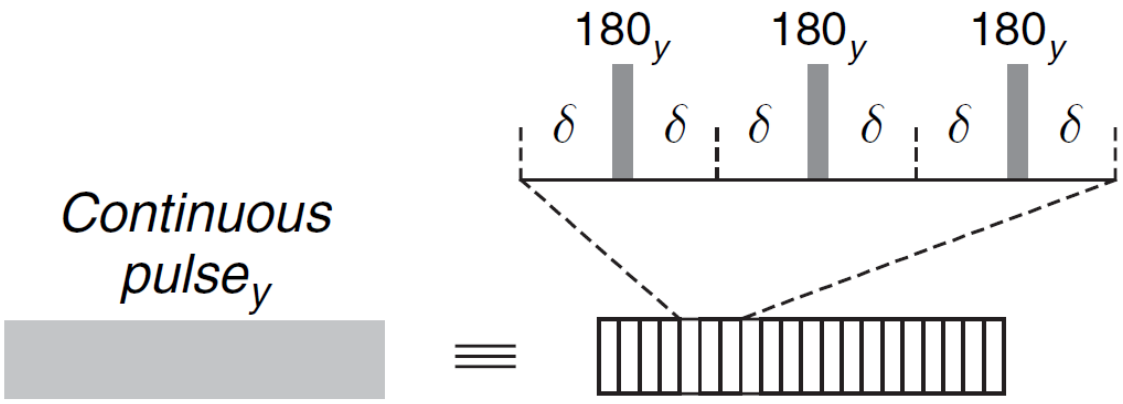

Figure II-2. The multiple pulse sequence in spin-lock period. This can be viewed as a continuous sequence of 180° pulses closely bracketed by infinitely small periods, δ.[21]

Materials and Methods

Materials

Daptomycin obtained from Eli Lilly Research Laboratories (Indianapolis, IN) was used as received. Sodium chloride, 0.01 or 0.1 M standard sodium hydroxide solutions, 0.1 or 1 M standard hydrochloric acid solutions were purchased from Fisher Scientific (Fair Lawn, NJ). Deuterium oxide (100% D_2O) was purchased from Cambridge Isotope Laboratories (Cambridge, MA). Standardized pH buffers of 2, 4, 7, and 10 were obtained from Fisher Scientific (Fair Lawn, NJ). All other chemicals used were reagent grade from Fisher Scientific (Pittsburgh, PA).

Methods

Analytical Methods

Daptomycin solutions were prepared in the pH range of 0.35 to 8.0. All solutions of daptomycin measured by spectroscopic methods were prepared at or below 0.12 mM in the non-aggregation states.

The pH measurements were made at room temperature using an Accumet Model 25 pH/Ion Meter and an Accumet 3 mm Ingold combination electrode with a AgCl reference electrode (Fisher Scientific, Fair Lawn, NJ). The pH meter was calibrated with three certified standards: pH 2, pH 4, and pH 7 (Fisher Scientific, Fair Lawn, NJ). No changes in sample pH values were observed before and after spectroscopic measurements. For the samples in 10% D_2O for NMR measurement, the reported pH values were not corrected for the deuterium isotope effect. The average ionic strength of the solutions of the daptomycin samples in NaCl solutions was about 150 mM. The ionic strength contribution from daptomycin is negligible since only 0.12 mM daptomycin was used.

Potentiometric titrations were carried out using a Mettler Toledo DL 50 Graphic Autotitrator (Mettler, Hightstown, NJ). The titrations were performed with constant stirring in a sealed, jacketed titration vessel, maintained under nitrogen atmosphere at 25±0.5°C. The initial pH values of daptomycin solutions at 2.95 and 5.88 mM concentrations and blank solutions were adjusted to pH around 7.0 by adding an accurate volume of standard 0.01 M standard sodium hydroxide solution, and then titrated with 1.0 M standard hydrochloric acid to pH 2.5. Bjerrum plots were used to estimate the pK_a values[22-24] although the sequence-specific pK_a values could not be assigned solely based on potentiometric titration.

UV absorbance spectra of 0.12 mM daptomycin solutions in the pH range from 0.35 to 4.19 were collected on a Hewlett-Packard 8453 diode-array UV-Visible spectrophotometer (Agilent, Palo Alto, CA).

Fluorescence spectra of 0.12 mM daptomycin solutions in the pH range from 0.35 to 4.19 were acquired using a LS55 luminescence spectrometer (Perkin Elmer Instruments, Norwalk, CT) at room temperature. At an excitation wavelength of 285 nm, emission spectra were collected from 300 to 550 nm with a 3 mm path length cuvette. The excitation and emission slit widths were set to 4 and 3 nm, respectively, and the scan rate was 250 nm/minute.

^{1}H 2D TOCSY homonuclear NMR spectra were collected on a Bruker Avance II 800 MHz NMR spectrometer equipped with a cryoprobe for 0.12 mM daptomycin at various pH values in 90% H_2O/10% D_2O. Daptomycin exists in a monomeric state at this concentration. All NMR experiments were performed at 25 ^oC. The spectra were acquired using TOPSPIN® software. The water signal was suppressed by employing a WATERGATE pulse sequence. All NMR spectra were processed with the NMRPipe® program[25] and analyzed using NMRView®.[26]

Determination of Apparent pK_a Values

Potentiometric pH titration data analysis (Bjerrum plot)

Due to the overlapping pK_a values of daptomycin, the individual pK_a values could not be directly extracted from the titration curves. Therefore, Bjerrum plots were used to obtain the individual pK_a values, though the specific pK_a values cannot be assigned. The Bjerrum curve is a plot of the average number of bound hydrogen atoms (n_H) per molecule versus pH. All pK_a values were determined at the pH values at half integral n_H in the Bjerrum plot.[22] Briefly, the total hydrogen ion (free and bound) concentrations were obtained from the dissociable protons of daptomycin in titrated solutions. The free hydrogen ion concentrations were measured from a pH probe. The bound hydrogen ion concentrations were calculated from the difference between the total and free concentrations. The detailed operational procedures to transform the titration curves to Bjerrum plot are described in the literature,[22-24] and the equations used to construct Bjerrum plots are derived in Appendix A. A correction for a blank solution titration has been made by performing an identical titration with water in the absence of daptomycin. The average number (n_H) of bound hydrogen atoms per molecule of daptomycin was plotted as a function of pH.[22] The apparent pK_a values of the carboxylic acid groups in daptomycin were estimated from the Bjerrum plots.

UV and fluorescence pH titration data analysis

The apparent pK_a values of spectroscopic titration methods were estimated by non-linear regression using the absorbance or emission intensity as a function of pH to the modified Henderson-Hasselbach equation as follows:[27]

$$pK_a = pH - \log [(A_{acid} - A_{obs})/A_{obs} - A_{base})]$$

where A_{obs} is the observed absorbance or emission intensity at each pH, and A_{acid} and A_{base} are absorbances or emission intensities of the protonated and unprotonated forms, respectively.

NMR pH titration data analysis

A modified Hill equation[28,29] was used to estimate the pK_a and Hill coefficient value by nonlinear least squares analysis (Kaleidagraph, Synergy Software, Essex Junction, VT):

$$\delta_{obs} = (\delta_{acid} + \delta_{base}\, 10^{n(pH-pKa)})/(1+ 10^{n(pH-pKa)})$$

Where δ_{obs} is the observed chemical shift at a given pH; δ_{acid} and δ_{base} are the chemical shifts of the protonated and fully unprotonated species, respectively; and n is the Hill coefficient, a measure of cooperativity.

Results and Discussion

Potentiometric Titration

The potentiometric titration curves of daptomycin at two representative concentrations of 2.95 and 5.88 mM are shown Figure II-3A. The choice of concentration for the titration in potentiometric titration method is recommended at 0.01 M.[30] As daptomycin in the non-aggregation state at 0.12 mM in the titration pH ranges from 7 to 2.5 would not be suitable for being titrated. Each titration curve reflects the overlapping ionization due to the four carboxylic acid groups (Asp-3, Asp-7, Asp-9, and mGlu-12) and the aromatic amine (Kyn-13). Moreover the titration curves were daptomycin concentration-dependent. The apparent dissociation constants were estimated from the values at half integral n_H positions of the Bjerrum plots as shown in Figure II-3B as described previously.[22,23] The dissociation constants of daptomycin at the concentration of 5.88 mM thus were estimated to be 4.3, 5.2, 5.6, and one value was less than 3 (Figure II-3B); the dissociation constants of daptomycin at 2.95 mM were 4.1, 5.1, and 5.6, and also one less than 3. However, with this method, the pK_a values cannot be assigned to individual ionizable groups. Moreover, the pK_a values determined by this potentiometric method are shown to be daptomycin concentration dependent. We found that the pK_a values generally increase with increasing daptomycin concentration as the side-chain

acidic residues are exposed to a hydrophobic environment due to the aggregation formation. The higher apparent pK_a values resulted from self-association.[31,32]

The critical aggregation concentrations of daptomycin as a function of pH has been determined by complementary techniques including dynamic light scattering, fluorescence, and NMR spectroscopy.[33,34] Illustrative NMR data are presented in Figure II-4 where daptomycin exists in the monomeric state at $\leq$ 0.15 mM at pH 4.2 as evidenced by the presence of sharp NMR lines in the NMR spectrum (Figure II-4A). However, significant line broadening was observed at higher concentrations due to daptomycin aggregation (Figure II-4B-D). The residues Trp-1 and Kyn-13 had the biggest increase in linewidth. An increase in the resonance linewidths results in a decrease in the proton spin-spin relaxation times T_2 and indicates an increase in "molecular weight" due to aggregate formation. The pH range for meaningful potentiometric titrations is dependent on the substrate concentration, therefore the pK_a values for monomeric daptomycin cannot be determined (without solvent modifiers) at the low concentrations required to avoid aggregation. Therefore, pH titrations with spectroscopic techniques such as NMR, UV, and fluorescence spectroscopy were used to determine pK_a values for daptomycin under non-aggregation state and to assign the estimated values to specific amino acid residues.

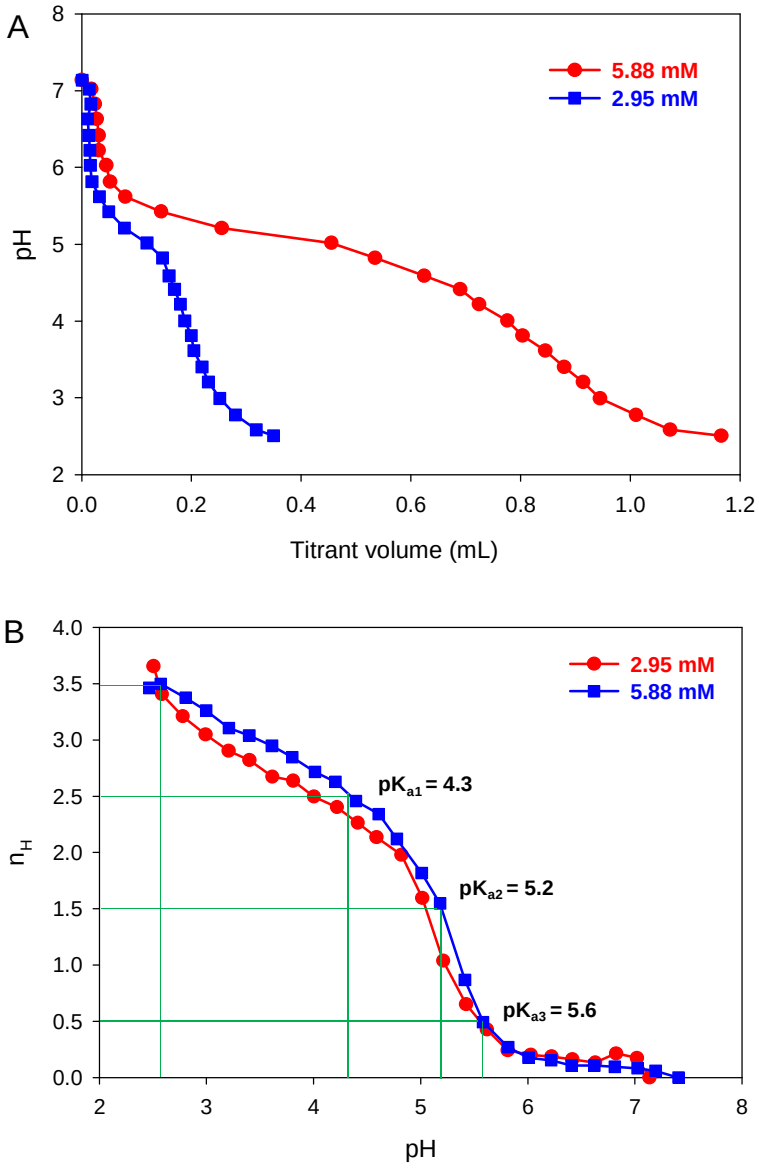

Figure II-3. (A) Daptomycin potentiometric titration curves. The pH values of the daptomycin solutions at 2.95 and 5.88 mM are plotted as a function of titrant (1M HCl) volume. (B) Bjerrum plot of daptomycin potentiometric titration curves. The molar equivalent number of hydrogen's bound (n_H) in these titrations is plotted as a function of pH for daptomycin at 2.95 and 5.88 mM. The estimated pK_a values obtained for daptomycin at 5.88 mM are indicated.

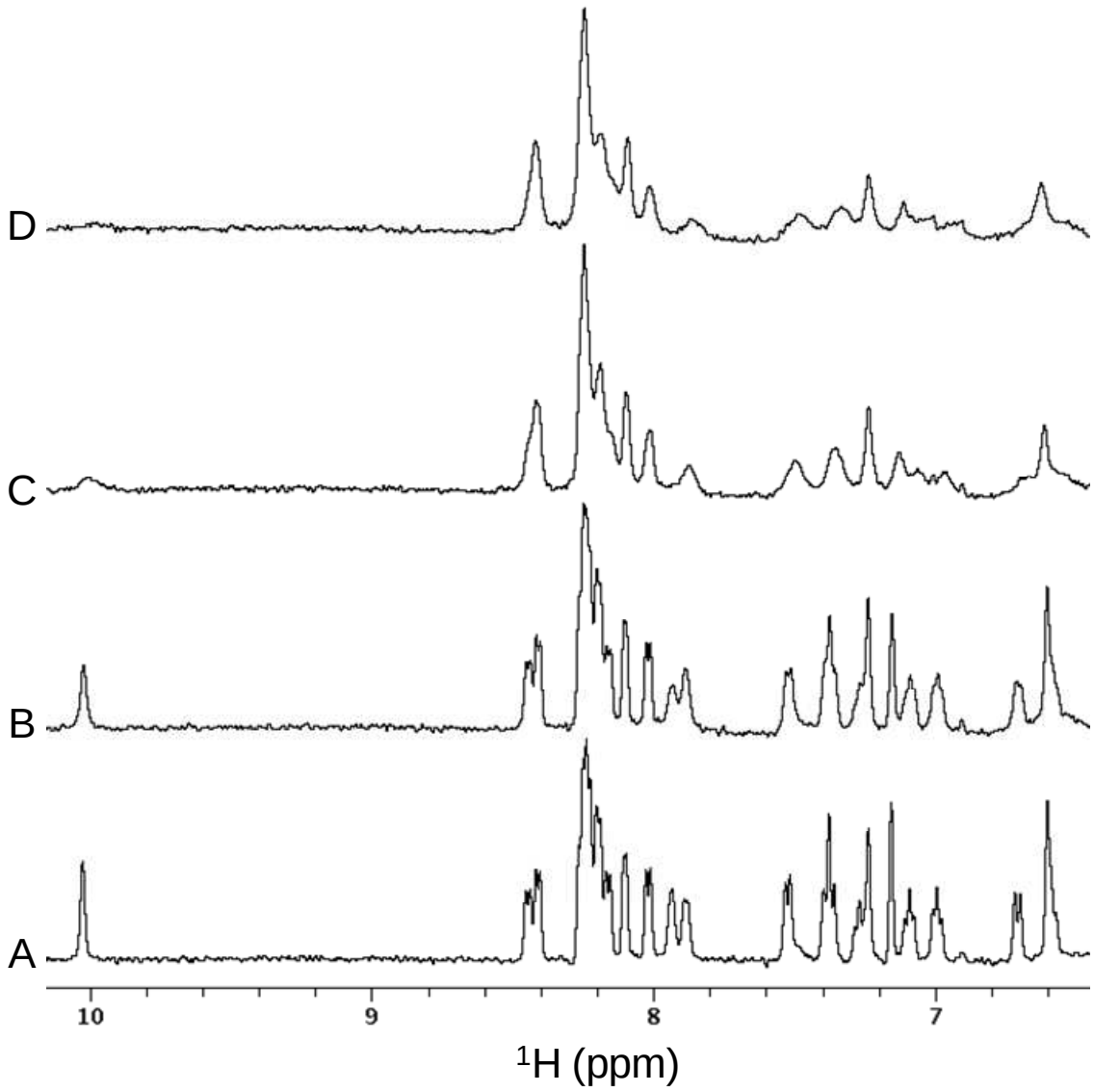

Figure II-4. Aromatic region of the ^{1}H 1D NMR spectra illustrating the concentration-dependent aggregation of the aqueous solutions at pH 4.2 for daptomycin at 0.15 mM (A), 0.18 mM (B), 0.21 mM (C), and 0.25 mM (D). The spectra were acquired on the Bruker Avance II 500 MHz NMR spectrometer.

NMR pH Titration

The ^{1}H resonances of daptomycin have been assigned previously[13,14] and confirmed in the present study. 2D ^{1}H TOCSY spectra were recorded for daptomycin solutions under non-aggregation state at 0.12 mM at pH values ranging from 1 to 8. The side chain resonances of the ionizable groups, particularly the ones close to ionizing residues, are severely overlapped with other peaks in the one-dimensional ^{1}H spectrum. Thus, we have taken the advantage of the high resolution/dispersion of the backbone amides and collected 2D ^{1}H TOCSY spectra for these samples in order to clearly and unambiguously trace the NH:$C_{\beta}H_2$ cross peaks for Asp residues and NH:$C_{\gamma}H_2$ cross peaks for the mGlu-12 residue as shown in Figure II-5A for their pK_a determination. ^{1}H TOCSY spectra for the aromatic resonances of Trp-1 and Kyn-13 are shown in Figure II-5B. As expected, the Trp-1 aromatic resonances showed no shift at these pH values because the protonated form of the indole group in Trp-1 has an apparent lower pK_a of -3.5.[35] However, the Kyn-13 aromatic resonances experienced larger changes in chemical shift at these pH values as indicated in Figure II-5B.

Following the pH-dependent chemical shifts of the cross peaks between amide protons and β-protons of Asp-3, Asp-7, and Asp-9, and γ-protons of mGlu-12, the sequence-specific pK_a values for these residues of daptomycin in the absence of salt were estimated by nonlinear regression using a modified Henderson-Hasselbalch equation (Figure II-6).

Large chemical shift changes were observed for Asp-3, Asp-9, and mGlu-12 over the pH titration range. The apparent pK_a values for Asp-3, Asp-9, and mGlu-12 were determined to be 4.15, 3.85, and 4.55, respectively, with no added NaCl. In contrast, very small changes in chemical shifts were observed for Asp-7. Although attempts were made to obtain additional data for daptomycin below pH 2, the backbone amide protons exhibited fast exchange with water under these more acidic conditions, preventing the acquisition of useful data below pH 2.0. The observed chemical shift change for the Asp-

7 β-proton was only 0.04 ppm above pH 2. Since the expected change in Asp β-proton chemical shifts over the course of pH titration would be about 0.20 ppm, the pK_a value of Asp-7 could be as low as 1.0 and is reported here in as low as 1.0 (Table II-1). This extremely acidic pK_a for Asp-7 could be caused by the nearby positively charged environment of Orn-6 which was reported to have a pK_a value of 10.7.[19] Thus, the formation of a salt bridge between a negatively charged Asp-7 and positively charged Orn-6 could account the unusually low pK_a value of Aps-7.[36,37] Asp-7 residues appear to more stabilized in the ionized state.

In order to corroborate this inference, a NMR titration experiment was performed in 150 mM NaCl. Under this condition, 2D ^{1}H NMR TOCSY spectra were obtained for samples at pH values down to 1.2. These additional points at lower pH values help better define the titration curve for Asp-7 (Figure II-7). The pK_a values of Asp-3, Asp-9, and mGlu-12 in 150 mM NaCl were determined to be 4.07, 3.83, and 4.39, respectively, which are similar to those obtained without added NaCl (Table II-1). The activity coefficients in 150 mM NaCl were not applied to the pK_a calculations. Moreover, the estimated fitted Hill coefficients for these residues were less than 1.0 in the presence and absence of added NaCl (Table II-1). The estimated pK_a value for Asp-7 was 1.27 in 150 mM NaCl. The estimated Hill coefficient was 0.72 in without NaCl and 1.31 in 150 mM NaCl.

The following is a typical Hill equation:

$$\alpha_0 = [H^+]^n / (K_d + [H^+]^n) = [H^+]^n / (K_a{}^n + [H^+]^n)$$

where α_0 is the fraction of protonated species, K_d and K_a are apparent or macroscopic dissociation constant and microscopic dissociation constant, respectively, $[H^+]$ is hydrogen ion concentration, and n is the Hill coefficient, describing the cooperativity of the hydrogen ion binding to titrable residues.

The Hill coefficient (n) describes the cooperativity of the hydrogen ion binding to ionizable residues: n=1, indicating completely independent H^+ binding; n<1, negative cooperative binding where once one H^+ is bound, the affinity for the subsequent H^+ is decreased; n>1, for positive cooperative binding where one H^+ binding facilitates the binding of subsequent H^+ at other sites. The higher Hill coefficient (n=1.31) suggests that the salt effect is positive cooperativity for the binding process, *i.e.* addition of salt promotes the binding of H^+ to the Asp-7 and as a result leads to an increase in its pK_a values. In other words, addition of salt reduces the electrostatic interaction between Asp-7 and Orn-6 and raises the pK_a of Asp-7. Thus, the increase in the Hill coefficient and pK_a value in 150 mM NaCl for Asp-7 is consistent with a salt bridge between the negatively charged Asp-7 and the positively charged Orn-6.

The Hill coefficient less than unity may be explained by the presence of one or more residues with overlapping pK_a values. Significant deviation of the fitted Hill coefficinet from unity suggests that the titration involves more than one dissociating group. The Hill coefficient of mGlu-12 residues was only about 0.5 (0.48), indicating that the mGlu-12 protonated was perturbed or inhibited by the neighbouring titrable Asp-9 or Asp-3 residues.

The pK_a value of the aromatic amine of Kyn-13 was determined to be ~1.3 (Figure II-8). The Hill coefficients of Kyn-13 were not affected by added salt.

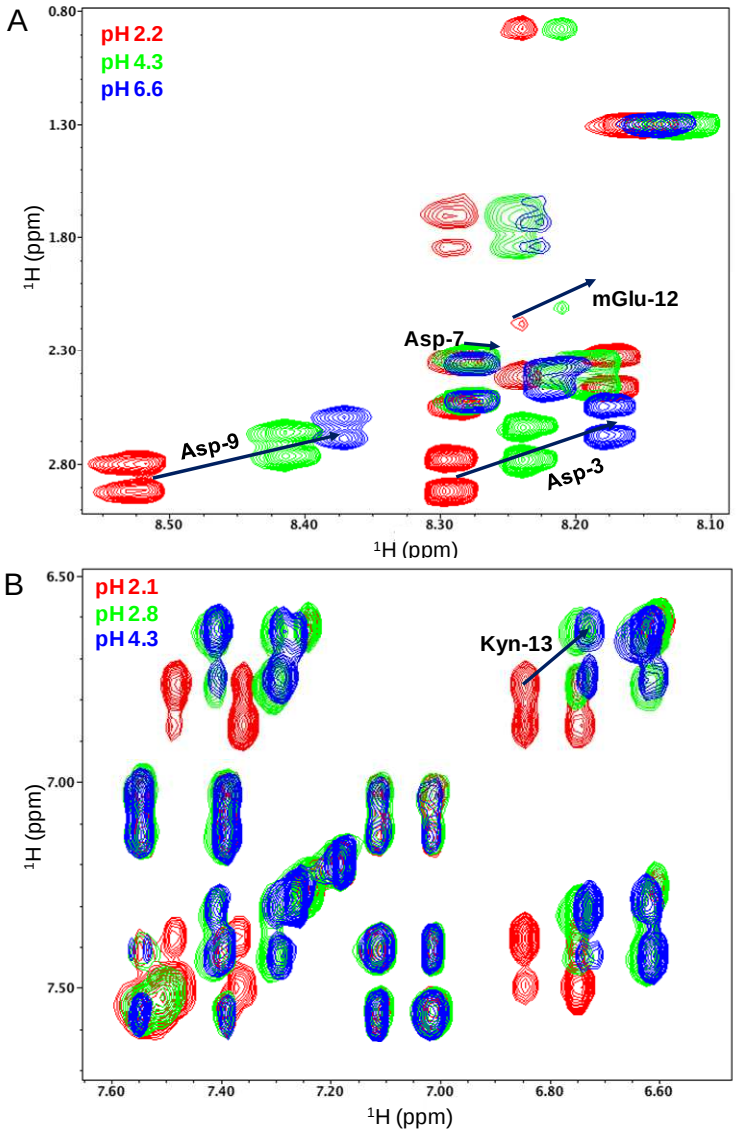

Figure II-5. ^{1}H TOCSY NMR spectra of daptomycin at 0.12 mM in aqueous solutions at different pH values. (A) Spectral region showing the pH-dependence for the acidic residues. For Asp-3, Asp-7, and Asp-9, the tracked cross-peaks are derived from the backbone amide proton and β protons. For mGlu-12, the tracked cross-peaks are from the backbone amide proton and γ-proton, and these cross-peaks are clearly presented at lower contour level. (B) Spectral region showing the pH-dependence for the aromatic residues. The pH-dependence for one of the aromatic resonances of Kyn-13 is indicated. No salt was added to the samples. The arrows indicate the directions of cross-peak movement with increasing pH.

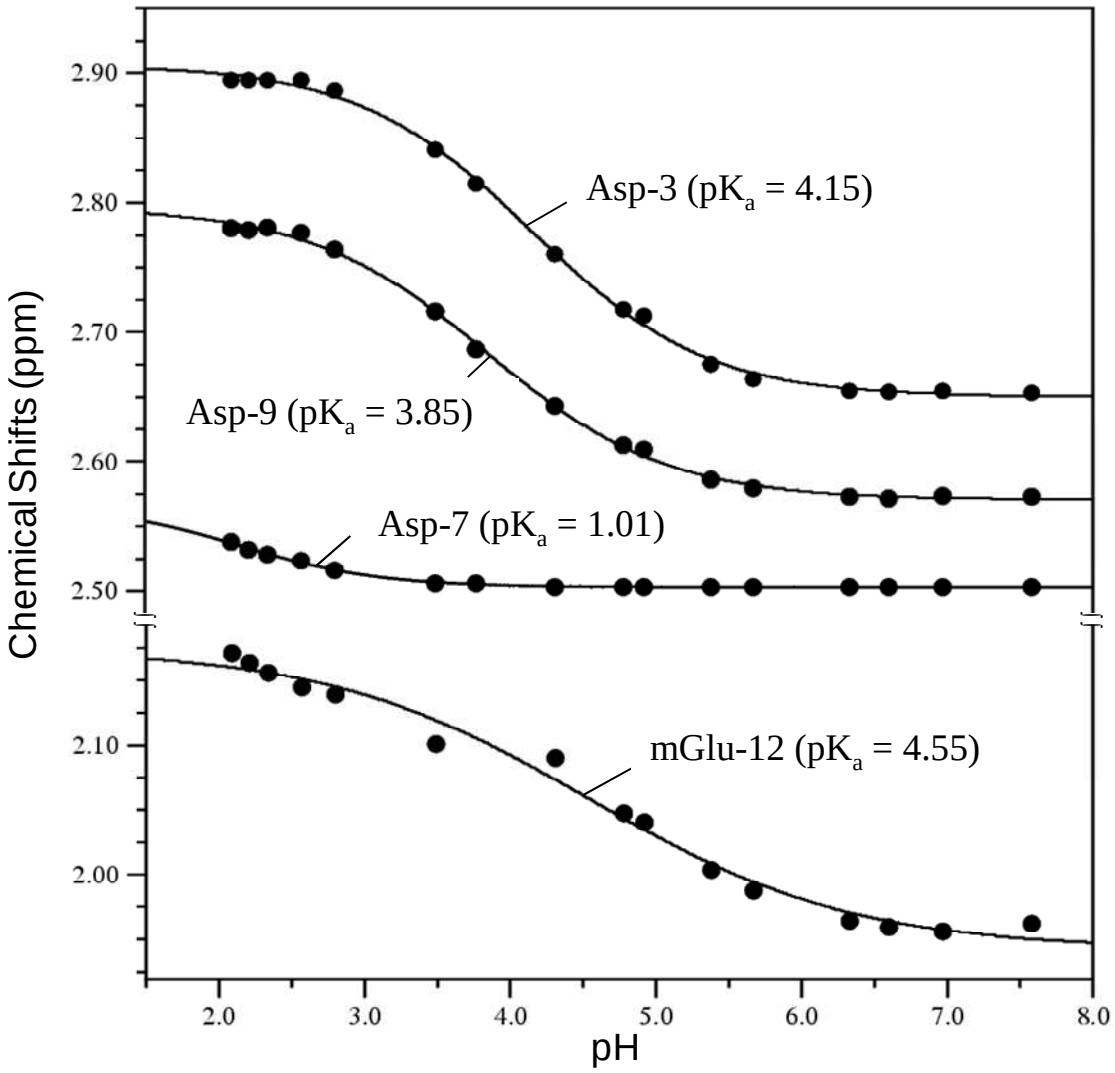

Figure II-6. ^{1}H TOCSY chemical shifts from pH titration of the β-protons of Asp-3, Asp-7, and Asp-9 and the γ-protons of γ-mGlu-12 of daptomycin without NaCl. The fitted modified Henderson-Hasselbalch titration curves are shown by the continuous curves.

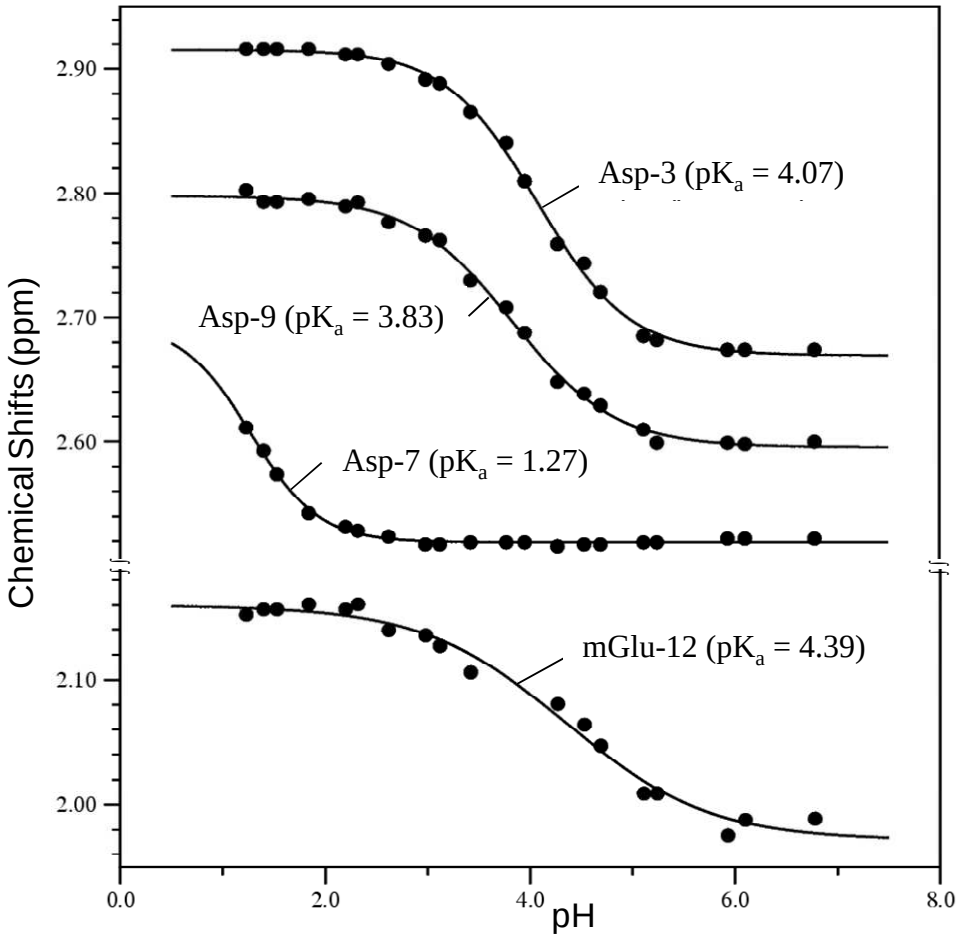

Figure II-7. ^{1}H TOCSY chemical shifts from pH titration of the β-protons of Asp-3, Asp-7, and Asp-9 and the γ-protons of γ-mGlu-12 of daptomycin in 150 mM NaCl. The fitted modified Henderson-Hasselbalch titration curves are shown by the continuous curves.

Table II-1. Estimated pK_a Values and Hill Coefficients of Daptomycin from ^1H TOCSY NMR pH Titration Data.

Residues	NaCl		150 mM NaCl	
	pK_a	Hill Coefficient (n)	pK_a	Hill Coefficient (n)
Asp-3	4.15 ± 0.03	0.73 ± 0.03	4.07 ± 0.02	0.97 ± 0.04
Asp-7	~1.01[a] ± 1.72	0.72 ± 0.16	1.27[b] ± 0.15	1.31 ± 0.16
Asp-9	3.85 ± 0.03	0.71 ± 0.04	3.83 ± 0.03	0.87 ± 0.05
mGlu-12	4.55 ± 0.15	0.48 ± 0.10	4.39 ± 0.12	0.73 ± 0.14
Kyn-13	1.30[b] ± 0.19	0.88 ± 0.11	1.30[b] ± 0.24	0.89 ± 0.07

[a]pK_a value was estimated from changes in chemical shift, with a maximum of 0.2 ppm for the Asp-7 β-protons over a complete titration.

[b]pK_a values were estimated from incomplete pH titration curves.

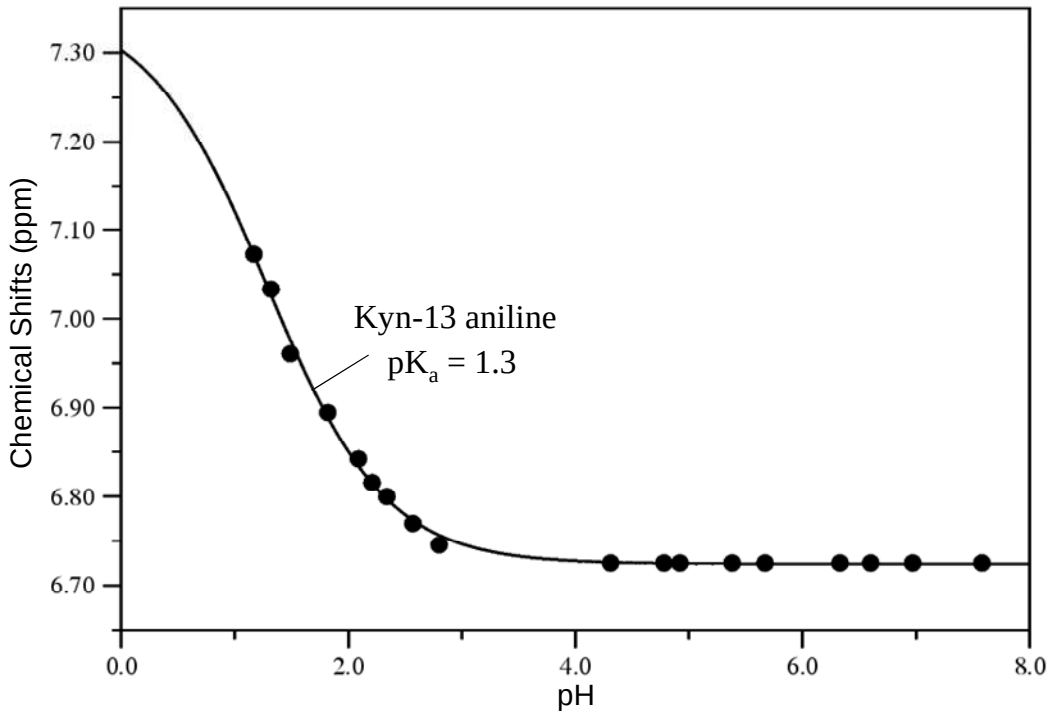

Figure II-8. ^{1}H TOCSY chemical shifts from pH titration of Kyn-13 aromatic protons of daptomycin with no NaCl added. The solid curve represents the best fitted modified Henderson-Hasselbalch to single ionization equilibrium by nonlinear regression.

UV and Fluorescence Spectroscopy

The aromatic amine of Kyn-13 has distinct UV and fluorescence spectroscopic properties. The spectral intensity changes of UV and fluorescence spectra due to the protonation of the amine of Kyn-13 were employed to determine the ionization constant.

The UV absorption spectra of daptomycin in aqueous solutions at different pH values are shown in Figure II-9A. The multiple isosbestic points were observed at 240 nm, 258 nm, 270 nm, and 295 nm. The pK_a value of Kyn-13 was determined to be 1.19 ± 0.02 by plotting the absorbance changes measured at 365 nm as a function of pH (Figure II-10).

The ionization of the aromatic amine in Kyn-13 was specifically observed using pH-dependent fluorescence emission changes (Figure II-9B). As pH values of daptomycin solutions decreased from pH 4.19 to 0.35, the emission intensity from Kyn-13 at 460 nm also decreased, while that from Trp-1 at 355 nm increased. The protonation of the amine group of Kyn-13 by acid titration reduced the efficiency of fluorescence resonance energy transfer between donor Trp-1 and acceptor Kyn-13. By plotting the emission intensity at 460 nm from Kyn-13 as a function pH, the pK_a value of Kyn-13 was determined to be 1.29 ± 0.03 (Figure II-10). The pK_a values measured by UV and fluorescence spectroscopy are expected to be slightly different, since fluorescence relates to the first excited state of the molecule, while UV measurement is related to the ground state. The lowest excited singlet state has an electronic distribution which is generally different from the ground electronic state of the molecule, thus the excited state may be more or less acidic than the ground state. Generally, the excited state pK_a values of the molecules containing an electron-withdrawing group are typically greater than those for the ground state.[38]

Understanding the intramolecular interactions in daptomycin is important for understanding its activity and solution properties. Asp-3 and Asp-7 are considered as essential groups for the bioactivity of daptomycin.[11] We have found here that Asp-7 has

unique ionization properties. Based on the sequence-specific pK_a values and Hill coefficients reported in this study, the pH-dependent daptomycin species distribution varied from di-cation (H_6A^{2+}), cation (H_6A^{+}), zwitterion ($H_4A^{\pm}$), monoanion (H_3A^{-}), dianion (H_2A^{2-}), and trianion (HA^{3-}) can be calculated as shown in Figure II-11 (Appendix B). This species distribution plot can be used to understand the interactions of molecular mechanism between daptomycin with other small and macromolecules under the different pH conditions.

Conclusions

The sequence-specific pK_a determination of daptomycin has not been reported previously. In this study, the chemical shifts of $C_\beta H_2$ of Asp residues and $C_\gamma H_2$ of the mGlu-12 residue were measured by using the highly resolved NH:$C_\beta H_2$ and NH:$C_\gamma H_2$ cross-peaks detected in the 2D ^{1}H NMR TOCSY spectra to obtain the pK_a values of the four carboxyl groups in daptomycin. The pK_a value of Kyn-13 has also been determined over this pH range using its aromatic proton chemical shifts.

The acidity of the side-chain ionizable group is strongly influenced by structural and electrostatic interactions in their local surroundings. The average pK_a values of aspartic acid and glutamic acid in folded proteins are 3.5 ± 1.2 and 4.2 ± 0.9, respectively.[39] The pK_a values of daptomycin provide valuable information about the local environment. The apparent pK_a values of 4.07, 1.27, and 3.83 for the three aspartic acid residues, Asp-3, Asp-7, and Asp-9, respectively, of daptomycin in 150 mM NaCl, are different than with added NaCl, suggesting that they are located in a different electrostatic environment. Asp-7 likely forms a salt bridge with Orn-6 leading to an abnormally low pK_a.[36,37] The slightly higher pK_a of Asp-3 than Asp-9 could be attributed to the fact that Asp-3 is located close to hydrophobic residue Trp-1 and lipophilic decanoyl tail.[39] The pK_a value determined for Kyn-13 by NMR spectroscopy agrees well with the values obtained by UV and fluorescence spectroscopy.

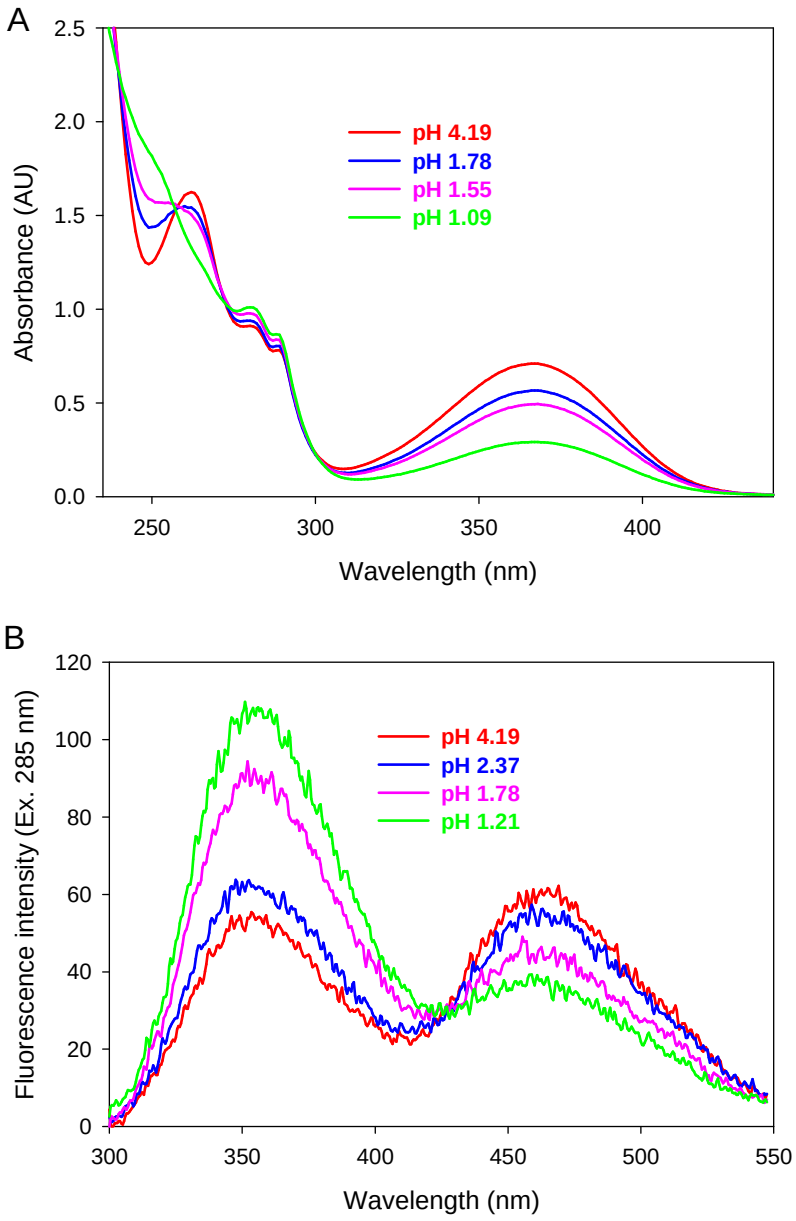

Figure II-9. The UV and fluorescence spectra of daptomycin at 0.12 mM in the different pH solutions with no NaCl added. (A) Representative pH-dependent UV absorbance spectra of daptomycin solutions. (B) Representative pH-dependent fluorescence emission spectra of daptomycin solutions. The excitation wavelength was 285 nm. Trp-1 fluorescent emission was at 355 nm, and Kyn-13 fluorescent emission was at 460 nm.

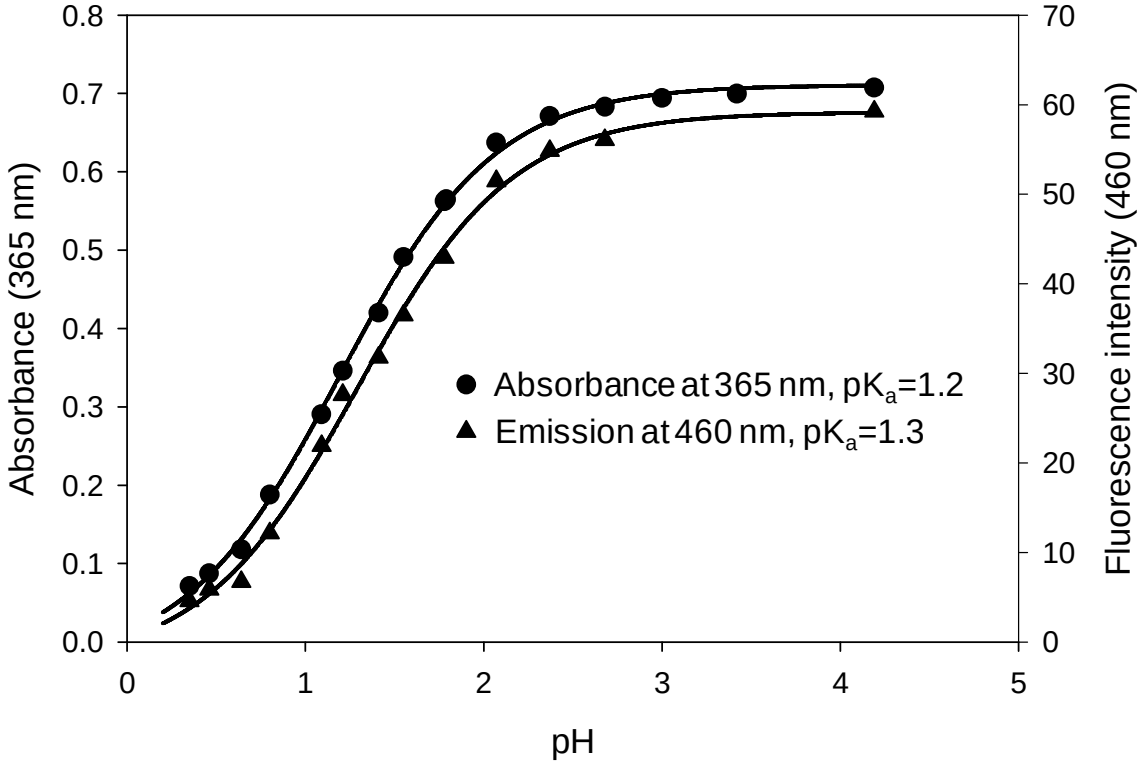

Figure II-10. UV and fluorescence pH titration of Kyn-13 of daptomycin with no NaCl added. The plots are UV absorbance (at 365 nm) and fluorescent emission intensity (at 460 nm) for Kyn-13 at 0.12 mM daptomycin as a function of pH. The solid curves represent the best fit Henderson-Hasselbalch equation to single ionization equilibrium by nonlinear regression.

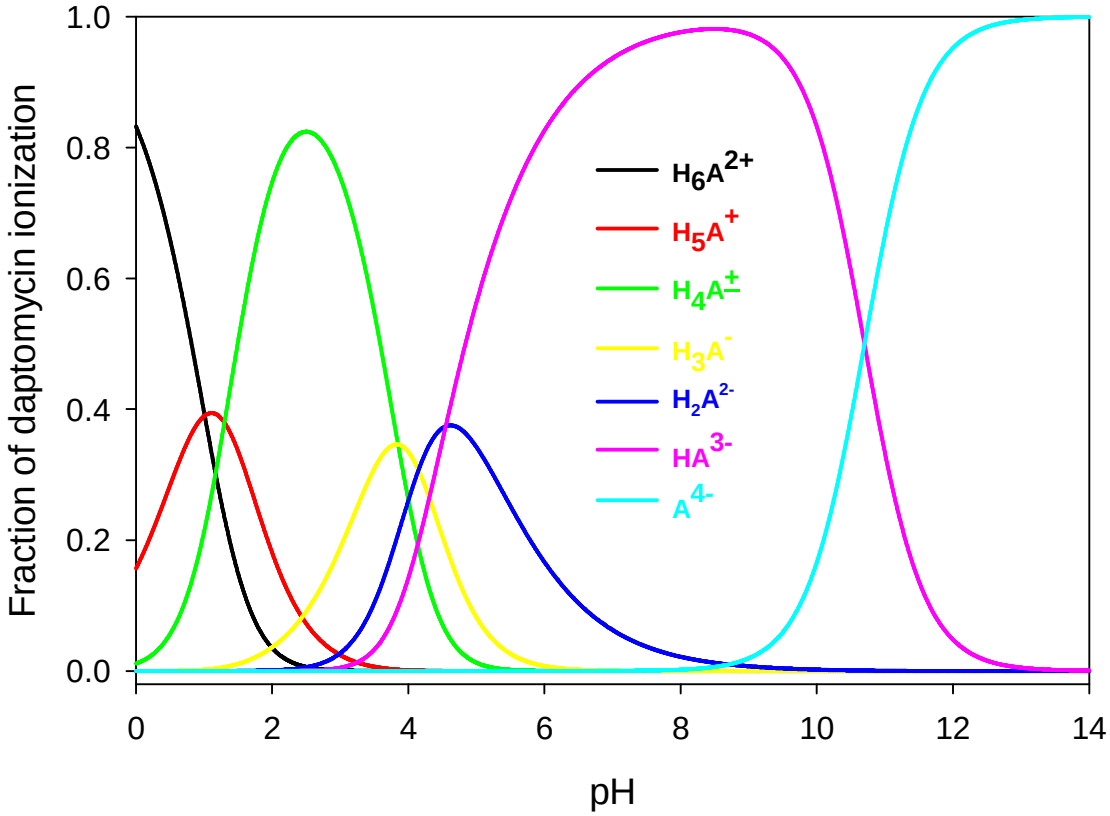

Figure II-11. pH-dependent species distribution for daptomycin in a non-aggregation state. The pK_a values and Hill coefficients used in this calculation are pK_{a1} = 1.01 (Asp-7), n_1 = 0.72; pK_{a2} = 1.30 (Kyn-13), n_2 = 0.88; pK_{a3} = 3.85 (Asp-9), n_3 = 0.71; pK_{a4} = 4.15 (Asp-3), n_4 = 0.73; pK_{a5} = 4.55 (mGlu-12), n_5 = 0.48; pK_{a6} = 10.7 (Orn-6), n_6 = 1.00; The calculations of pH-dependent species distribution for daptomycin are described in Appendix B.

CHAPTER III EVALUATION OF METHODS TO DETERMINE DAPTOMYCIN AGGREGATION

Introduction

This chapter describes the development of methods to study daptomycin aggregation. Daptomycin is a lipopeptide that contains thirteen amino acid residues including hydrophobic aromatic residues, such as Trp-1 and Kyn-13, a lipophilic decanoyl tail, and hydrophilic ionizable side-chains (Asp-3, Asp-7, Asp-9, and mGlu-12).

Various methods have been used to investigate the mechanism and stoichiometry of peptide/protein aggregation. Broadly, these analytical methods can be classified as size determination methods and molecular spectroscopic detection. Size determination methods include size exclusion chromatography (SEC), static and dynamic light scattering. Molecular spectroscopic detection includes circular dichronism (CD), Fourier transform infrared (FTIR), fluorescence spectroscopy, and nuclear magnetic resonance (NMR).[40,41]

According to the literature, daptomycin aggregation is induced by calcium ion, pH variation, or substrate concentration.[7,13,42,43] Below the critical aggregation concentration (CAC), daptomycin molecules are in monomeric form, while aggregation occurs at and above the CAC. However a systematic determination of CAC values of daptomycin has not been made. Lakey and Ptak[42] observed that the ratio of fluorescence yield Kyn-13/Trp-1 increased at daptomycin concentrations of 5 mM, possibly due to aggregation effects increasing the fluorescence energy transfer from Trp-1 to Kyn-13; moreover ^{1}H NMR results from aqueous solutions were reported to show significant line broadening consistent with aggregation although representative spectra were not published. Calcium-induced daptomycin aggregation was observed using NMR.[12-14] The pronounced broadening of resonances in NMR pH titration of daptomycin were observed as decreasing pH up to 2.[13] The CAC value of daptomycin in borate buffer solution (pH

10) was determined to be 2 mM by surface tension measurement.[43] An observed deviation in hydrolytic reaction order at higher substrate concentration in alkaline solutions was attributed to daptomycin aggregation.

Aggregates are defined as protein assembles of higher molecular order formed by unfolded (denatured) and/or partially unfolded monomers. By contrast, protein associates are built up of native monomers and can be re-dissociated to yield native monomers.[44] Strictly speaking, daptomycin "aggregation" is also "association". Thus, the analytical techniques involving dilution such as size exclusion chromatography and flow field fractionation (FFF) may not be suitable for CAC determination.

Daptomycin (Figure I-1) contains two aromatic fluorescent residues, Trp-1 and Kyn-13. The C-terminal carboxyl group of Kyn-13 is connected with the hydroxyl group of Thr-4 via an ester bond, forming a 10-membered ring. The N-terminal Trp-1 residue is acylated with a decanoyl aliphatic chain and situated between the lipid chain and the Kyn-13 residue. The proximity of these two fluorophores arises from a lactone bond, which connects threonine (Thr-4) side chain with the C-terminal Kyn-13 residue. Due to the proximity of the two fluorophores and the overlap of the donor Trp-1 emission spectrum (maximum emission wavelength at 355 nm) and acceptor Kyn-13 excitation spectrum (excitation wavelength about 355 nm), fluorescence resonance energy transfer (FRET) occurs between the two fluorophores.[14,45] FRET is a distance-dependent interaction between the electronic excited states of two functional groups in which excitation is transferred from a donor (e.g. Trp-1) to an acceptor (e.g. Kyn-13) without emission of a photon.

The extent of energy transfer is determined by the distance between the donor and acceptor and the extent of spectral overlap. The distance at which FRET is 50% efficient is called the "Förster distance".[46] The spectral overlap is described in terms of the Förster distance (R_0). The rate of energy transfer $k_T(r)$ is given by

$$k_T(r) = 1/\tau_D \, (R_0/r)^6$$

where τ_D is the decay time of the donor in the absence of energy transfer, R_0 is the Förster distance, and r is the distance between the donor (D) and the acceptor (A). When the D-A distance (r) is equal to the Förster distance (R_0), the rate of transfer is equal to the decay rate ($1/\tau_D$) of the donor. Hence, the rate of energy transfer is strongly distance-dependent ($1/ r^6$).[46]

The efficiency of FRET is dependent on the inverse sixth power of the distance between the donor and the acceptor, the relative orientation of the donor emission dipole moment and the acceptor absorption dipole moment, and the spectral overlap of the donor emission spectrum and the acceptor absorption spectrum.[46] Therefore, the fluorescence emission patterns are expected to be useful to detect conformational transitions and aggregation of daptomycin. The emission fluorescence from Kyn-13 in daptomycin at 460 nm was shown to be a sensitive probe for daptomycin-phospholipid membrane interactions.[14] FRET as a probe of peptide cyclization was exploited to detect the cyclic ring opening during alkaline hydrolysis and the differences of Kyn-13 fluorescence between the linear and cyclized peptide.[42,47]

Besides utilizing the fluorescence properties to detect daptomycin aggregation, dynamic light scattering (DLS) is also potentially useful for measuring CAC and hydrodynamic radius of daptomycin aggregates, particle size distribution of the aggregates. DLS is a sensitive, noninvasive, and nondestructive technique to detect the presence of small aggregates (< 1 μm). DLS measures temporal fluctuation in the intensity of scattered light as a result of Brownian motion. Smaller particles move faster, and the larger ones move slower. The dynamic properties of the scattering solute molecules are derived from the autocorrelation function $G(\tau)$ calculated from the fluctuations of the scattered light. The autocorrelation function $G(\tau)$ can be expressed as following:

$$G(\tau) = \int_0^\infty I(t)I(t+\tau)dt = B + Ae^{-2q^2D\tau}$$

Where *I(t)* is the intensity of the scattered light at initial time *t*, *τ* is the delay time, *B* is the baseline, *A* is the amplitude, *D* is diffusion coefficient, and *q* is the scattering vector:

$$q = (4\pi n_0/\lambda_0)\sin(\theta/2)$$

where,

n_0 = the refractive index of the solvent

λ_0 = the wavelength of laser light

θ = the scattering angle

The relationship between hydrodynamic radius and diffusion coefficient is expressed by the Stokes-Einstein equation:

$R_h = kT/6\pi\eta_0 D$

where,

R_h = apparent hydrodynamic radius

T = absolute temperature

k = Boltzmann constant

η_0 = solvent viscosity

G(τ) decays exponentially as a function of the time delay, τ. The rate of the intensity fluctuation is directly related to the translational diffusion coefficient (D).

At low τ values, the positions of the solute molecules and the intensities of the scattered light are highly correlated, and G(τ) is large. At higher τ values, the positions of the solute molecules become less correlated, and G(τ) progressively decreases. When a large number of monodisperse solute molecules/particles are moving randomly, G(τ) decays exponentially as a function of the time delay, τ. Analysis of these intensity fluctuations also enables the determination of a size distribution of particles using established models.[48]

Compared with the hydrodynamic radius (R_h) values and molecular weights of proteins (e.g., lysozyme, 14 kDa at 1.9 nm; insulin, 34 kDa at 2.7 nm; and immunoglobulin G, 160 kDa at 7.2 nm), daptomycin is a relative small lipopeptide with molecular weight 1.6 kDa. The expected hydrodynamic radius of aggregated daptomycin is expected to be ≤ 10 nm depending on the aggregation number. A sensitive light scattering instrument with a non-invasive-back-scatter (NIBS) detection angle at 173º was selected to directly measure the hydrodynamic radius and size distribution because it can measure a minimum particle size < 1 nm. The backscatter detection can extend the range of sizes and concentrations of samples, improve detection sensitivity, reduce the multiple scattering and measure higher concentration samples.

With multiple ionizable side-chain residues, ionization states and net charge of daptomycin varying with pH, daptomycin aggregation is predicted to be sensitive to both pH and substrate concentration. The sequence-specific pK_a values for the four acidic residues and one aromatic amine (Kyn-13) in daptomycin were determined by 2D TOCSY NMR pH titration as reported in Chapter II. The estimated pK_a values for Asp-3, Asp-7, Asp-9, mGlu-12, and Kyn-13 were determined to be 4.3, 1.0, 3.8, 4.6, and 1.3 in aqueous solution. The pK_a value of the primary aliphatic amine (Orn-6) was estimated by potentiometric titration to be 10.7.[19] The aromatic amine (Kyn-13) is a much weaker base due to resonance delocalization of the nonbonding electrons in the free amine.

The objective of the work presented in this chapter was to evaluate methods for determining the CAC of daptomycin using fluorescence spectroscopy, DLS, and NMR. A method for estimating CAC based on FRET was developed. Supporting evidence for the estimated CAC values was obtained using the intensity correlation function and hydrodynamic radius distribution from DLS measurement and from the changes of proton resonance intensities and linewidths using NMR spectroscopy.

Materials and Methods

Materials

Daptomycin obtained from Eli Lilly Research Laboratories (Indianapolis, IN) was used as received. L-kynurenine was purchased from MP Biomedicals, LLC (Solon, OH). Sodium chloride, sodium hydroxide solutions, hydrochloric acid solutions were purchased from Fisher Scientific (Fair Lawn, NJ). Deuterium oxide (100% D_2O) was purchased from Cambridge Isotope Laboratories (Cambridge, MA). Standardized pH buffers of 2, 4, 7, and 10 were obtained from Fisher Scientific (Fair Lawn, NJ). All other chemicals used were reagent grade or higher quality from Sigma-Aldrich (St. Louis, MO) and Fisher Scientific (Pittsburgh, PA).

Methods

Preparation of daptomycin solutions

To compare the fluorescence properties of kynurenine and Kyn-13 in daptomycin, daptomycin and kynurenine aqueous solutions at pH 4.0 were separately prepared at 0.23 and 0.24 mM, respectively.

Based on the estimated pK_a values of daptomycin, the four side chain acids are completely ionized at pH 6.5, and the net charge of daptomycin is negative 3. At pH 4.0, the side-chain acidic residues are partially ionized. Thus, these two pH conditions (pH 4.0 and 6.5) were used to investigate the utility of various analytical methods.

Aqueous solutions of daptomycin were prepared in the concentration range from 0.05 to 21.21 mM. The solution pH values were adjusted with diluted sodium hydroxide or hydrochloric acid solution and diluted to the targeted concentrations with the same pH values of deionized water at pH 4.0 or 6.5. The pH measurements were made at room temperature using an Accumet Model 25 pH/Ion Meter and an Accumet 3 mm Ingold combination electrode with an AgCl reference electrode (Fisher Scientific, Fair Lawn,

NJ). The pH meter was calibrated with three certified standards pH 2, pH 4, and pH 7 (Fisher Scientific, Fair Lawn, NJ). Sample pH was measured before and after spectroscopic measurements.

Fluorescence spectroscopy

Fluorescence spectra were recorded using a Perkin-Elmer LS55 luminescence spectrometer (Perkin Elmer Inc., Norwalk, CT) at room temperature. To measure the emission intensities from both Trp-1 and Kyn-13, daptomycin solutions were excited at 285 nm. The emission spectra were collected from 250 to 550 nm. The scan rate was set at 250 nm/minute. The excitation and emission slit widths were set to 4 and 3 nm, respectively. Initially a cuvette with a 10 mm path length was used. But to expand the measured concentration range in the presence of self-quenching, 3 and 1 mm path length cuvettes (Starna Cells, Inc., Atascadero, CA) were used.

Dynamic light scattering

Dynamic light scattering (DLS) experiments were conducted at 298 K with an ALV-NIBS High Performance Particle Sizer (Model No ALV-NIBS/HPPS, S/D: NIBS-20034, ALV-Laser Vertriebsgesellschaft m.b.H Langen, Germany). Scattered light intensity (He-Ne laser 632.8 nm) was detected at an angle of 173^0 with an ALV-5000/E multiple tau digital correlator. Prior to performing measurements, samples were filtered through a 0.2 μm filter membrane (Anotop Inorganic Membrane Filter, Whatman). The ALV correlator setup was 3 runs each of 10 second duration. The CONTIIN algorithm was used to estimate hydrodynamic radius and particle size distribution.

NMR spectroscopy

1D proton NMR spectra were collected with a Bruker Avance II 500 MHz US2 spectrometer in 90% H_2O/10% D_2O at daptomycin concentrations from 0.11 to 21 mM in pH 4.0 and 6.5.

Results

Fluorescence Spectroscopy

Fluorescence spectra of daptomycin and kynurenine

The emission spectra of daptomycin and kynurenine at 0.23 and 0.24 mM concentration and pH 4.0 are shown in Figure III-1. Kynurenine showed only weak fluorescence around 420 nm (excitation at 285 nm). The emission peaks of daptomycin were 355 nm from Trp-1 and 460 nm from Kyn-13 (excitation at 285 nm). The fluorescent emission intensity from Kyn-13 of daptomycin was much stronger than that from kynurenine, and the emission wavelength also shifted due to the fluorescence resonance energy transfer (FRET) between Trp-1 and Kyn-13.

Aggregation detection by fluorescence spectroscopy

Shown in Figures III-2 and 3 are the fluorescence spectra of daptomycin solutions at pH 4.0 (III-2) and 6.5 (III-3). In pH 4.0 solutions, the emission intensities from both Trp-1 at 355 nm and Kyn-13 at 460 nm increased as the daptomycin concentration was increased from 0.06 to 0.11 mM. At higher concentrations, e.g. at 0.23 mM and 0.57 mM, the magnitudes of the concentration-dependent emission intensities at 460 nm from Kyn-13 increased dramatically, while the emission intensities of Trp-1 at 355 nm decreased. The fluorescence emission intensities from Trp-1 and Kyn-13 changed differently with an increase in daptomycin concentration, which indicated a occurrence of either a conformational transition or aggregation. At pH 6.5, both the fluorescence emission intensities at 460 nm (Kyn-13) and at 355 nm (Trp-1) increased in the concentration ranges 0.05 to 0.50 mM. The concentration emission intensities at 460 nm at both pH values are compared in Figure III-4. The intensities at 460 nm abruptly increase at pH 4.0 (> 0.12 mM) whereas a gradual increase at pH 6.5 can be observed. The fluorescence intensity changes as a function of daptomycin concentration at pH 4.0 (III-5A and 6A)

and 6.5 (III-5B and 6B) with 3 mm and 10 mm path length cuvettes are plotted. At pH 6.5, no upward inflection point of the emission intensities at 460 nm was observed, and the fluorescent emission patterns from Trp-1 and Kyn-13 changed similarly as daptomycin concentration increased.

Since the emission patterns at 355 nm and 460 nm are associated with daptomycin concentration, the plot of fluorescent response calculated by the ratio of fluorescent intensity to daptomycin concentration is also an indicator of CAC. In Figure III-7, the normalized fluorescent responses are plotted against the concentration. The abrupt change of fluorescent response was detected at pH 4.0 (III-7A), but not at pH 6.5 (III-7B).

In Figure III-8, the fluorescent intensity at 460 nm (left Y-axis) and the maximum emission wavelength from Trp-1 between 300 to 375 nm (right Y-axis) are displayed together. Corresponding to the fluorescent intensity increase at 460 nm, the maximum emission wavelength shifted to short wavelength (354 to 338 nm). The emission wavelength of Kyn-13 at 460 nm did not change.

Taken together these results suggest that the CAC for daptomycin at pH 4.0 was 0.12 mM, while no observable CAC was detected at pH 6.5. Confirmation that the observed fluorescent changes are due to aggregation was obtained using DLS and NMR.

Dynamic Light Scattering

The normalized autocorrelation function plots of daptomycin at pH 4.0 and 6.5 are shown in Figure III-9. The correlation function is expected to drop rapidly for small particles and more slowly for larger particles. At pH 6.5, the normalized intensity correlation function of both 0.25 and 3.65 mM daptomycin solutions rapidly decreased. The hydrodynamic radii were extracted from normalized intensity correlation functions based on number weighting. The normalized distributions of hydrodynamic radii (logarithmic scale) of daptomycin at pH 6.5 and 4.0 are shown in Figures III-10. The

hydrodynamic radius of daptomycin at pH 6.5 remained constant at the smallest measurable size (0.6 nm) up to 7.32 mM (Figure III-10A), suggesting the absence of aggregation in solutions.

In contrast, at pH 4.0, the normalized intensity correlation function of daptomycin solutions drastically decreased from solutions at 0.11 mM, but dropped off more slowly at 0.21 mM and 3.30 mM. The hydrodynamic radius of daptomycin at pH 4.0 above 0.20 mM increased to 2 – 3 nm (Figure III-10B), which indicated that daptomycin aggregates were formed at higher concentrations.

The count rate plots of daptomycin solutions at pH 4.0 and pH 6.5 are shown in Figure III-11. The CAC value of daptomycin at pH 4.0 was observed at 0.12 mM from the inflection point of the plot of count rate versus daptomycin concentration. The count rate plot of daptomycin solutions at pH 6.5 was a flat line. Daptomycin aggregated at higher concentrations at pH 4.0, but not at pH 6.5.

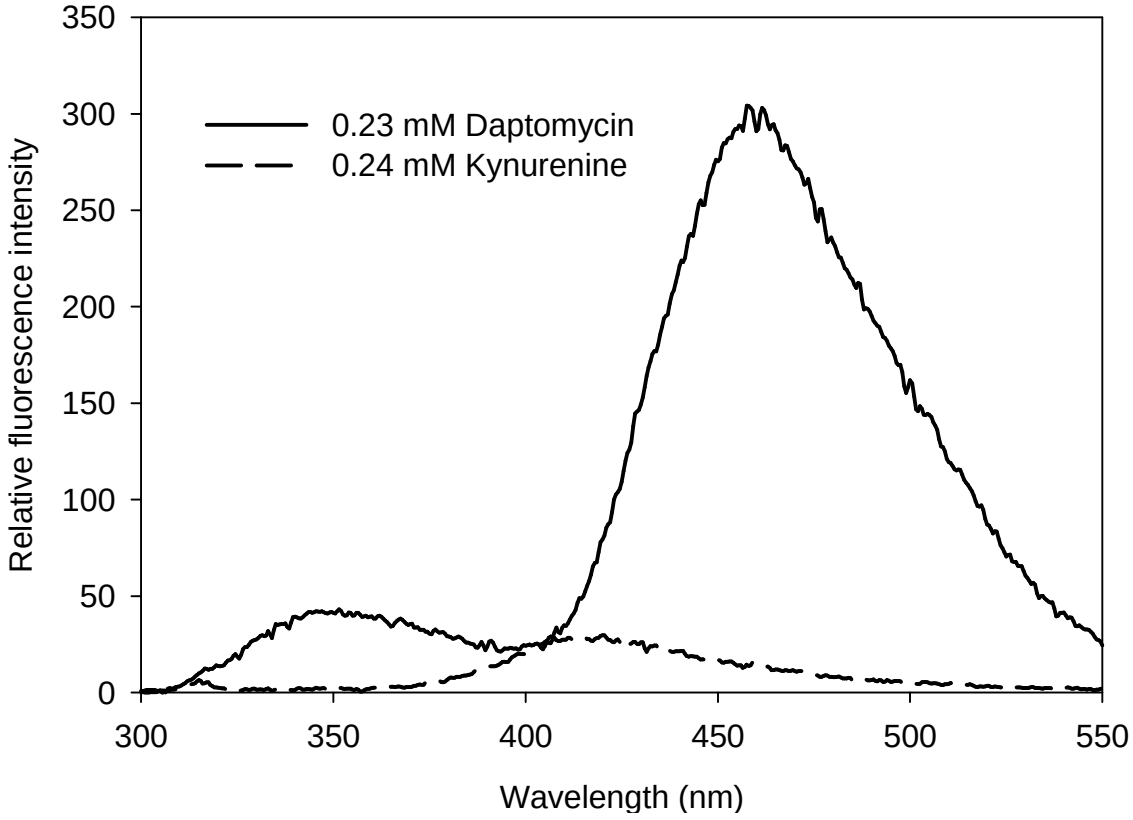

Figure III-1. Emission spectra of daptomycin and kynurenine in aqueous solutions at pH 4.0. (cuvette path length 10 mm; excitation wavelength at 285 nm).

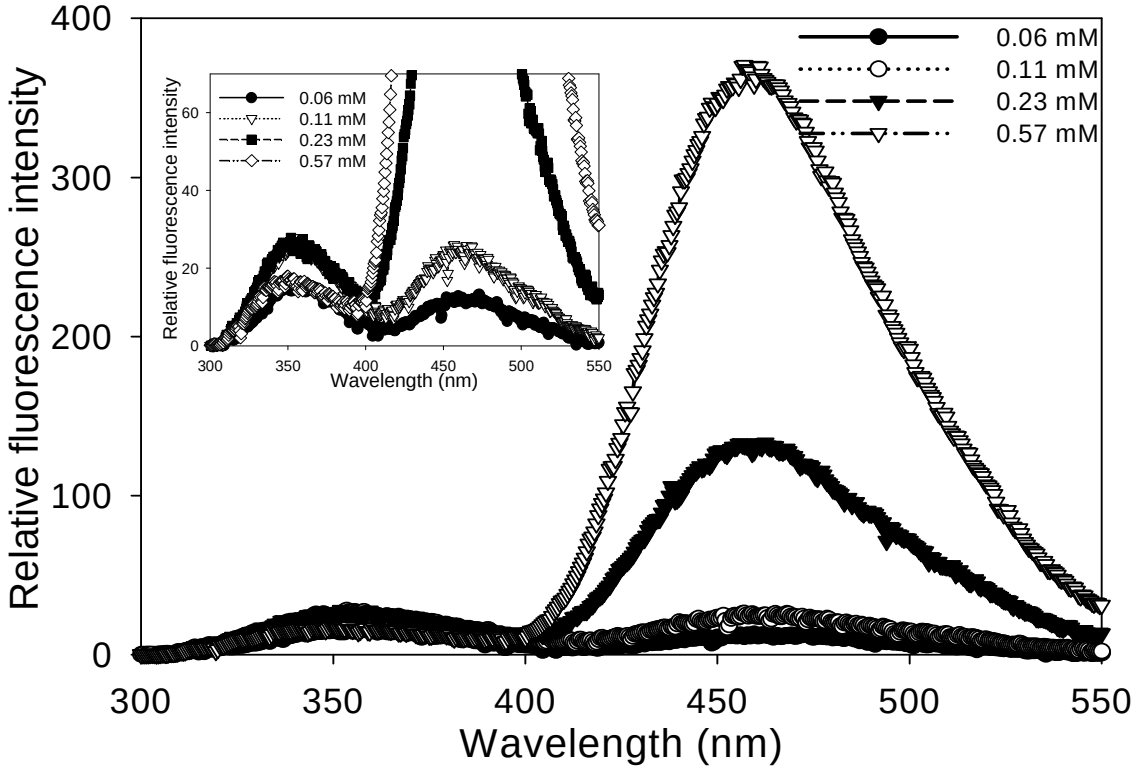

Figure III-2. Emission spectra of daptomycin aqueous solutions at pH 4.0 (cuvette path length 3 mm; excitation wavelength at 285 nm).

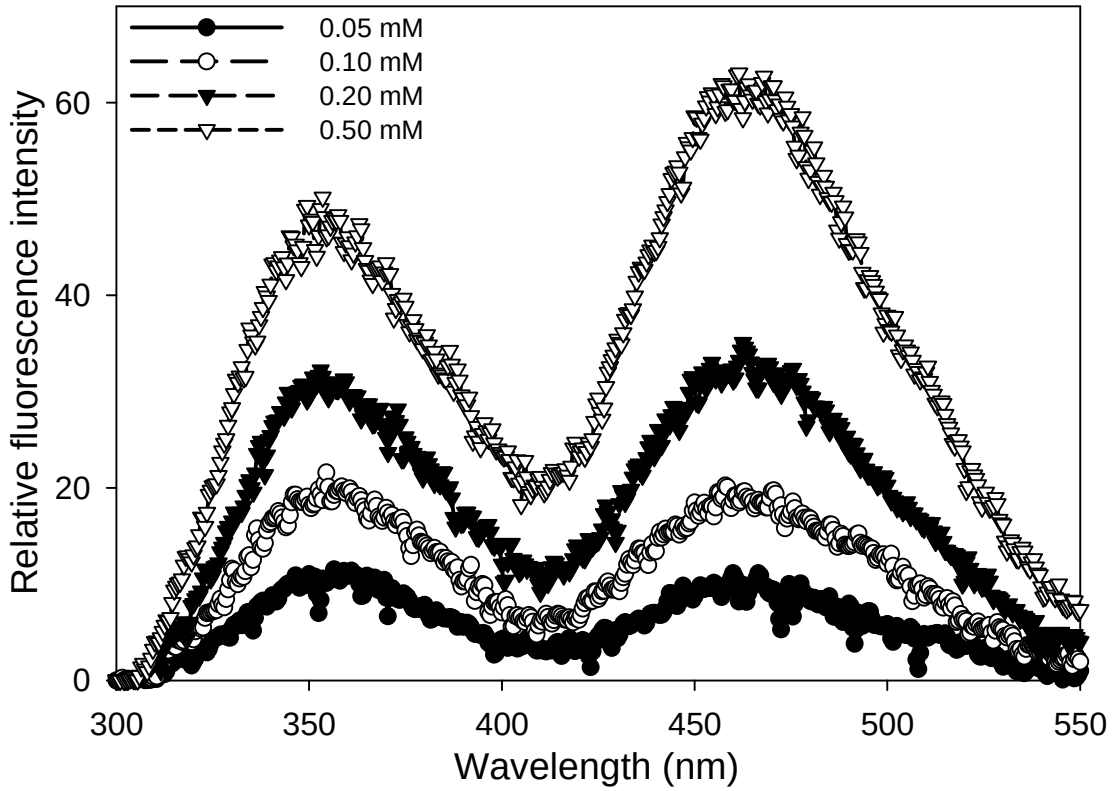

Figure III-3. Emission spectra of daptomycin aqueous solutions at pH 6.5 (cuvette path length 3 mm; excitation wavelength at 285 nm).

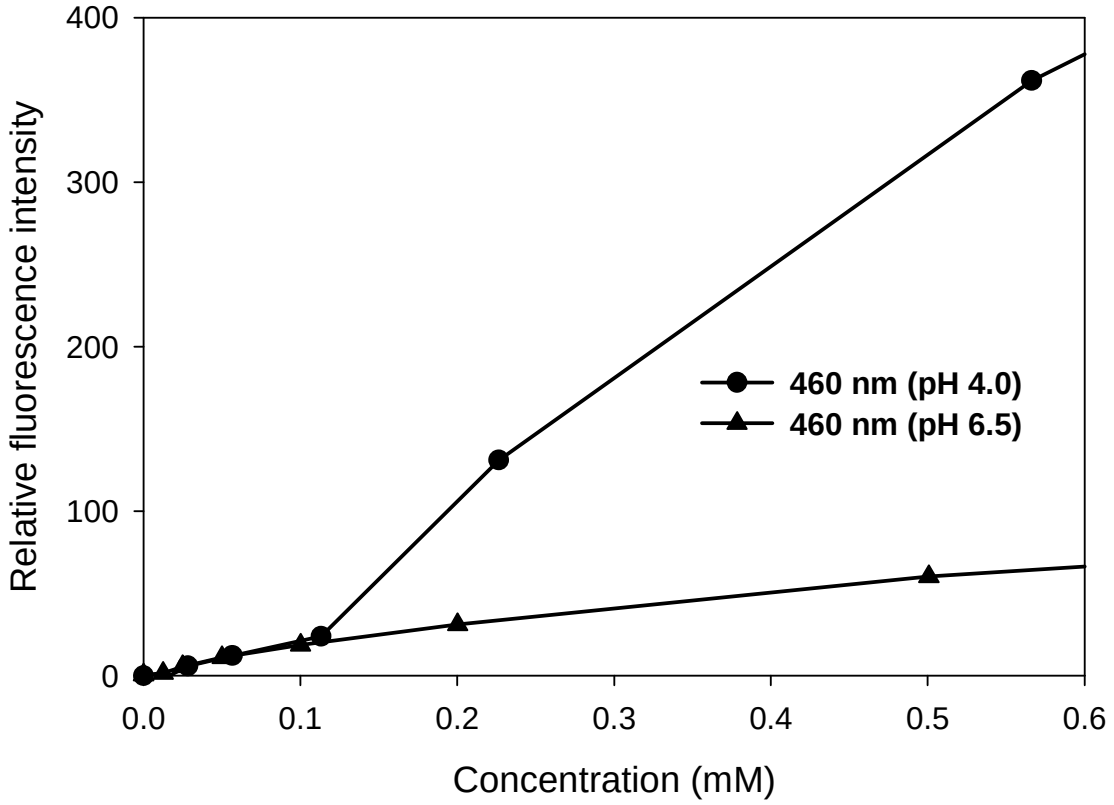

Figure III-4. Changes in the fluorescence intensities of the different daptomycin concentrations at pH 4.0 and 6.5. (cuvette path length 3 mm; excitation wavelength at 285 nm).

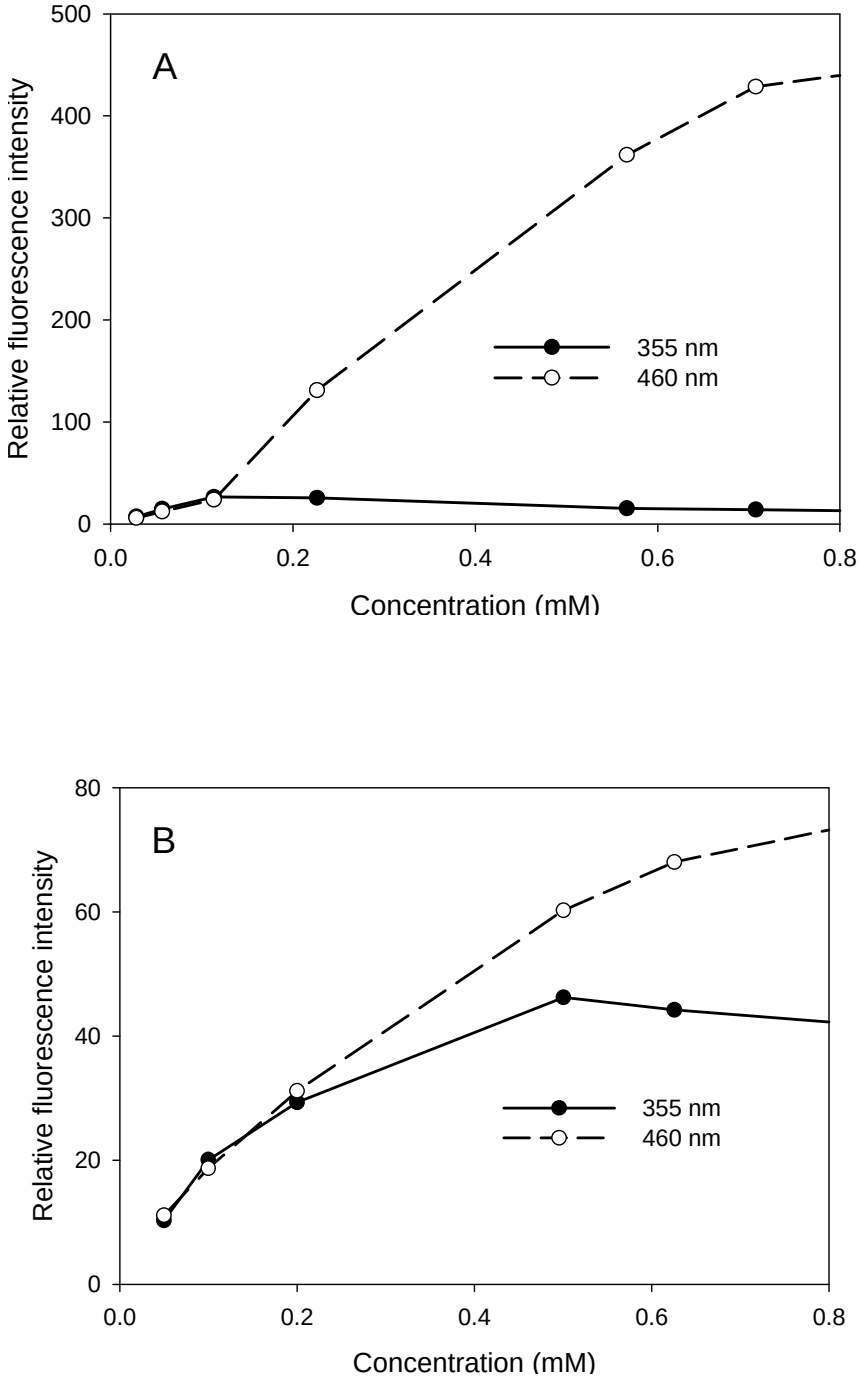

Figures III-5. Changes in the fluorescence intensities of the different daptomycin concentrations at pH 4.0 (A) and pH 6.5 (B). (cuvette path length 3 mm; excitation wavelength at 285 nm).

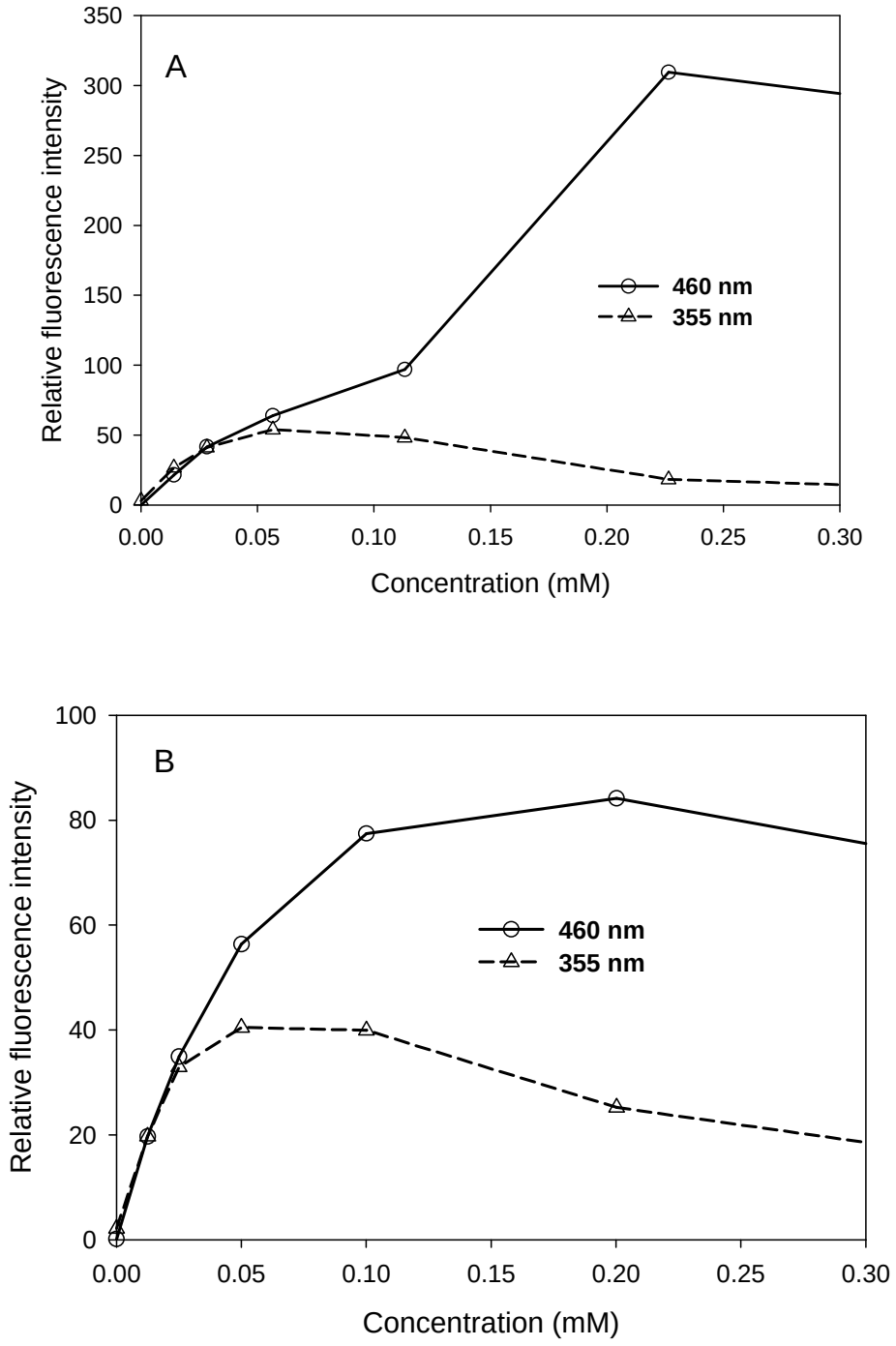

Figures III-6. Changes in the fluorescence intensities of the different daptomycin concentrations at pH 4.0 (A) and pH 6.5 (B). (cuvette path length 10 mm; excitation wavelength at 285 nm).

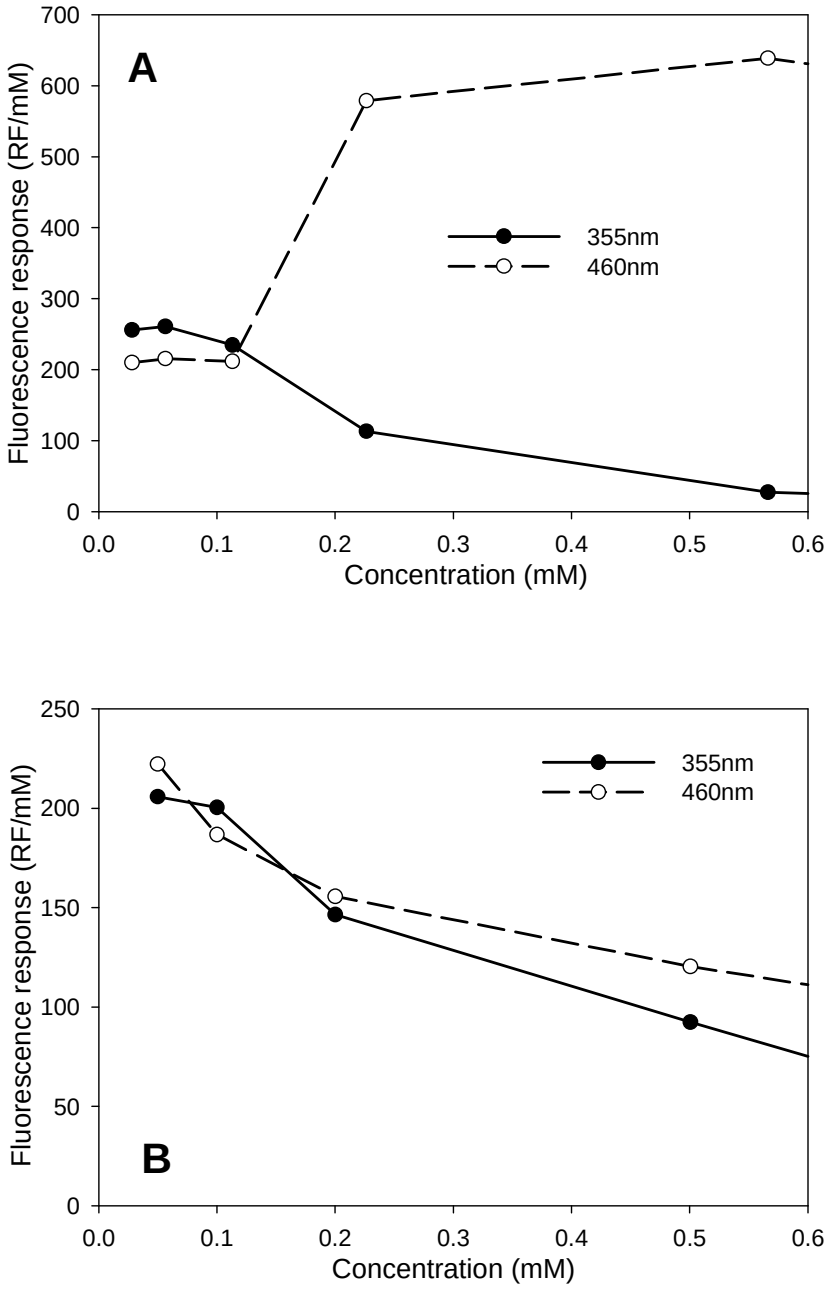

Figures III-7. Plots of fluorescence responses (the ratio of the fluorescence intensity to daptomycin concentration) at pH 4.0 (A) and pH 6.5 (B). (cuvette path length 3 mm; excitation wavelength at 285 nm).

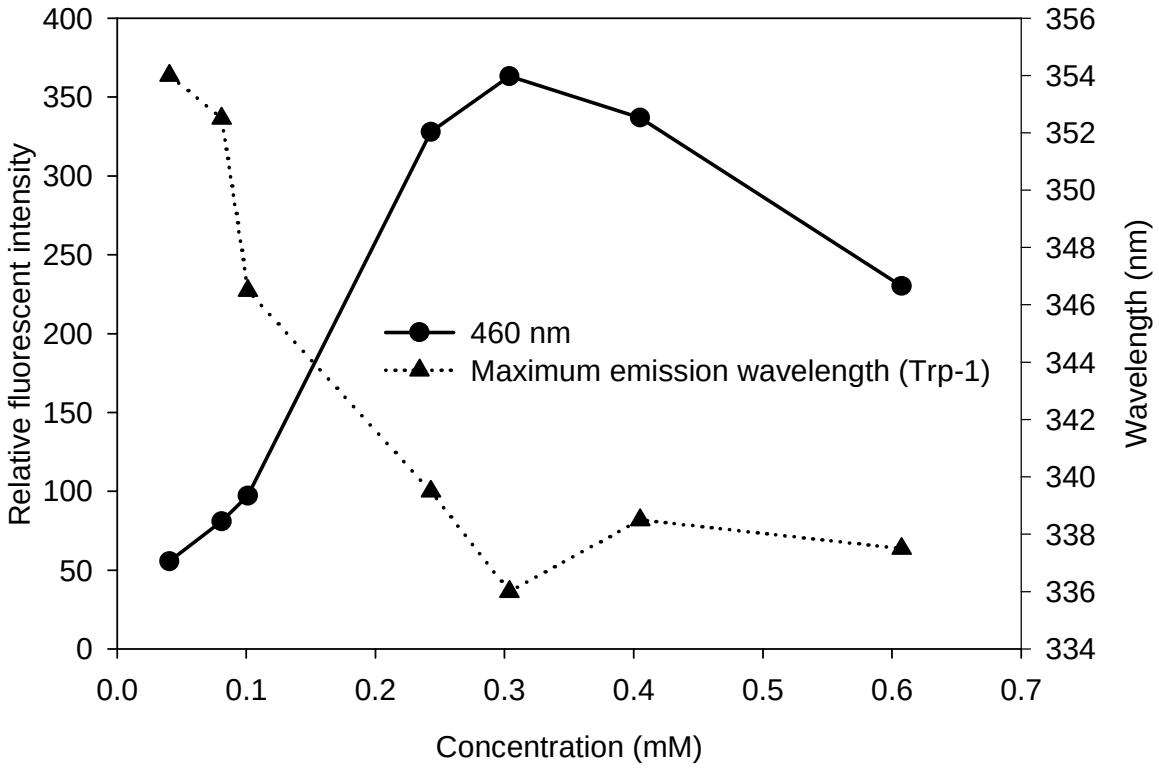

Figure III-8. Plots of emission intensities at 460 nm and maximum emission wavelength (300 – 375 nm) as a function of daptomycin concentration at pH 4.0. (cuvette path length 10 mm; excitation wavelength at 285 nm).

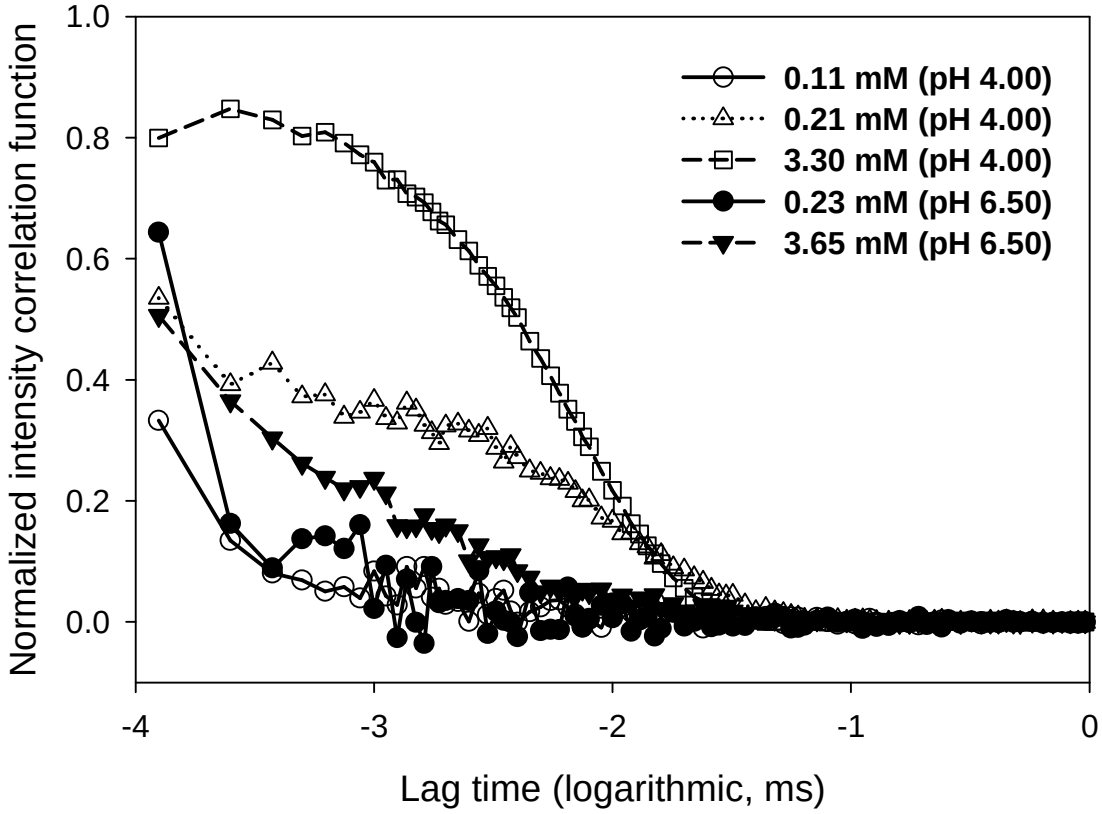

Figure III-9. Dynamic light scattering correlation functions of daptomycin at pH 4.0 and pH 6.5 solutions.

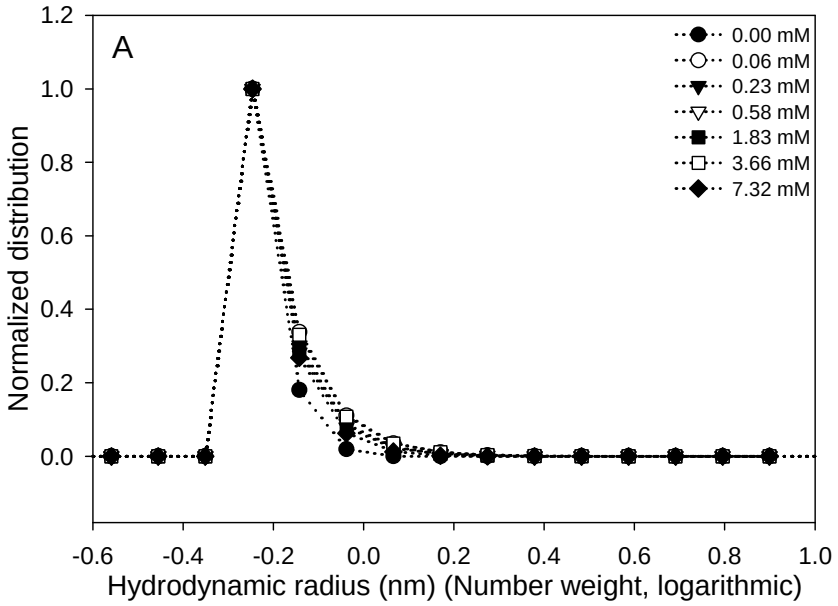

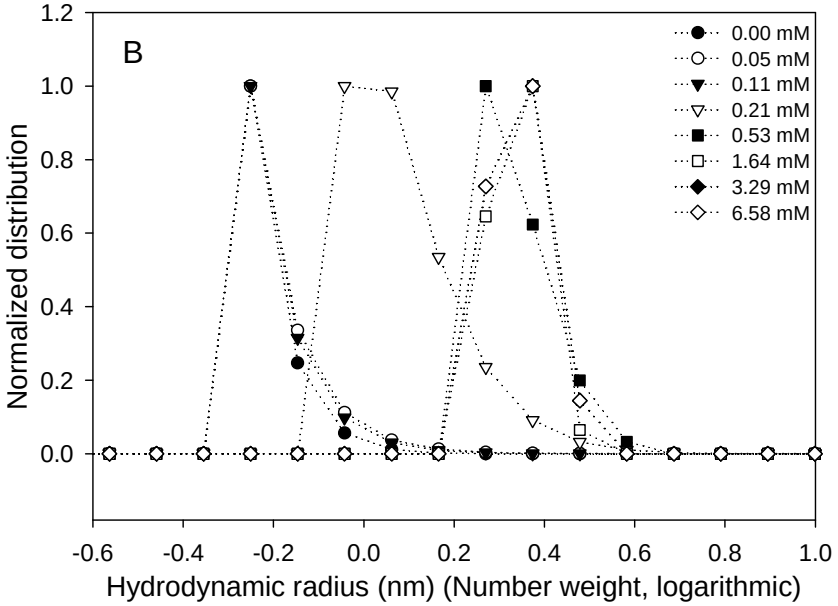

Figures III-10. Hydrodynamic radius distribution (logarithmic) of daptomycin solutions at pH 6.5 (A) and 4.0 (B).

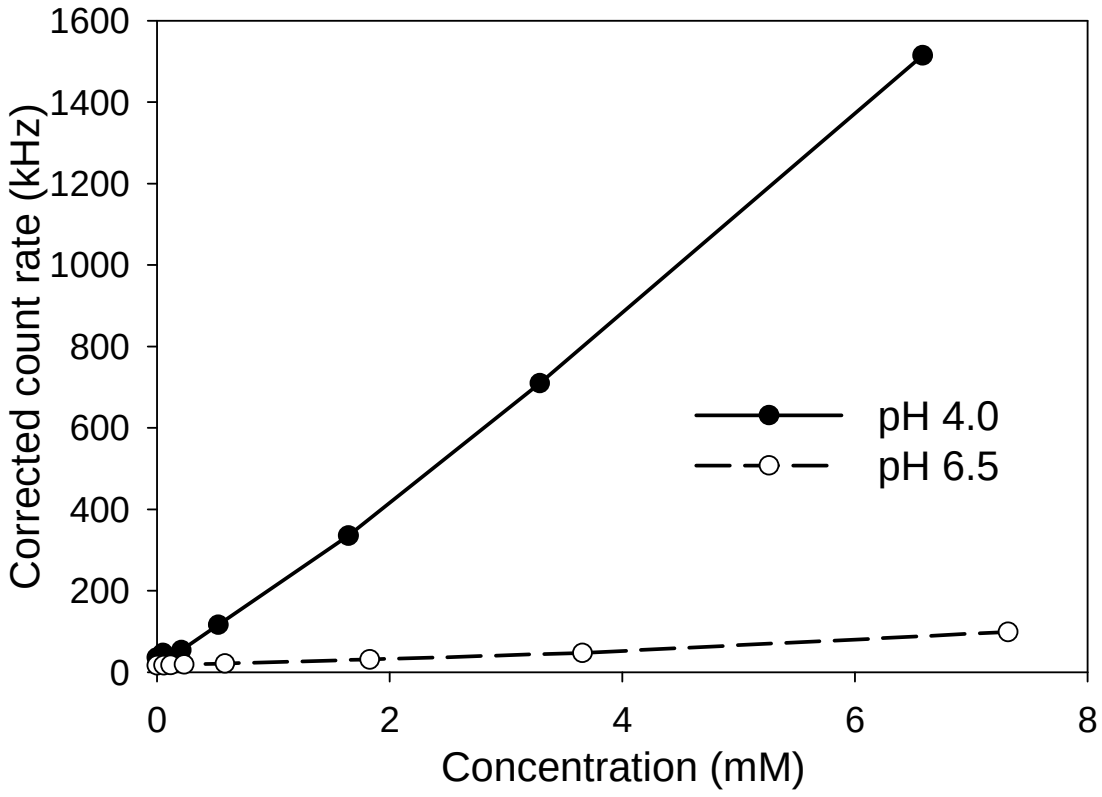

Figure III-11. Dynamic light scattering count rate plots of daptomycin solutions as a function of concentration at pH 4.0 and 6.5.

NMR Spectroscopy

The aggregation of daptomycin was further confirmed by analyzing the changes of the resonance linewidth and intensity of NMR spectra as a function of concentration. Illustrative NMR data at 21.21 mM are presented in Figure III-12 where daptomycin exists in the monomeric non-aggregated state at pH 6.5 as evidenced by the presence of sharp lines in the NMR spectrum. In 1D proton NMR spectra of daptomycin solutions at pH 4.0 (Figure III-13), the resonance linewidth broadened as the concentration of daptomycin solutions at pH 4.0 increased from 0.11 to 0.17 mM. The aromatic proton resonances of the residues Trp-1 and Kyn-13 between 6.50 to 7.70 ppm showed an increase in linewidth and a decrease in resonance intensities. The distinct proton resonance at 10.18 ppm of the N-H in the indole of the Trp-1 residue almost completely disappeared due to molecular aggregation.

Conclusions

The fluorescence approach for aggregation determination utilizes the fluorescent properties of either intrinsic or extrinsic probes,[49] which are affected by the polarity of their environments.[50,51] Below the CAC, fluorescent probes are mainly in an aqueous-like medium, where as above the CAC, they are exposed to less polar environment. Based on FRET from donor Trp-1 to acceptor Kyn-13, the aggregation and conformation of daptomycin was studied. The abrupt upward emission intensity inflection at 460 nm from Kyn-13 is due to the increase of the efficiency of FRET from Trp-1 to Kyn-13. The CAC of daptomycin at pH 4.0 was determined to be 0.12 mM by the upward inflection of the fluorescence emission at 460 nm as a function of daptomycin concentration. Above the CAC, a significant enhancement of fluorescence intensity at 460 nm from Kyn-13 occurred, while the emission intensity at 355 nm from Trp-1 decreased (Figure III-5A).

The emission spectrum of Trp-1 residue is highly sensitive to solvent polarity.[46] As daptomycin aggregates, the emission wavelength blue-shifted from Trp-1 was also observed due to its less polar environment.

The concentration-dependent aggregation of daptomycin solution at pH 4.0 was also observed from DLS data manifested as concentration dependent correlation function changes (Figure III-9). The hydrodynamic radius normalized distribution of daptomycin at pH 4.0 (Figure III-10B) shows daptomycin aggregates were observed at higher concentrations. At pH 6.5, no aggregates were detected in the daptomycin concentration ranges from 0.06 to 7.32 mM (Figure III-10A).

While the correlation function data are not suitable for complicated mathematical regression calculations at the lower concentration or smaller particles, the count rate values that measure the number of photons detected per second can be used for CAC measurement. Both the particle sizes and concentrations of species in samples affect the count rate values. The intensity of scattered light is proportional to the sixth power of the particle radius, so the effect of particle size is high as aggregation occurs. The inflection point of the count rate plot at pH 4.0 correlated with that observed for concentration-dependent fluorescence intensity. The plots of count rate versus daptomycin concentration (Figure III-11) demonstrated the presence and absence of aggregation at pH 4.0 and 6.5, respectively. The count rate is essentially a turbidity measurement, but the conventional UV/Vis/NIR spectrometers do not detect the subtle scattering intensity changes of daptomycin solutions.

A similar CAC value at pH 4.0 was also identified from NMR spectra. The considerable resonance intensity decrease of daptomycin NMR spectra from 0.11 to 0.17 mM at pH 4.0 is shown in Figure III-12. Daptomycin aggregation causes the peak intensity decrease and line broadening due to rapid transverse spin relaxation (i.e., rapid return from excited to ground state).[52] Combined with DLS and NMR techniques, the

CAC value at pH 4.0 has been successfully detected. The CAC obtained with fluorescence spectroscopy conforms to that using dynamic light scattering and NMR.

Ionization differences of daptomycin between pH 4.0 and 6.5 are expected to result in significant differences in aggregation behavior wherein the increased negative charge at higher pH results in electrostatic repulsion and no aggregation. CAC detection of daptomycin by an upward inflection of fluorescent emission at 460 nm, a broader NMR resonance linewidth, and DLS methods are in general agreement. The effects of factors such as concentration, pH, temperature, and calcium ion on daptomycin aggregation will be further discussed in Chapter IV.

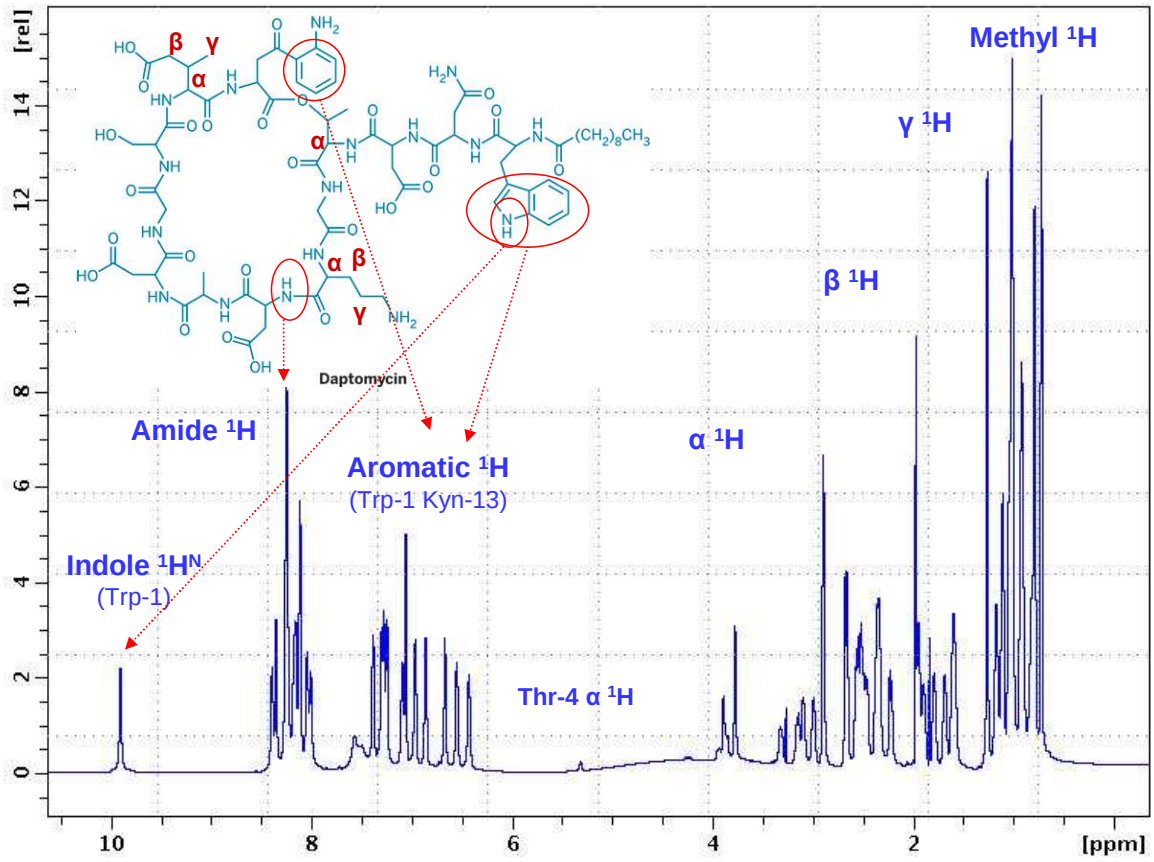

Figure III-12. 1D proton NMR spectrum of daptomycin solution at pH 6.5 at 21.21 mM.

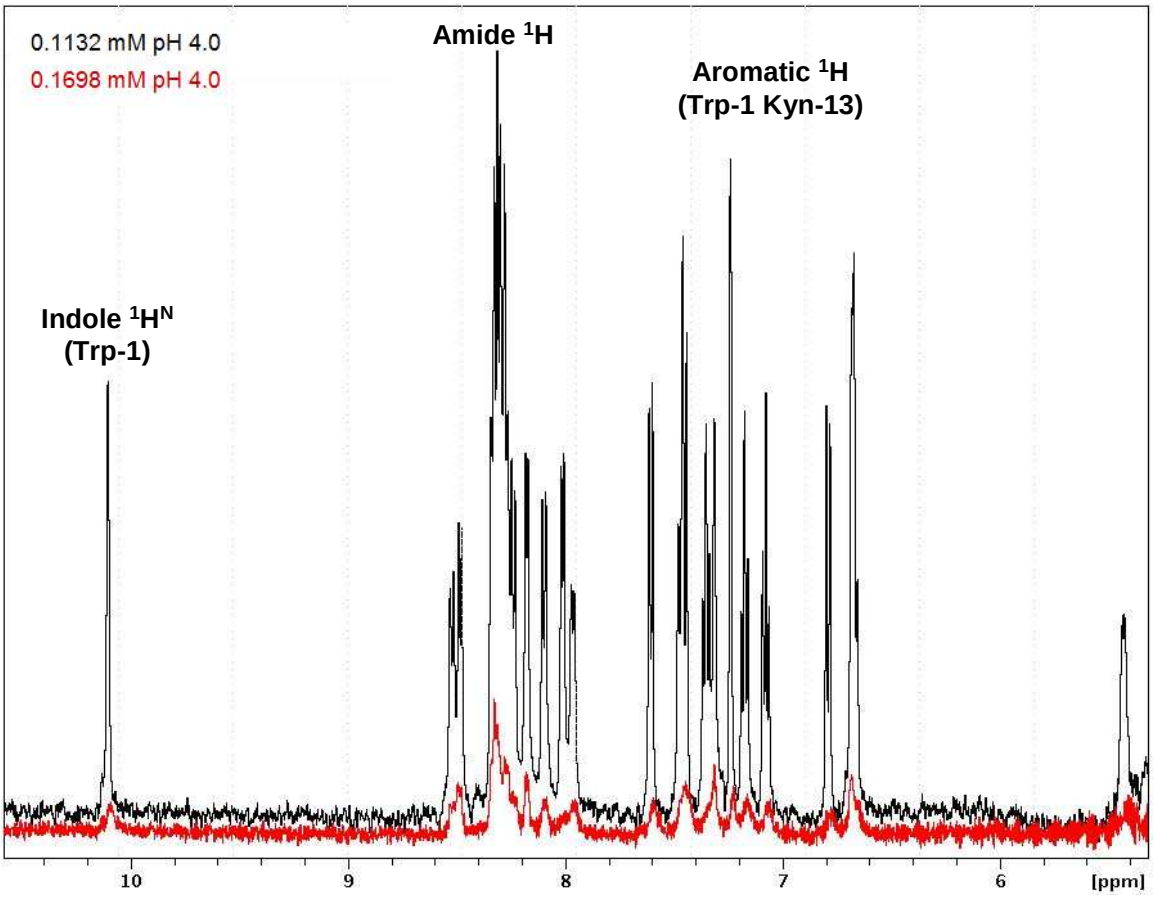

Figure III-13. 1D proton NMR spectra in aromatic region of daptomycin at pH 4.0 at two concentrations (0.11 and 0.17 mM).

CHAPTER IV EFFECTS SOLUTION COMPOSITION ON DAPTOMYCIN AGGREGATION

Introduction

In the previous chapter, an effective method for estimating CAC of daptomycin using FRET was presented. In this chapter, the effects of concentration, pH, temperature, and calcium ions on daptomycin aggregation will be presented using FRET, NMR spectroscopy, dynamic light scattering (DLS), and static light scattering (SLS).

In contrast to DLS which depends on fluctuations of the scattered light as a function of time, SLS measures the time-averaged fluctuations of scattered light intensity and provides a direct measure of absolute molecular weight and the 2nd virial coefficient (B_{22}). The 2nd viral coefficient (B_{22}) is related to the interaction strength between the particles and the solvent or appropriate dispersant medium.

The intensity of scattered light of macromolecules is dependent on concentration, size and shape of the molecule, and experimental conditions. When the particles in solution are much smaller than the wavelength of incident light (hydrodynamic radius less than $\lambda/20$), the intensity of the scattered light is uniform in all directions (Rayleigh scattering). To characterize the normalized intensity of the scattered light, the Rayleigh ratio (R_θ) is defined as:

$$R_\theta = r^2 I_\theta / I_0 = KcM$$

Where I_0 is the intensity of the incident light, I_θ is the total intensity of the scattered light (per unit scattering volume) measured at an angle θ at a distance r from the scattering volume by the detector, c is the concentration, and M is the molecular weight of the solute, K is the optical constant explained below. To obtain $I_{\theta,}$ the scattering intensity of the solvent has to be measured and subtracted from the scattering intensity of the solution to know the contribution of the particles/macromolecules. The intensity of scattered light is proportional to the product of the weight-average molecular weight and

the concentration of the particle. Thus by measuring the scattered intensity of a sample one can determine the average molecular weight. However, the concentration and the refractive index increment must be known with accuracy to measure the molecular weight accurately.

In the non-ideal polymer solutions, Rayleigh ratio (R_θ) is expressed as following equation:

$Kc/R_\theta = 1/M_w + 2B_{22}c$

where,

$K = 4\pi^2 n_0^2 (dn/dc)^2 / N_A \lambda^4$

C = the concentration of the scattering species

dn/dc = the differential refractive index increment (the specific refractive index, dn/dc), which is the change in refractive index as a function of the change in concentration.

N_A = Avogadro's number

λ = the wavelength of the incident laser light

n_0 = the refractive index of the solvent

R_θ = Rayleigh ratio at θ scattering angle

B_{22} = the second osmotic virial coefficient of the scattering solutes

By measuring the intensity of scattered light (Kc/R_θ) of various concentrations of sample at one angle and comparing with the scattering produced from a standard (i.e. toluene), a Debye plot of scattered light intensity (Kc/R_θ) versus concentration (c) can be obtained. The intercept will give the molecular weight (intercept = $1/M_w$), and the slope will give the second viral coefficient (slope = $2B_{22}$).[53,54]

The purpose of this research is to investigate the factors on daptomycin aggregation using the developed method.

Materials and Methods

Material

Daptomycin obtained from Eli Lilly Research Laboratories (Indianapolis, IN) was used as received. Sodium chloride, calcium chloride, 0.01 or 0.1 M sodium hydroxide solutions, 0.1 or 1 M hydrochloric acid solutions, toluene (HPLC grade), phosphate buffered saline (PBS) were purchased from Fisher Scientific (Fair Lawn, NJ). Deuterium oxide (100% D_2O) was purchased from Cambridge Isotope Laboratories (Cambridge, MA). Standardized pH buffers of 2, 4, 7, and 10 were obtained from Fisher Scientific (Fair Lawn, NJ). All other chemicals used were reagent grade from Fisher Scientific (Pittsburgh, PA).

Methods

Preparation of daptomycin solutions

Daptomycin aggregation behavior was studied in aqueous solutions in the pH range 2.5 to 6.5. The daptomycin concentration ranged from 0.00 to 21.21 mM. The pH values of daptomycin solutions were carefully controlled and measured before and after analytical measurements. The pH measurements were made at room temperature by using an Accumet Model 25 pH/Ion Meter and an Accumet 3 mm Ingold combination electrode with an AgCl reference (Fisher Scientific, Fair Lawn, NJ). The pH meter was calibrated with three certified standards pH 2, pH 4, and pH 7 (Fisher Scientific, Fair Lawn, NJ).

The temperature effect on daptomycin aggregation was performed in the concentration range from 0.06 to 3.11 mM at pH 4.0 aqueous solution. The samples in fluorescence quarts cuvette were thermostatted at 25 and 40 °C using circulating water with a Thermo Hakke C10-B3 Heating Circulator Bath (Thermo Hakke, Newington, NH).

The calcium ion effect on daptomycin aggregation was carried out in the daptomycin concentration range from 0.0026 to 0.26 mM at pH 7.4 and 6.5 in presence of calcium ion concentrations at 1.0 and 10 mM, respectively.

Dynamic light scattering

Dynamic light scattering experiments were conducted at 298 K with an ALV-NIBS High Performance Particle Sizer (Model No ALV-NIBS/HPPS, S/D: NIBS-20034, ALV-Laser Vertriebsgesellschaft m.b.H Langen, Germany). Scattered light intensity (He-Ne laser 632.8 nm) was detected at an angle of 173^0 with an ALV-5000/E multiple tau digital correlator. Prior to performing measurements, samples were filtered with a 0.2 μm filter membrane (Anotop Inorganic Membrane Filter, Whatman). The ALV Correlator setup was 3 runs each of 10 second duration. The CONTIIN algorithm was used to extract hydrodynamic radius and particle size distribution.

Static light scattering

Static light scattering experiments were conducted with the same ALV-NIBS/HPPS High Performance Particle Sizer as described in dynamic light scattering measurement. The scattering intensity of toluene with a known Rayleigh ratio and refraction index was first measured as a standard.

The differential refractive index increments (the specific refractive index, dn/dc) of daptomycin solutions at pH 4.0 and 6.5 were measured by using an ABBE refractometer (Bellingham & Stanley, Ltd.) at 25 ^{0}C circulated with a water bath (Fisher Scientific). A laser light source with the same wavelength (632.8 nm) as the light scattering instrument was used.

Fluorescence spectroscopy

Fluorescence spectra were recorded using a Perkin-Elmer LS55 luminescence spectrometer (Perkin Elmer Inc., Norwalk, CT) at room temperature. To measure the

emission intensities from both Trp-1 and Kyn-13, daptomycin solutions were excited at 285 nm, and the emission spectra were collected from 250 to 550 nm. The scan rate was set at 250 nm/minute. The excitation and emission slit widths were set to 4 and 3 nm, respectively. To reduce self-absorbing quenching effects in high concentration solutions, besides a 10 mm quartz cuvette, a 3 mm, or 1 mm path length quartz cuvette (Starna Cells, Inc. Atascadero, CA) was used based on the solution concentration.

NMR spectroscopy

1D homonuclear proton NMR spectra were collected with either a Bruker Avance II 500 MHz or 800 MHz US2 spectrometer in 90% H_2O/10% D_2O at daptomycin concentrations from 0.11 to 21 mM in the pH range of 2.5 to 6.5.

Results

Solvent pH Effects

With multiple ionizable groups, daptomycin aggregation is expected to be pH-dependent. The CAC values of daptomycin aqueous solutions in the range from 2.5 to 6.5 were first identified using fluorescence spectroscopy by the upward inflection points of fluorescence emission at 460 nm with increasing daptomycin concentration; then confirmed by dynamic light scattering, measuring the upward inflection points of count rate versus concentration and hydrodynamic radius; and by NMR spectroscopy, analyzing the changes of the resonance linewidth and intensity of NMR spectra.

The emission intensities at 355 and 460 nm of daptomycin solutions in pH 2.5 are shown in Figure IV-1. Below 0.20 mM, both emission intensities increased with daptomycin. Above 0.20 mM, the upward inflection point of emission intensity at 460 nm was observed, and the emission intensities at 355 nm decreased. There were linear relationships between daptomycin emission intensities at 460 nm and its concentrations below and above the inflection point CAC whereas the concentration quenching did not

occur. The inflection point of emission intensity at 460 nm was estimated by the intersection of the two lines drawn using data immediate above and below the apparent inflection. The linear regression equations with high R values between fluorescence intensity at 460 nm and daptomycin concentration are displayed in Figure IV-1, Y_1 = 2.6127 + 228.9449X, and R = 0.9998; Y_2 = -121.3470 + 834.9690X, and R = 0.9997; where, X is daptomycin concentration in mM, and Y_1 and Y_2 are the emission intensities at 460 nm below and above the inflection point, respectively. The upper inflection point or CAC value of daptomycin at pH 2.5 was estimated to be 0.20 mM from the intersection point of the two linear lines. Shown in Figure IV-2 are the count rate plot and the emission intensity at 460 nm versus daptomycin concentration in pH 2.50 aqueous solutions. The inflection point of the count rate versus daptomycin concentration also appeared at 0.20 mM. In Figure IV-3 displayed are the aromatic proton NMR spectra of daptomycin in pH 2.5 aqueous solutions at the concentrations of 0.20, 0.25, and 0.50 mM. As daptomycin concentration increased from 0.20 to 0.25 mM, the resonance intensity decreased, and linewidth became broader, (e.g. the chemical shift of proton at N-H in indole at 10.07 ppm).

The emission intensities at 355 and 460 nm of daptomycin in pH 3.0 aqueous solutions are shown in Figure IV-4. The upward inflection point of the emission intensity at 460 nm was identified to be > 0.12 mM. Similarly as described the estimation of daptomycin CAC value at pH 2.5, the CAC value of daptomycin at pH 3.0 shown in Figure IV-4 was estimated to be 0.14 mM from the intersection point of the two lines, where Y_1 = -0.3249 + 229.1160X, and R = 0.9984; Y_2 = -127.3552 + 1107.2745X, and R = 0.9990; X is daptomycin concentration in mM, and Y_1 and Y_2 are the emission intensities at 460 nm below and above the inflection point, respectively. The variations of the normalized intensity of the correlation functions at the concentration < 0.31 mM are displayed in Figure IV-5. The mean hydrodynamic radii extracted based on number weight calculation from the correlation functions is shown in Figure IV-6. Daptomycin

hydrodynamic radius started increased with concentration above 0.18 mM. The hydrodynamic radius of daptomycin aggregates was estimated to be about 2 nm in pH 3.0 aqueous solutions. Shown in Figure IV-7 are the fluorescence intensity at 460 nm and the count rate as a function of daptomycin concentration in pH 3.0 aqueous solutions. The inflection point of fluorescence intensity at 460 nm matched that of the count rate plot.

Similarly, the emission intensity changes at 355 and 460 nm, the normalized intensity of the correlation functions, and the count rates and emission intensities at 460 nm as a function of daptomycin concentrations in pH 4.0 aqueous solutions are shown in Figure IV-8, IV-9, and IV-10, respectively. In Figure IV-8, the CAC value of daptomycin at pH 4.0 was estimated to be 0.12 mM from the intersection point of the two lines, where Y_1 = -0.5455 + 223.3124X, and R = 0.9953; Y_2 = -109.0445 + 1120.8506X, and R = 0.9989; X is daptomycin concentration in mM, and Y_1 and Y_2 are the emission intensities at 460 nm below and above the inflection point, respectively. The hydrodynamic radius of daptomycin aggregation based on number weight calculation from correlation functions in pH 4.0 solutions is about 2 – 3 nm. The inflection points from fluorescence intensity at 460 nm and count rate of daptomycin were similar.

Shown in Figure IV-11 are the emission intensities at 355 and 460 nm of daptomycin in pH 5.0 aqueous solutions. The CAC value of daptomycin at pH 5.0 was estimated to be 0.20 mM from the intersection point of the two lines, where Y_1 = 3.5684 + 225.0065X, and R = 0.9995; Y_2 = -75.4243 + 620.8618X, and R = 0.9999; X is daptomycin concentration in mM, and Y_1 and Y_2 are the emission intensities at 460 nm below and above the inflection point, respectively. The normalized intensity of correlation functions of daptomycin solutions in pH 5.0 are shown in IV-12. The intensities and patterns of the correlations functions were observed to be quite different above and below the critical concentration at 0.20 mM concentrations. In Figure IV-13, 1D aromatic protons NMR spectra of daptomycin in pH 5.0 aqueous solutions also demonstrated that the resonance linewidths became broader as the daptomycin

concentration above 0.25 and 0.50 mM. The hydrodynamic radius of daptomycin aggregation in pH 5.0 solutions is also about 2–4 nm which were calculated based on the number weight from the normalized intensity of correlation functions DLS data.

Daptomycin behaves differently in aqueous solutions wherein the pH value was > 5.0. At pH 5.5, the upward inflection point of the emission intensity at 460 nm shown in Figure IV-14 was not apparent. Up to 2.5 mM, 1D NMR spectra (Figure IV-15) of daptomycin in pH 5.5 solutions still showed sharp resonance peaks and the resonance intensities increased with daptomycin concentration. Daptomycin did not form detectable aggregates in solutions prepared at pH 5.5 and substrate concentration up to 2.5 mM.

Since the workable concentration range of the sensitive fluorescence spectroscopy is very low, to lessen the effects of concentration quenching, the smallest path length cuvette (1.5 mm) was used. Shown in Figure IV-16 are the emission intensities at 460 nm from Kyn-13 of daptomycin in both pH 4.0 and 6.5 solutions. The concentration induced quench was significantly reduced, and the emission intensities at 460 nm of daptomycin solutions were not drastically reduced up to 10 mM concentration.

To minimize the concentration-quenching effect, the shorter path length cuvettes (3 and 1.5 mm) were used to collect the fluorescence spectra of daptomycin in higher concentrations in pH 6.0 and 6.5 aqueous solutions.

The fluorescence intensities at 355 and 460 nm as a function of daptomycin concentration in pH 6.0 and 6.5 solutions using both 3 and 1.5 mm path length cuvettes are shown in Figure IV-17 and IV-18, respectively. In a 3 mm path length cuvette, both emission intensities from Trp-1 and Kyn-13 started decreasing as daptomycin concentration at 2 mM. In a 1.5 mm path length cuvette, up to 20 mM, the emission intensity from Kyn-13 increase with the decreasing of that from Trp-1. As the shortest path length cuvettes was used, the upward inflection points of the emission intensities at 460 nm were observed. The similar results were found as daptomycin in pH 6.0 and 6.5 solutions. The 1D NMR spectra of daptomycin in pH 6.0 (Figure IV-19) and 6.5 (Figure

IV-20) solutions also exhibited sharp proton resonance peaks. However, as the concentration increased from 10.6 to 21.2 mM in Figure IV-20, the chemical shifts in Trp-1 residue changed from 10.02 to 9.95 (N-H in indole ring) and from 7.9 to 7.7 (amide proton). The chemical shifts of the aliphatic protons away from the two aromatic residues remained unchanged over the same concentration range (Figure IV-20). The normalized intensities of the correlation functions of daptomycin in pH 6.50 aqueous solutions up to 10 mM are displayed in Figure IV-21. There was no significant lag time observed from the normalized intensity of correlation function in the range of daptomycin concentration between 0.53 to 10.56 mM in pH 6.5 solutions. The hydrodynamic radius based on the correlation functions (Figure IV-21) measured by DLS was below 1 nm or not detectable. In Figure IV-22, the count rates as a function of daptomycin concentration in pH 6.5 was almost a straight line, and the inflection point of the count rate plot was not found up to 10 mM.

In summary, the fluorescence intensities at 460 nm as a function of concentration in various pH aqueous solutions from pH 2.5 to 6.5 are shown in Figure IV-23. The CAC values of daptomycin the different pH solutions were investigated. Below pH 5.5, the upward inflection points of fluorescence intensities at 460 nm were identified. The CAC values of daptomycin were estimated to be 0.14 mM at pH 3.0, 0.12 mM at pH 4.0, and at 0.20 mM at pH 2.5 and 5.0. Above pH 5.5, the sensitive upward inflection points of emission intensity changes as a function of concentration at 460 nm from Kyn-13 were not distinctly found.

Static Light Scattering

The aggregation status of daptomycin in pH 4.0 and 6.5 aqueous solutions was also characterized by SLS. In Figure IV-24, the measured specific refractive index (dn/dC) values of daptomycin aqueous solutions in pH 4.0 and pH 6.5 are 0.1842 and 0.1906, respectively. Listed in Table IV-1 are the measured average molecular weights

and the calculated aggregation numbers of daptomycin based on the molecular weight 1620.67 at the concentrations 1.50, 3.75, 6.30, and 12.70 mM in pH 4.0 and 6.5 solutions. The aggregation numbers of daptomycin were estimated between 16 to 20 in pH 4.0 and around 1 in pH 6.5 from 1.50 to 12.7 mM concentration range, respectively. These SLS results confirmed the aggregation of daptomycin was formed in pH 4.0 solutions, but not detected in higher pH solutions, e.g. pH 6.5. In the concentration range between 1.50 to 12.70 mM shown in Table IV-1, daptomycin was in monomeric state in pH 6.5, but in multimeric state in pH 4.0.

Effect of Temperature

The temperature effect on daptomycin aggregation was investigated using fluorescence spectroscopy. Figure IV-25 shows the plots of fluorescence intensities of daptomycin in pH 4.0 aqueous solutions at 25°C and 40°C. From the inflection points of the emission intensity at 460 nm, the CAC values of daptomycin aqueous solutions in pH 4.0 at 25°C and 40°C were identified to be 0.12 mM and 0.27 mM, respectively. The emission intensities at 460 nm from Kyn-13 above CAC at 25°C were much stronger than those at 40°C, while there were no differences of the emission intensities at 355 nm from Trp-1.

Effect of Calcium Ions

Calcium ions are known to neutralize the negative charges of daptomycin and induce daptomycin aggregation.[13,14] Due to the fluorescence energy transfer between the Trp-1 and Kyn-13, the fluorescence emission patterns of daptomycin at 355 and 460 nm are closely related with pH, daptomycin concentration, and calcium ion concentrations. The fluorescence properties of daptomycin induced by calcium ions were investigated in pH 7.4 and 6.5 solutions. In the absence of calcium ions, the CAC values of daptomycin in pH 6.5 solutions were not observed using any of the methods described including fluorescence, dynamic light scattering, and NMR. In 1.0 mM calcium ions phosphate

buffer (pH 7.4) solutions, the fluorescence spectra of daptomycin are shown in Figure IV-26. As daptomycin concentrations increased from 0.011 to 0.026 mM, the fluorescence spectral patterns were not changed, and both emission intensities at 355 nm and 460 nm increased with daptomycin concentration. However, the fluorescence spectral patterns were noticeably changed at the very low concentration range between 0.065 to 0.157 mM, the enhancement of the emission intensity from Kyn-13 along with the decrease of the emission from Trp-1. The emission intensities at both 355 and 460 nm are plotted in Figure IV-27. The upward inflection point of the emission at 460 was not observed. However, the increase of the emission intensity at 460 nm from Kyn-13 corresponded with the decrease in the emission intensity at 355 from Trp-1.

In 10.0 mM calcium ion pH 6.5 solutions, the fluorescence spectra of daptomycin are displayed in Figure IV-28. Similarly, at lower concentration ranges (e.g., 0.25 and 0.50 mM), the spectral pattern were not changed. At higher concentrations (e.g., 1.01 and 2.02 mM), the spectral patterns were manifestly altered, and the emission intensity at 460 nm increased greatly. Shown in Figure IV-29 are the fluorescence intensities of daptomycin in pH 6.5 solutions in the absence calcium ions and in 10.0 mM calcium ions solutions. In 10.0 mM calcium ions pH 6.5 solutions, and at daptomycin concentration > 0.50 mM, the emission intensities from Kyn-13 greatly increased as those from Trp-1 decreased. These changes were not observed in the absence of calcium ions.

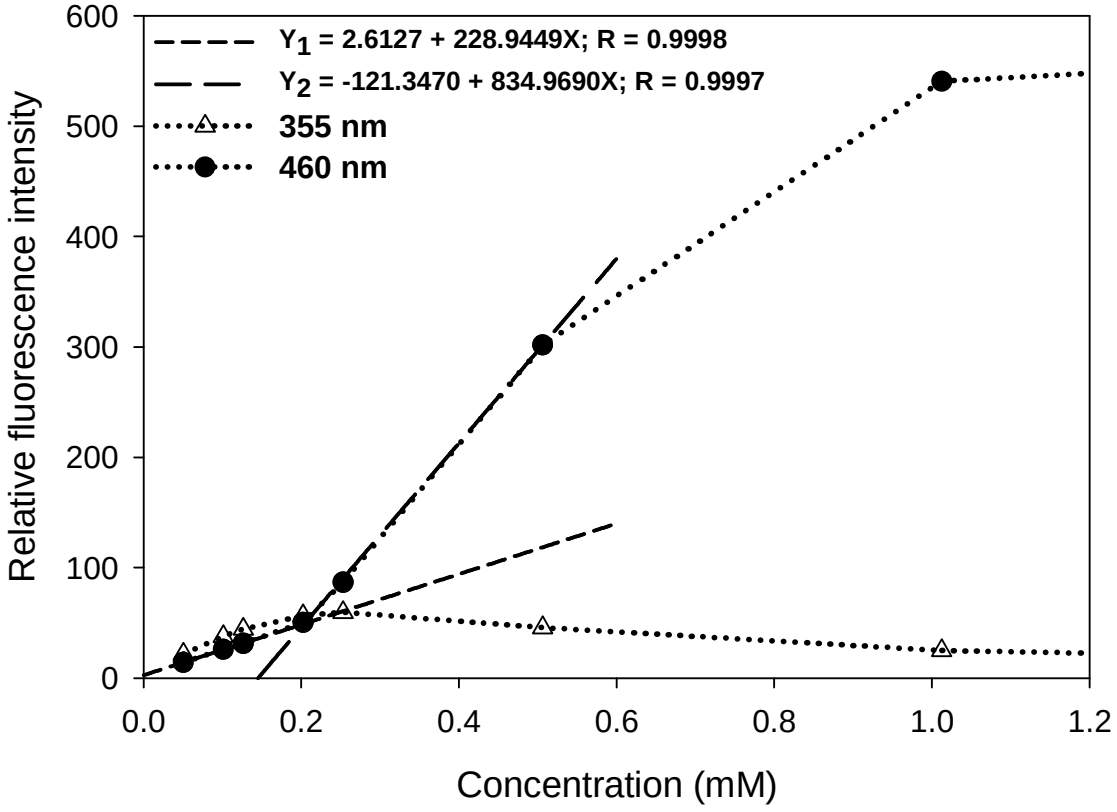

Figure IV-1. Plots of fluorescence intensities at 355 and 460 nm as a function of daptomycin concentration in pH 2.5 aqueous solutions. (cuvette path length 3 mm; excitation wavelength at 285 nm). The estimated CAC value of daptomycin in pH 2.5 aqueous solution was 0.20 mM.

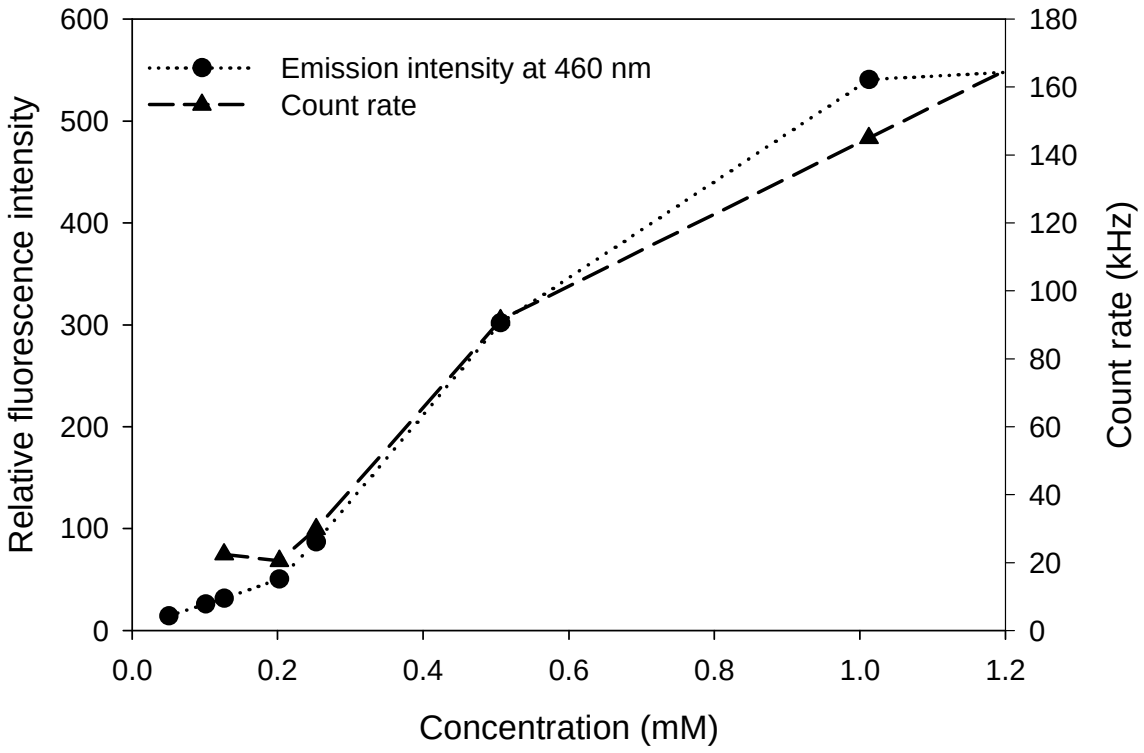

Figure IV-2. Plots of fluorescence intensity at 460 nm and count rate as a function of daptomycin concentration in pH 2.5 aqueous solutions.

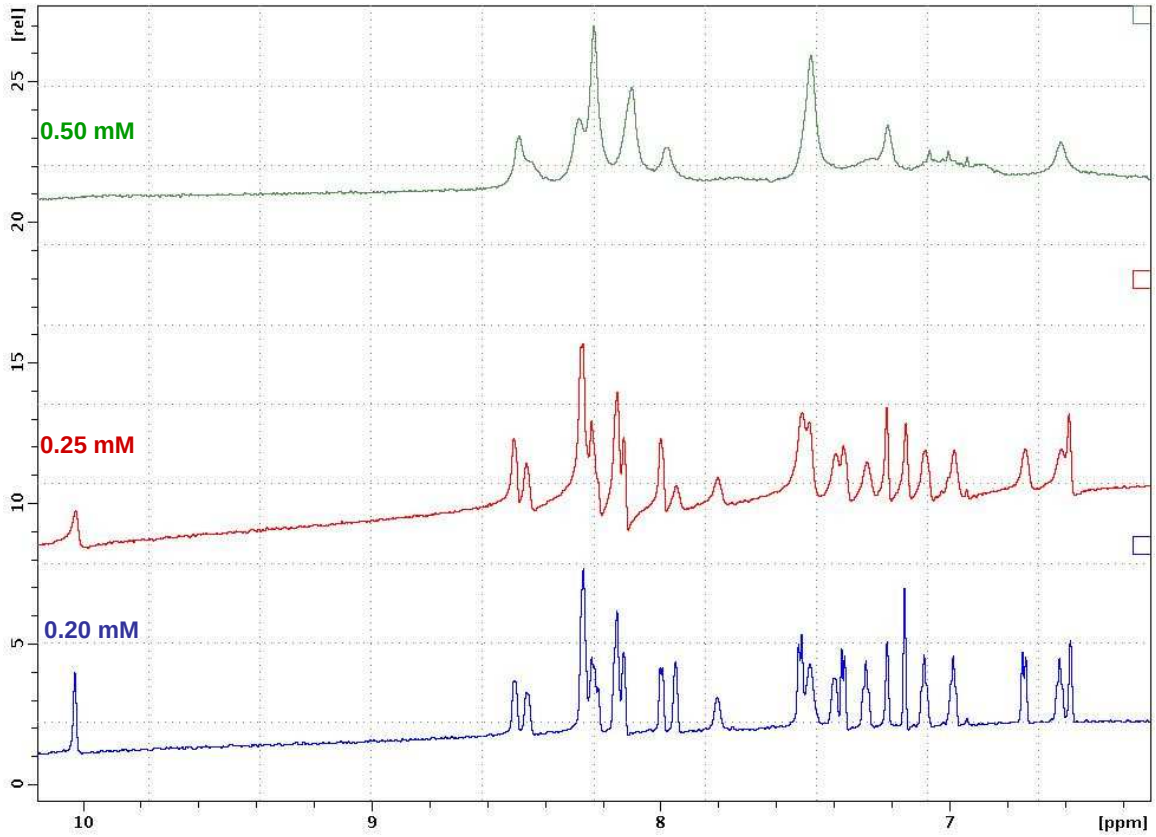

Figure IV-3. 1D proton NMR spectra in aromatic region of daptomycin in pH 2.5 solutions at three concentrations (0.20, 0.25, and 0.50 mM).

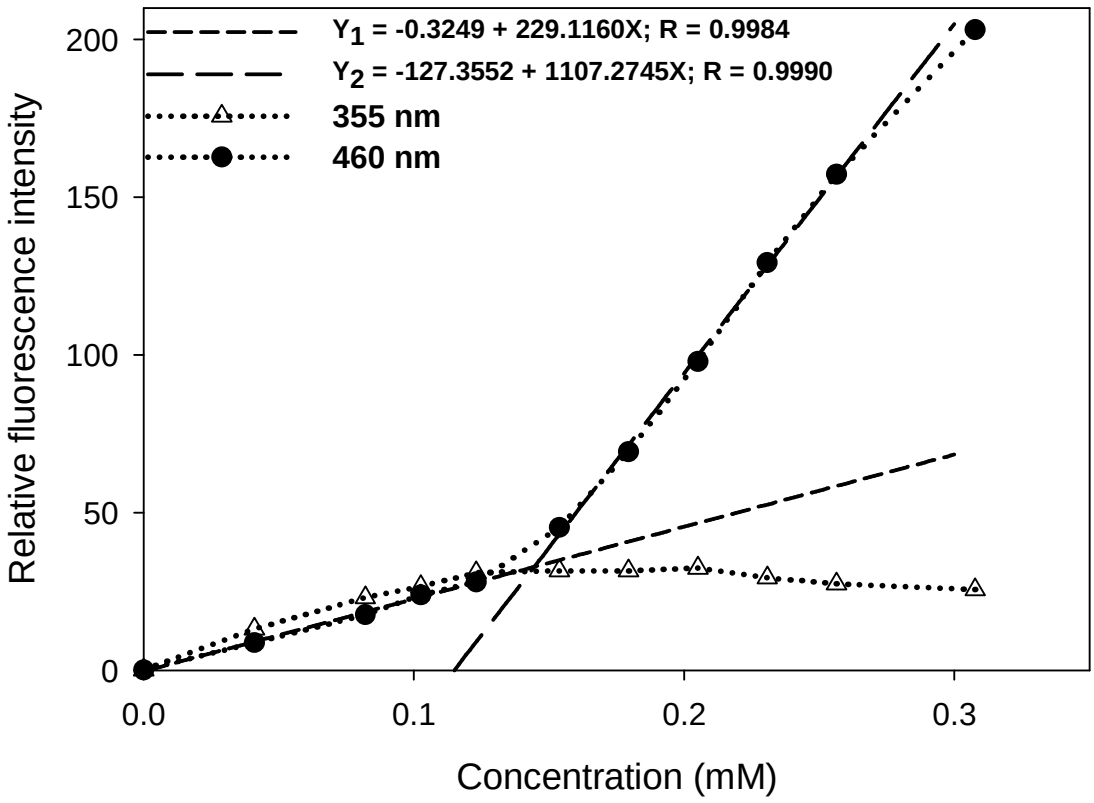

Figure IV-4. Plots of fluorescence intensity at 355 and 460 nm as a function of daptomycin concentration in pH 3.0 aqueous solutions. (cuvette path length 3 mm; excitation wavelength at 285 nm). The estimated CAC value of daptomycin in pH 3.0 aqueous solution was 0.14 mM.

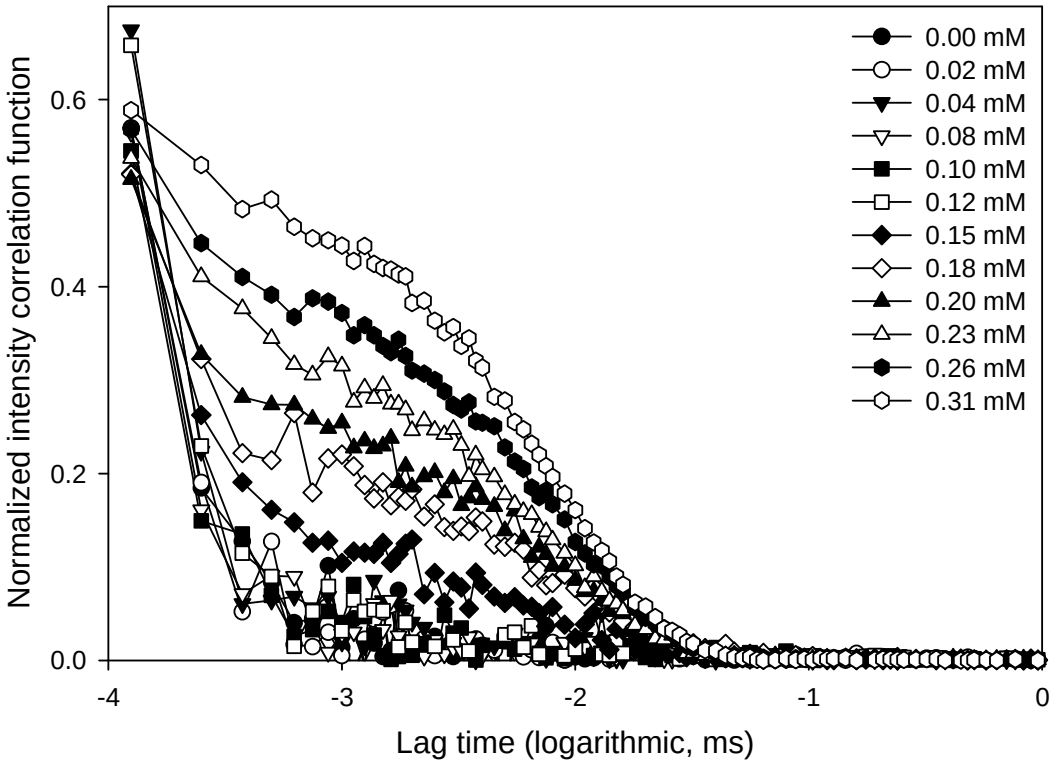

Figure IV-5. Dynamic light scattering correlation functions of daptomycin in pH 3.0 aqueous solutions.

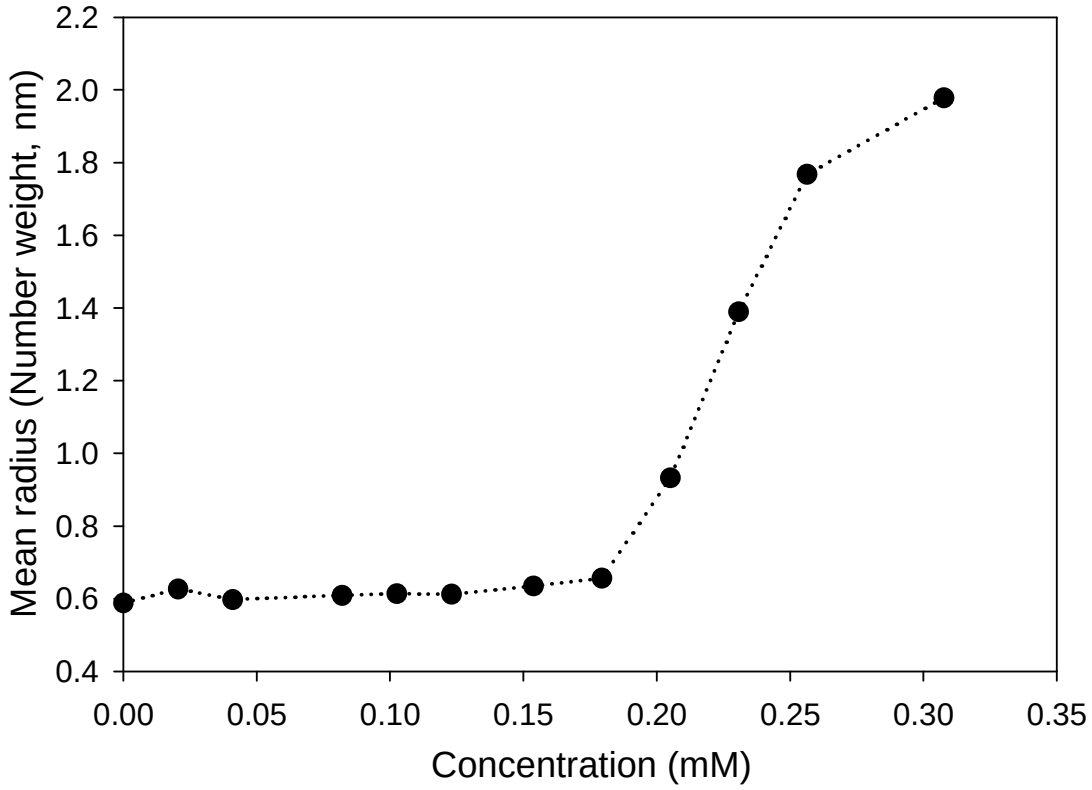

Figure IV-6. Mean hydrodynamic radius (number weight) of daptomycin in pH 3.0 aqueous solutions.

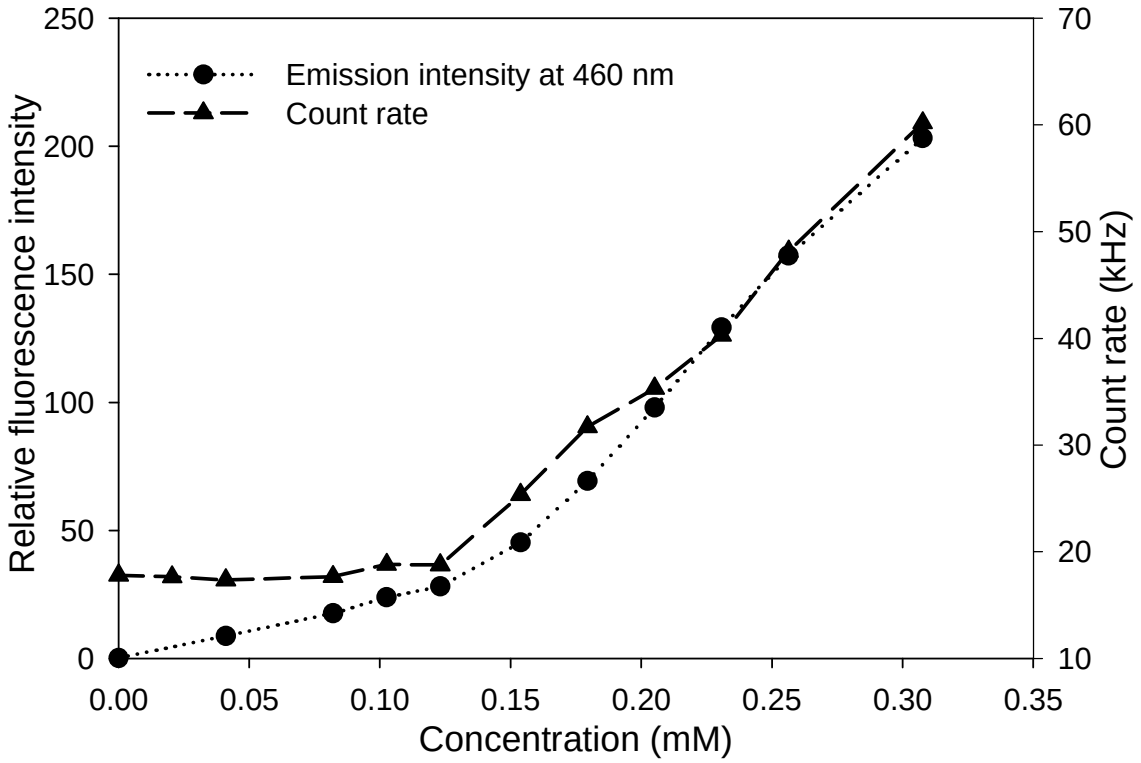

Figure IV-7. Plots of fluorescence intensity at 460 nm and count rate as a function of daptomycin concentration in pH 3.0 aqueous solutions.

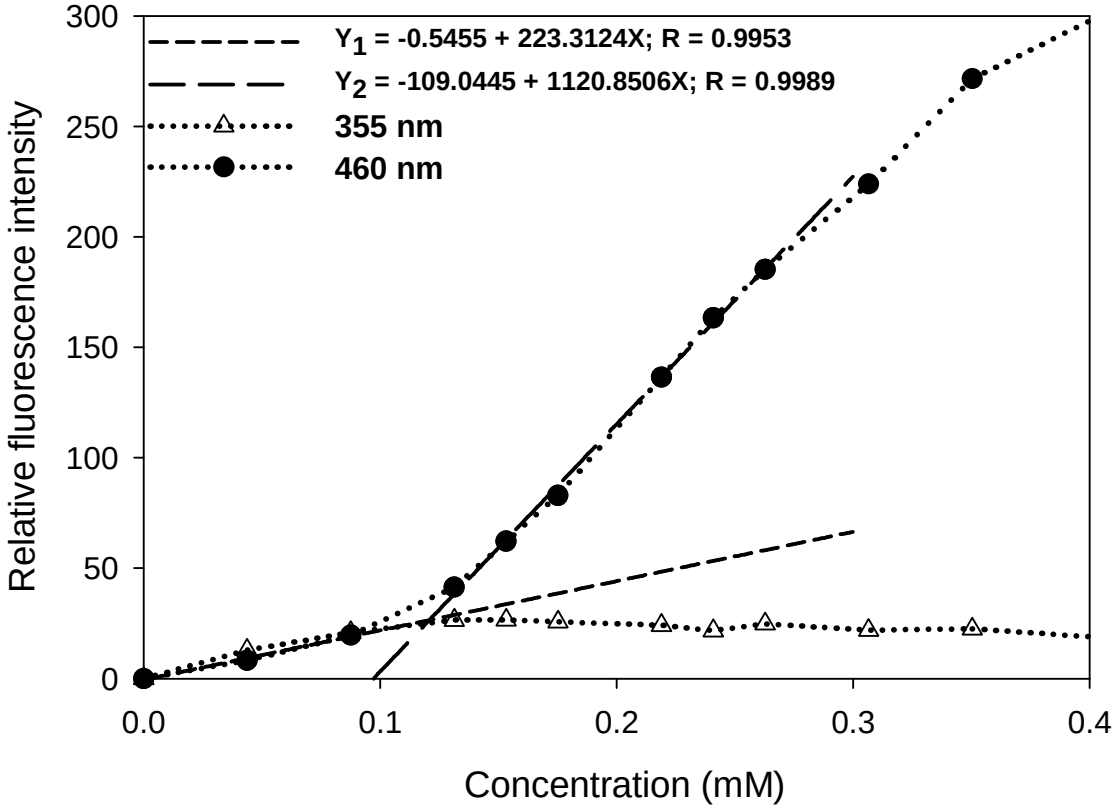

Figure IV-8. Plots of fluorescence intensities at 355 and 460 nm as a function of daptomycin concentration in pH 4.0 aqueous solutions. (cuvette path length 3 mm; excitation wavelength at 285 nm). The estimated CAC value of daptomycin in pH 4.0 aqueous solution was 0.12 mM.

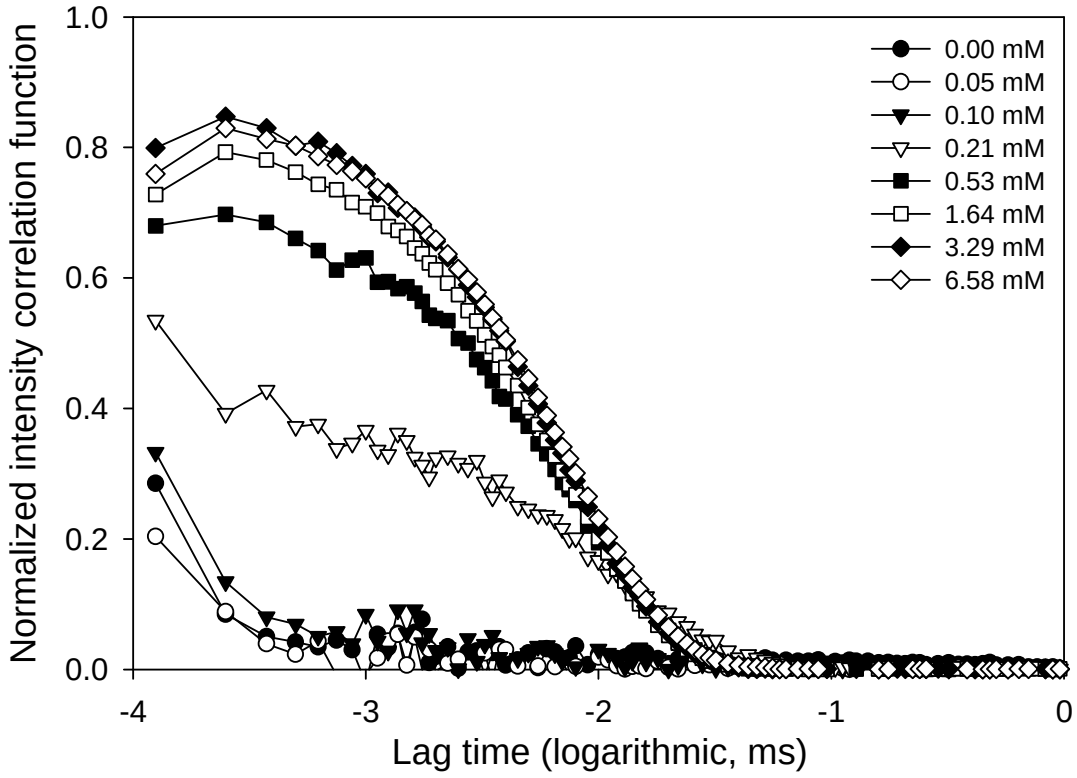

Figure IV-9. Dynamic light scattering correlation functions of daptomycin in pH 4.0 aqueous solutions.

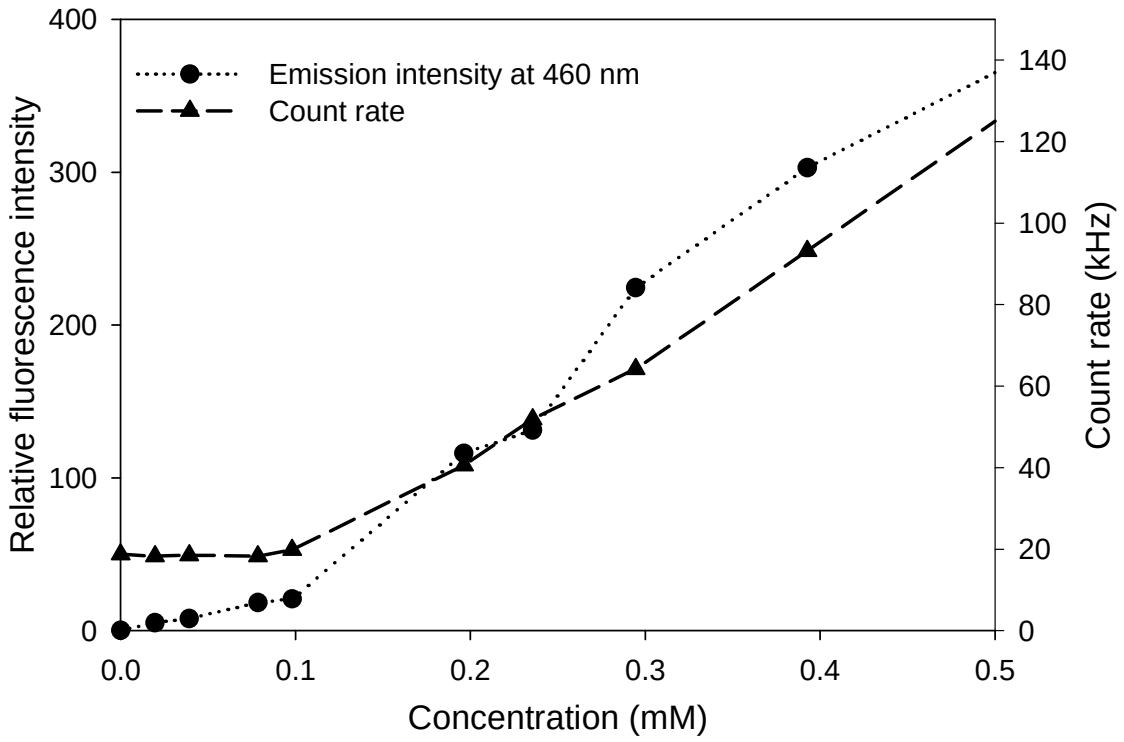

Figure IV-10. Plots of fluorescence intensity and count rate as a function of daptomycin concentration in pH 4.0 aqueous solutions.

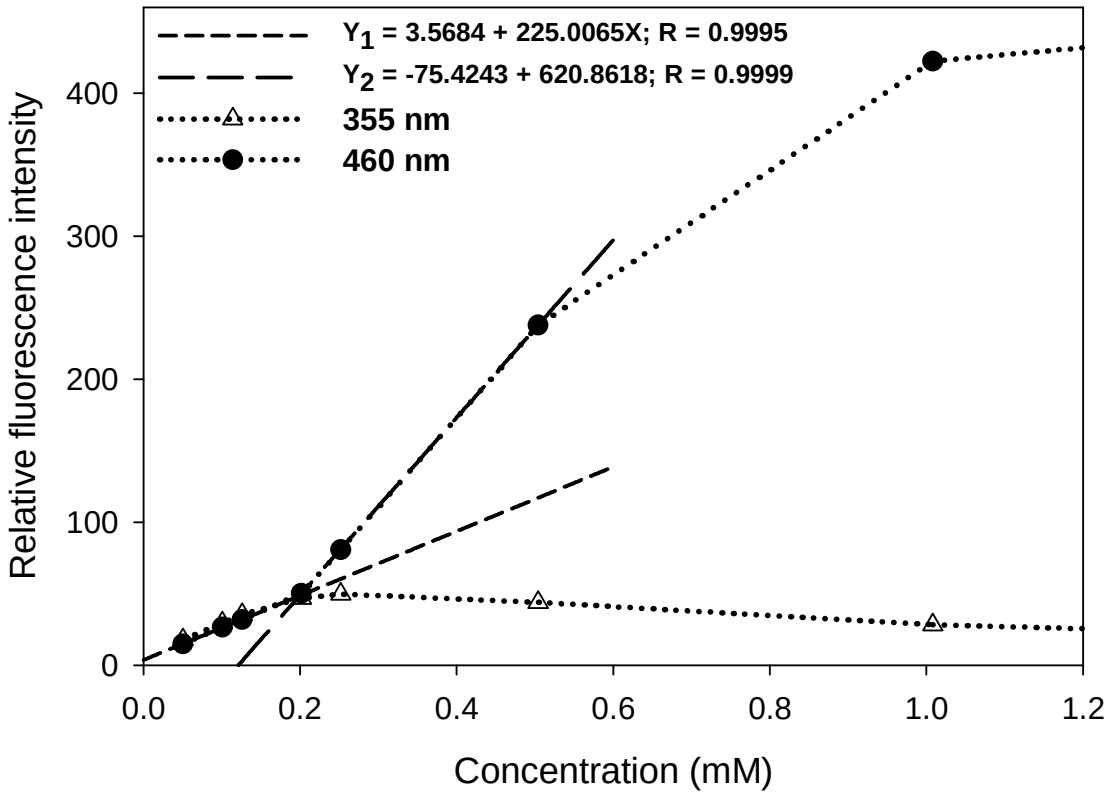

Figure IV-11. Plots of fluorescence intensities at 355 and 460 nm as a function of daptomycin concentration in pH 5.0 aqueous solutions. (cuvette path length 3 mm; excitation wavelength at 285 nm). The estimated CAC value of daptomycin in pH 5.0 aqueous solution was 0.20 mM.

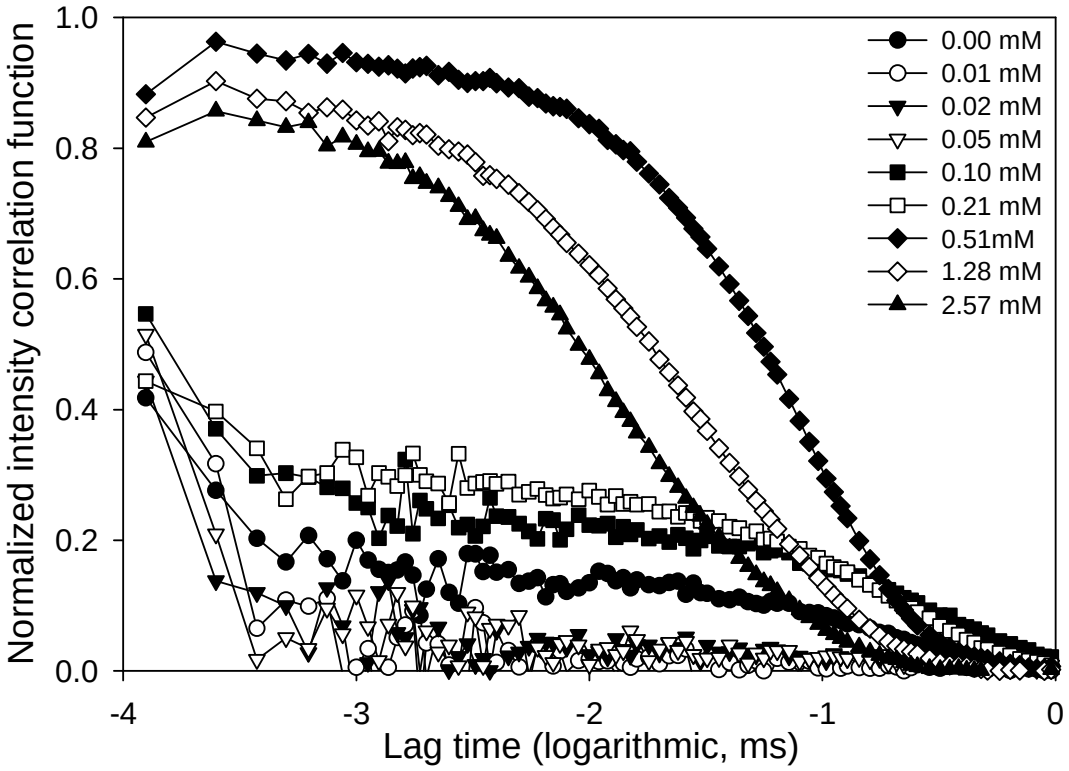

Figure IV-12. Dynamic light scattering correlation functions of daptomycin in pH 5.0 aqueous solutions.

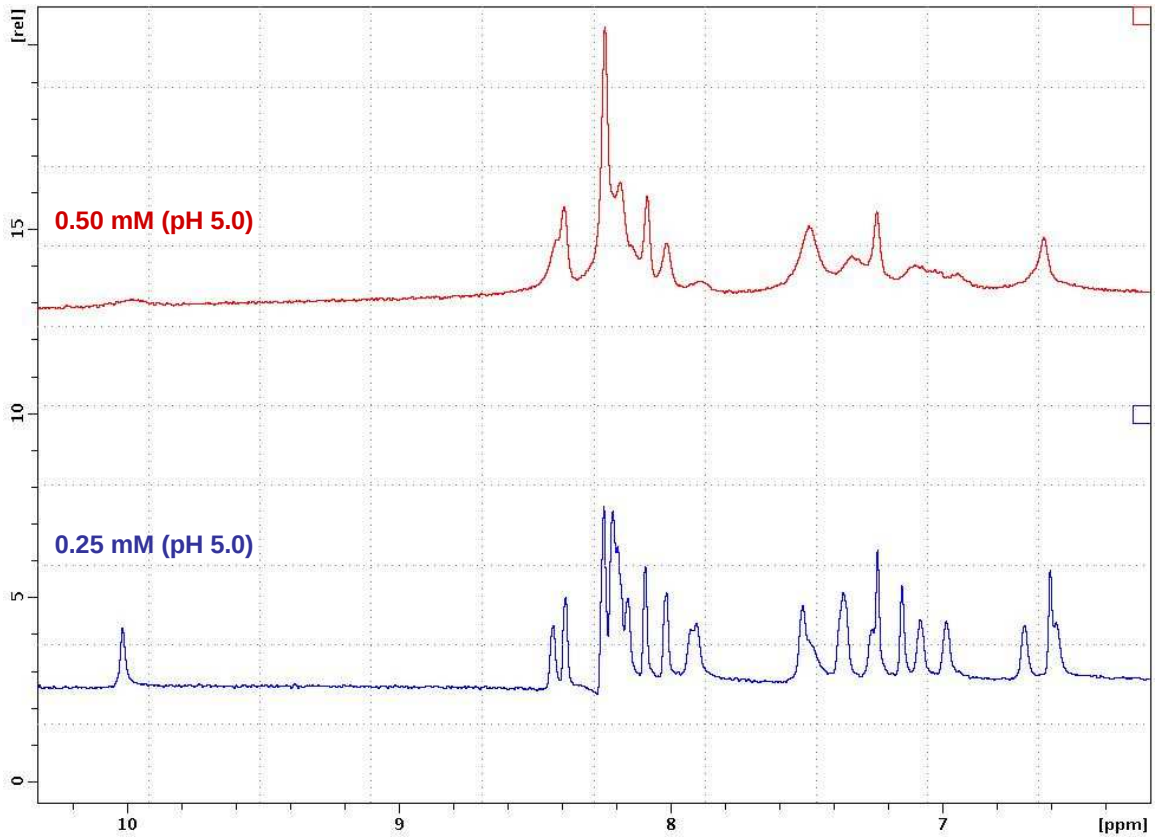

Figure IV-13. 1D proton NMR spectra in aromatic region of daptomycin in pH 5.0 at two concentrations (0.25 and 0.50 mM).

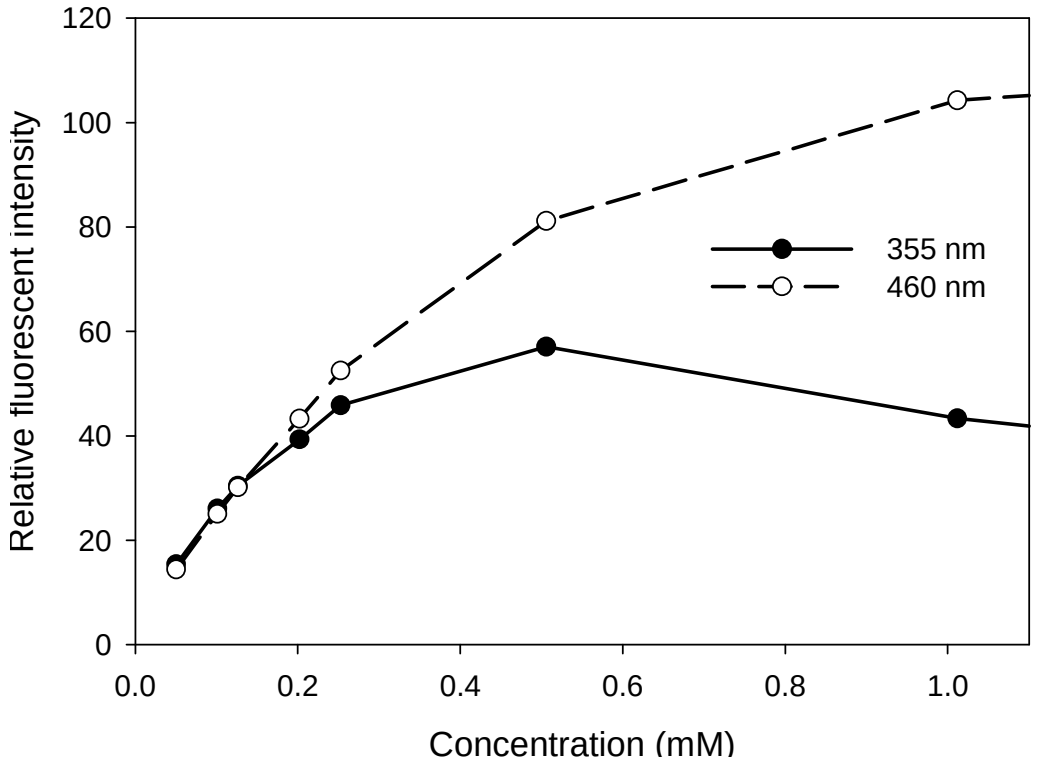

Figure IV-14. Plots of fluorescence intensities at 355 and 460 nm as a function of daptomycin concentration in pH 5.5 aqueous solutions. (cuvette path length 3 mm; excitation wavelength at 285 nm).

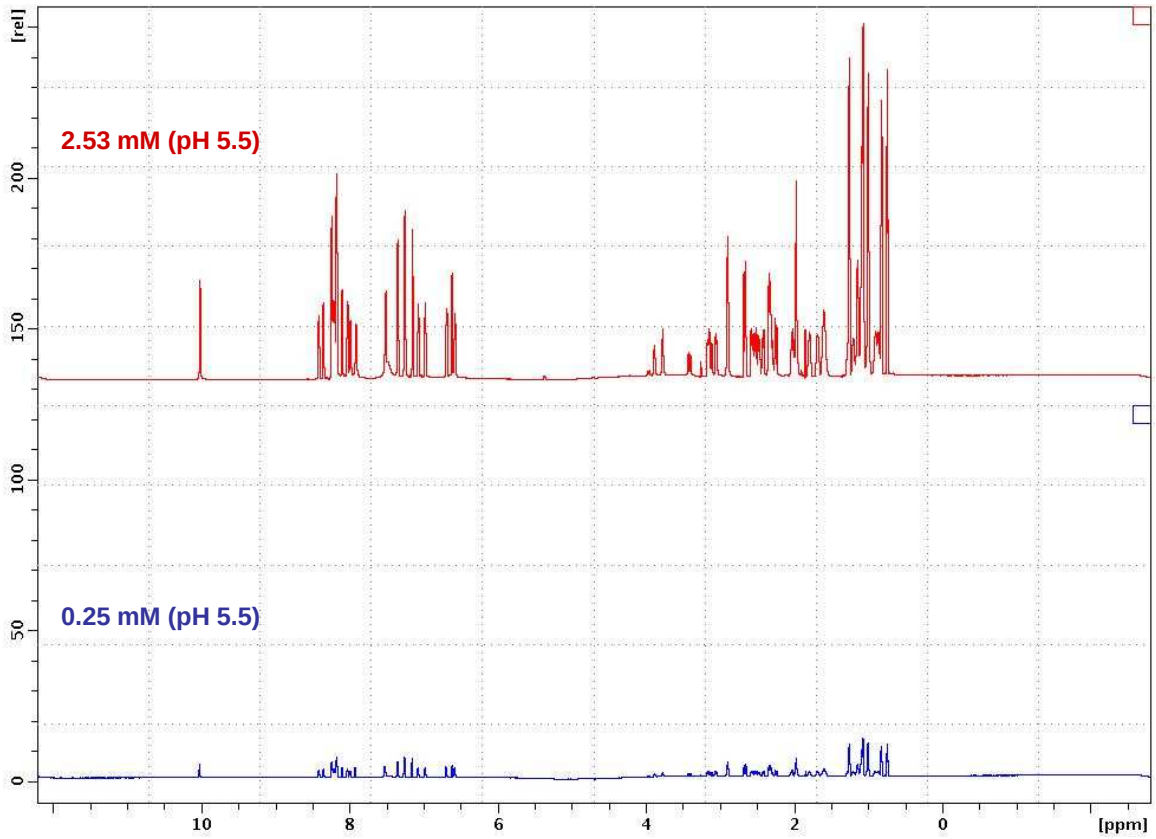

Figure IV-15. 1D proton NMR spectra of daptomycin in pH 5.5 at two concentrations (0.25 and 2.53 mM).

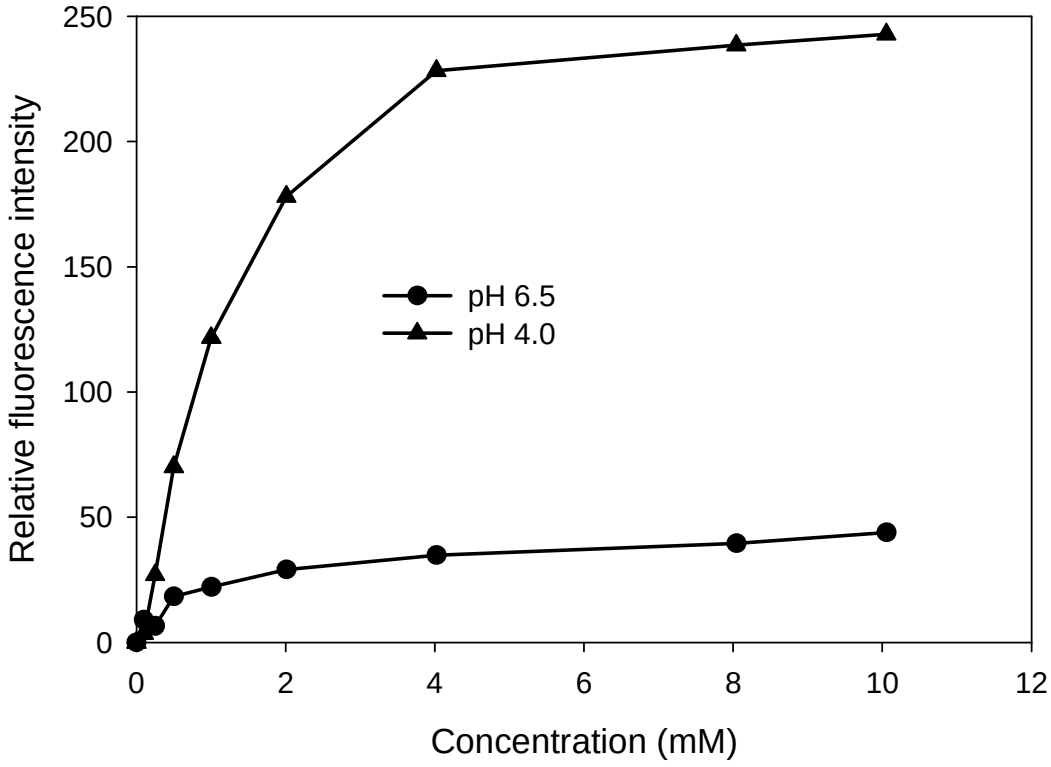

Figure IV-16. Plots of fluorescence intensities at 460 nm in pH 4.0 and pH 6.5 solutions as a function of daptomycin concentration. (cuvette path length 1.5 mm; excitation wavelength at 285 nm).

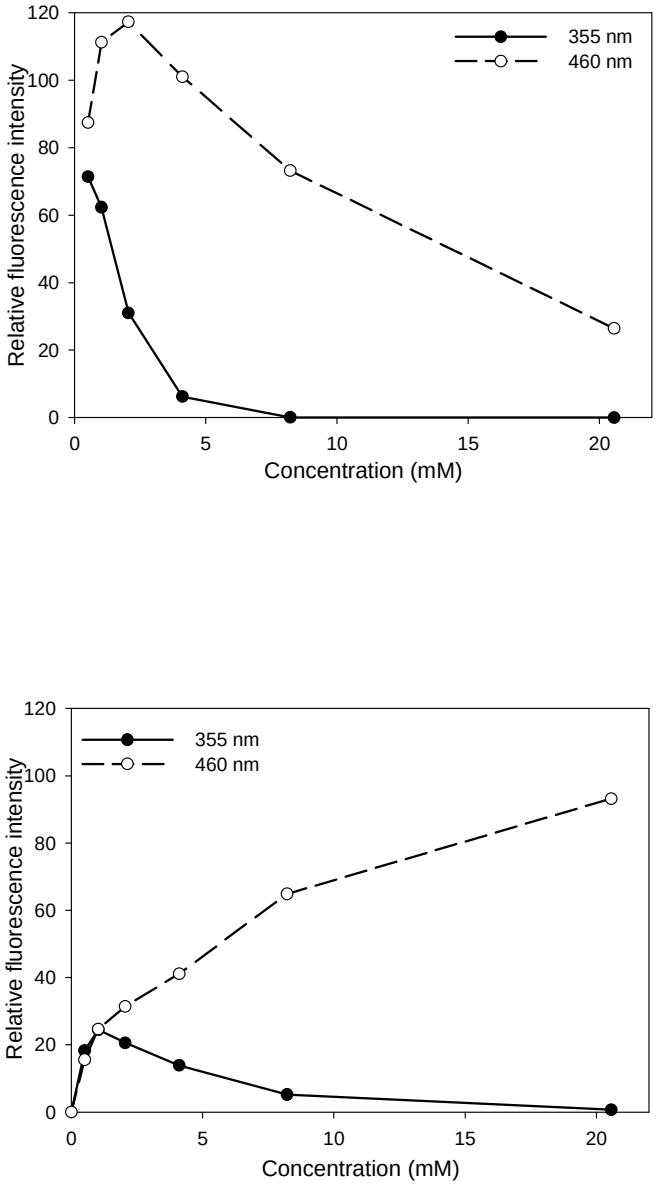

Figures IV-17. Plots of fluorescence intensities at 355 and 460 nm as a function of daptomycin concentration in pH 6.0 aqueous solutions. (Top: cuvette path length 3mm; Bottom: cuvette path length 1.5 mm; excitation wavelength at 285 nm).

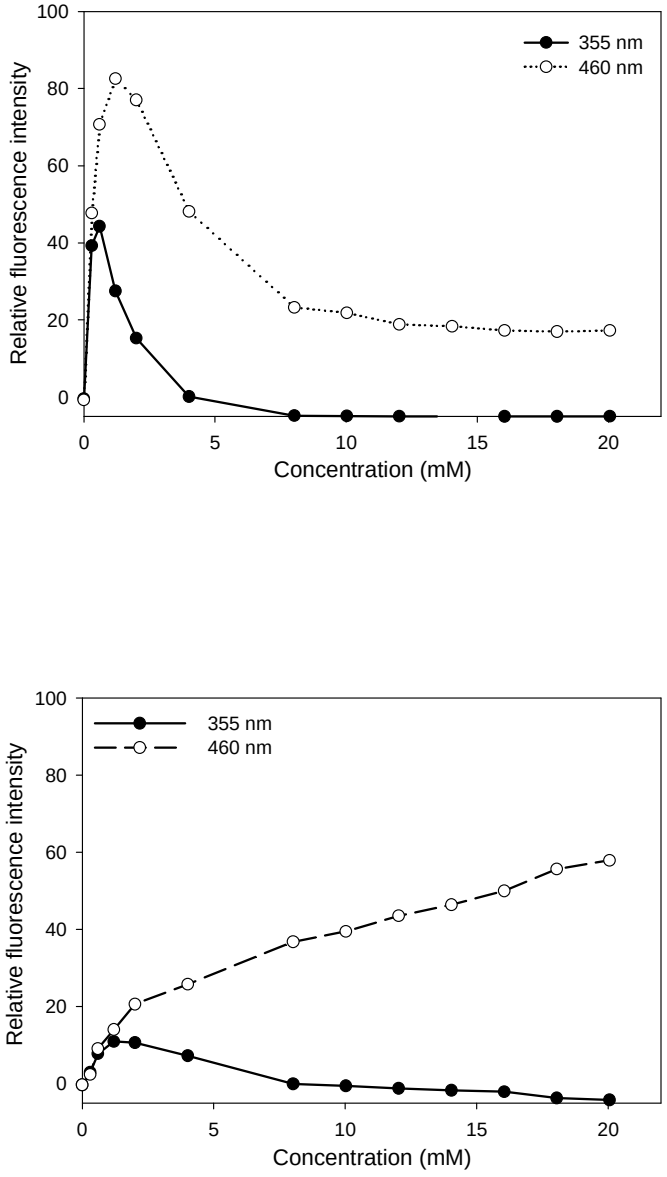

Figures IV-18. Plots of fluorescence intensities at 350 and 460 nm as a function of daptomycin concentration in pH 6.5 aqueous solutions. (Top: cuvette path length 3 mm; Bottom: cuvette path length 1.5 mm; excitation wavelength at 285 nm).

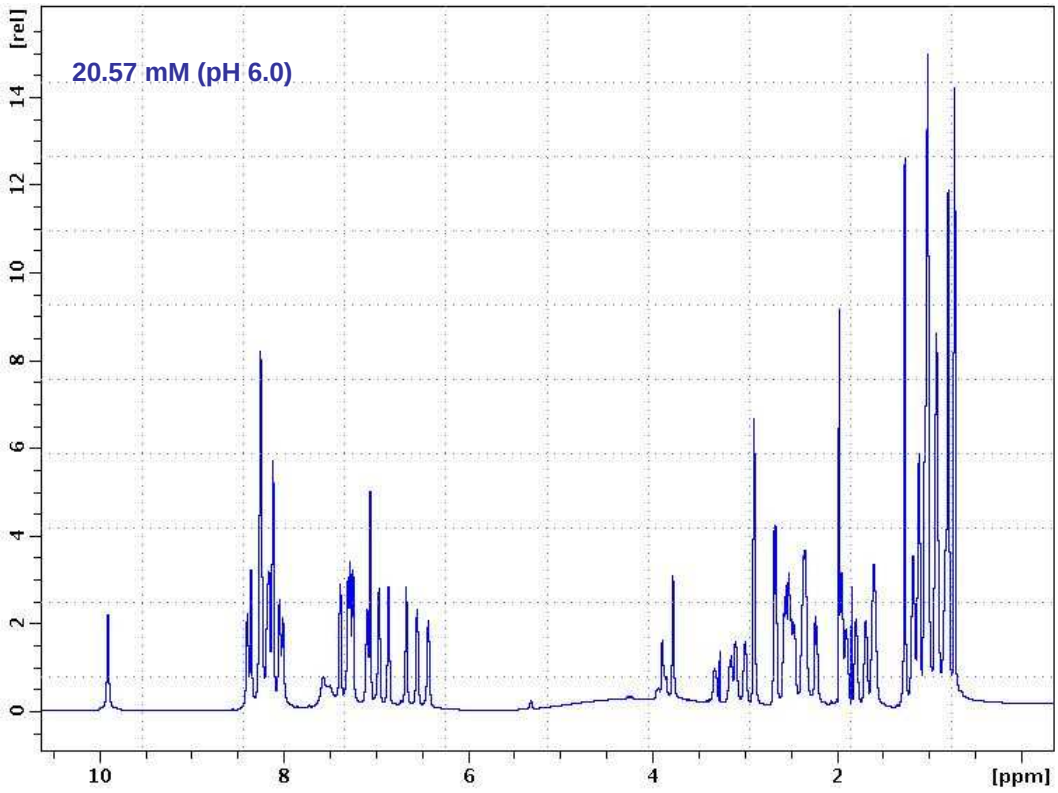

Figure IV-19. 1D proton NMR spectrum of daptomycin in pH 6.0 at 20.57 mM.

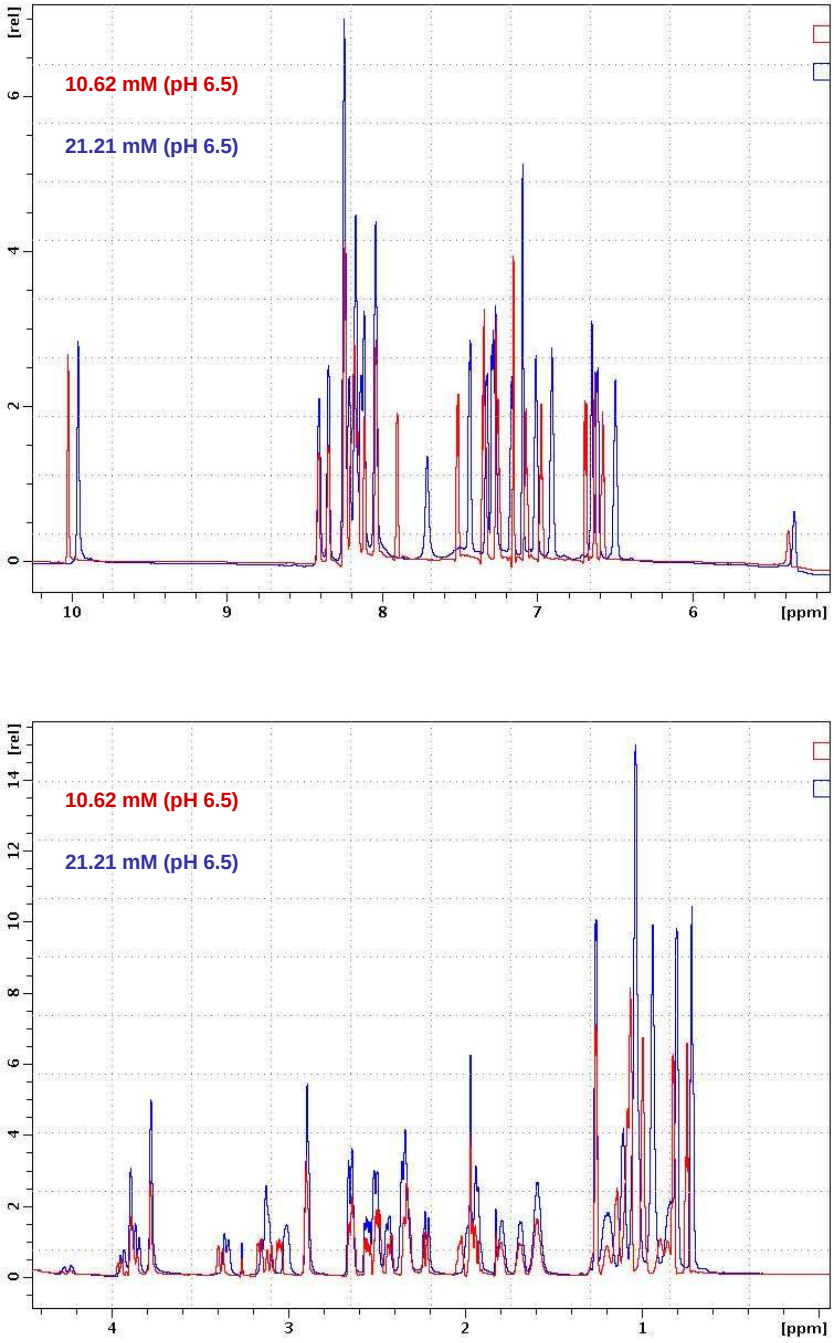

Figures IV-20. 1D proton NMR spectra of daptomycin in pH 6.5 at two concentrations (10.62 and 21.21 mM). (Top: amide and aromatic protons; Bottom: aliphatic protons).

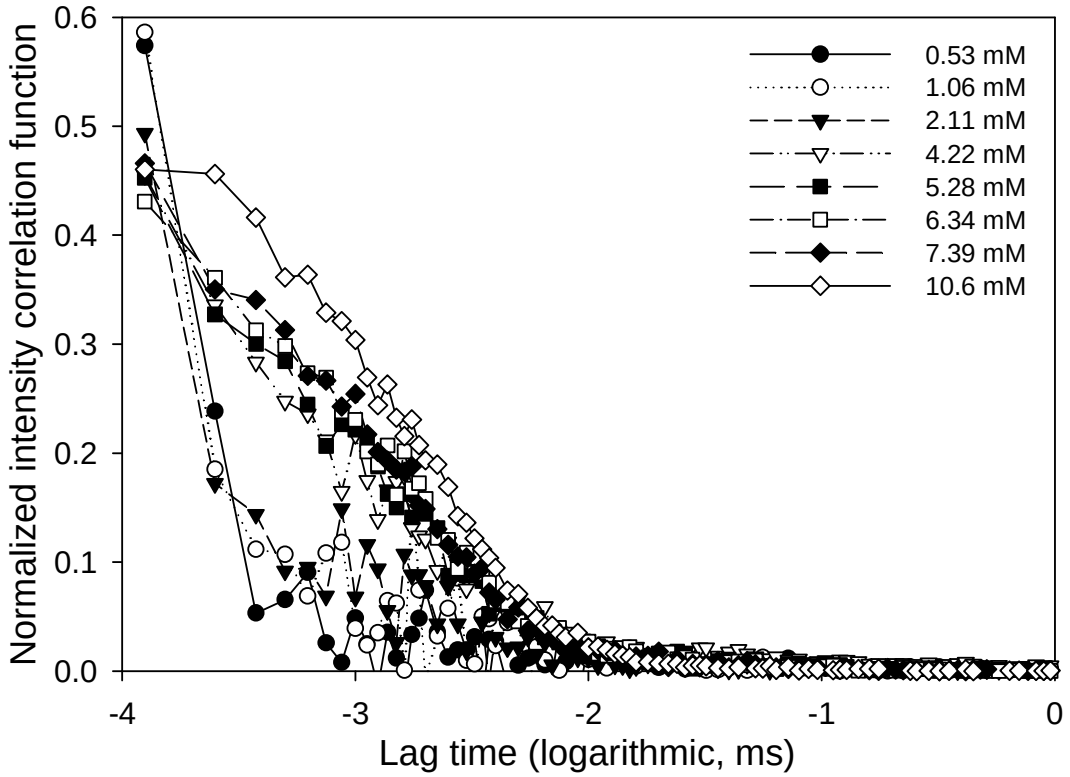

Figure IV-21. Dynamic light scattering correlation functions of daptomycin in pH 6.5 aqueous solutions.

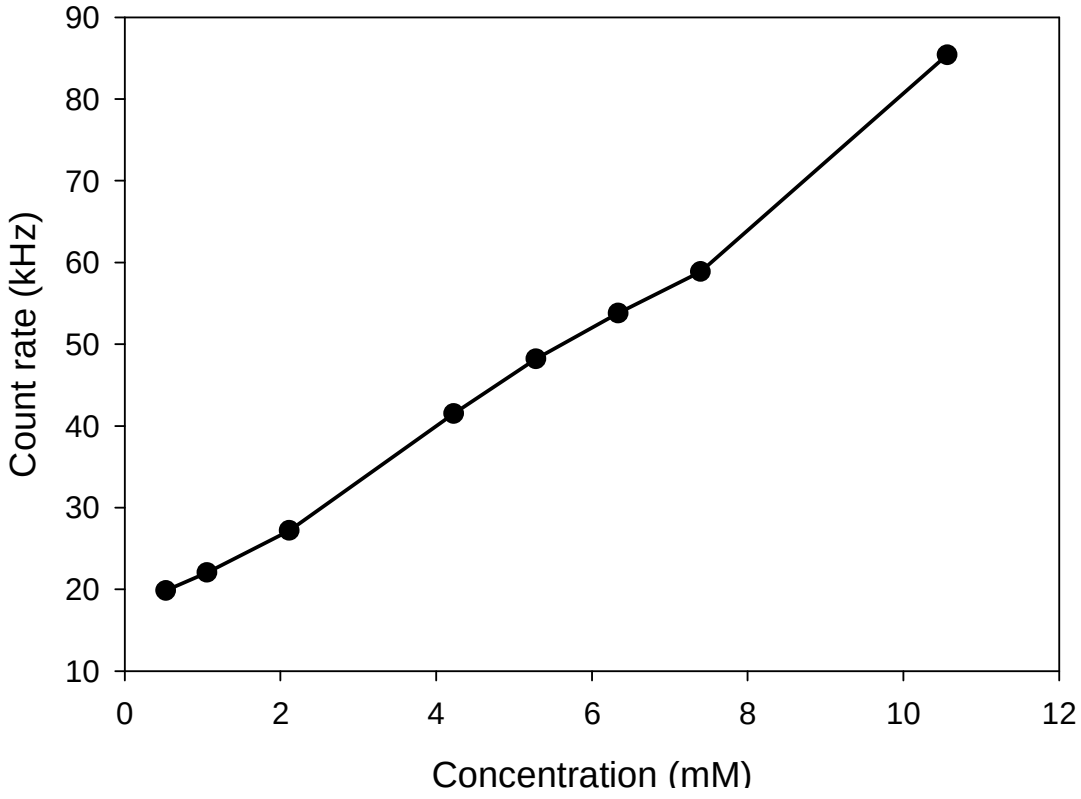

Figure IV-22. Dynamic light scattering count rate of daptomycin in pH 6.5 aqueous solutions as a function of concentration.

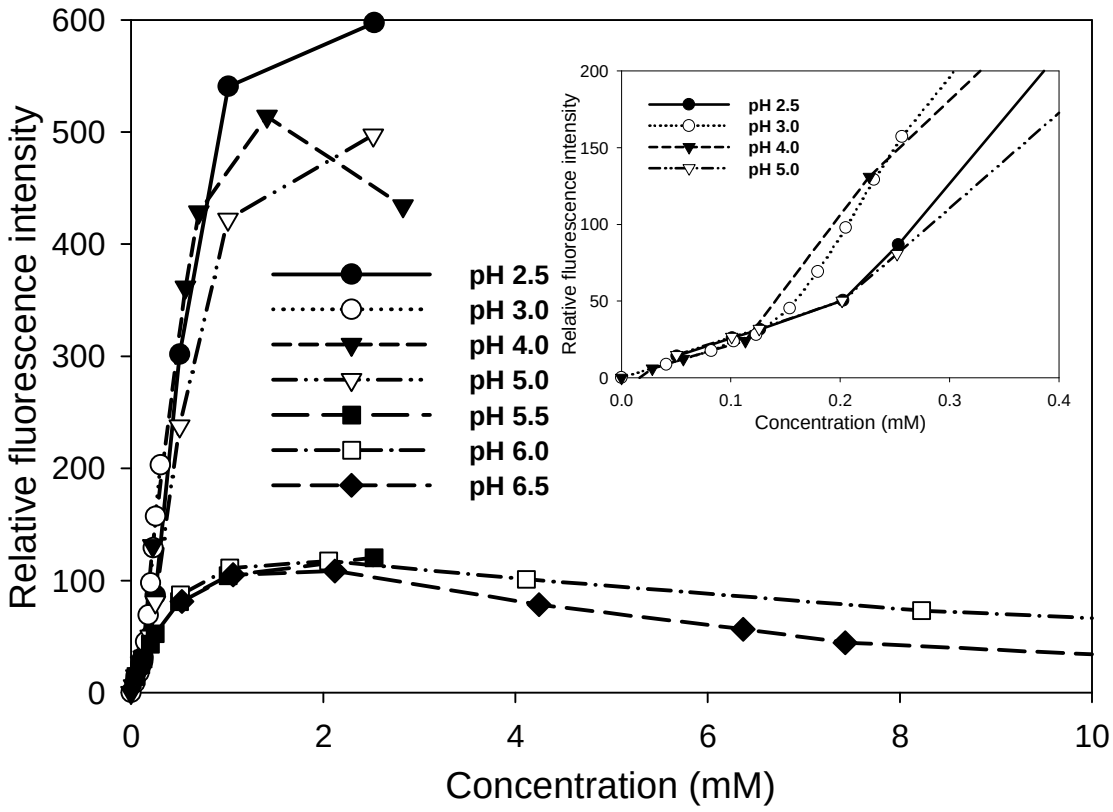

Figure IV-23. Plots of fluorescence intensities at 460 nm as a function of daptomycin concentration in various pH aqueous solutions. (cuvette path length 3 mm; excitation wavelength at 285 nm).

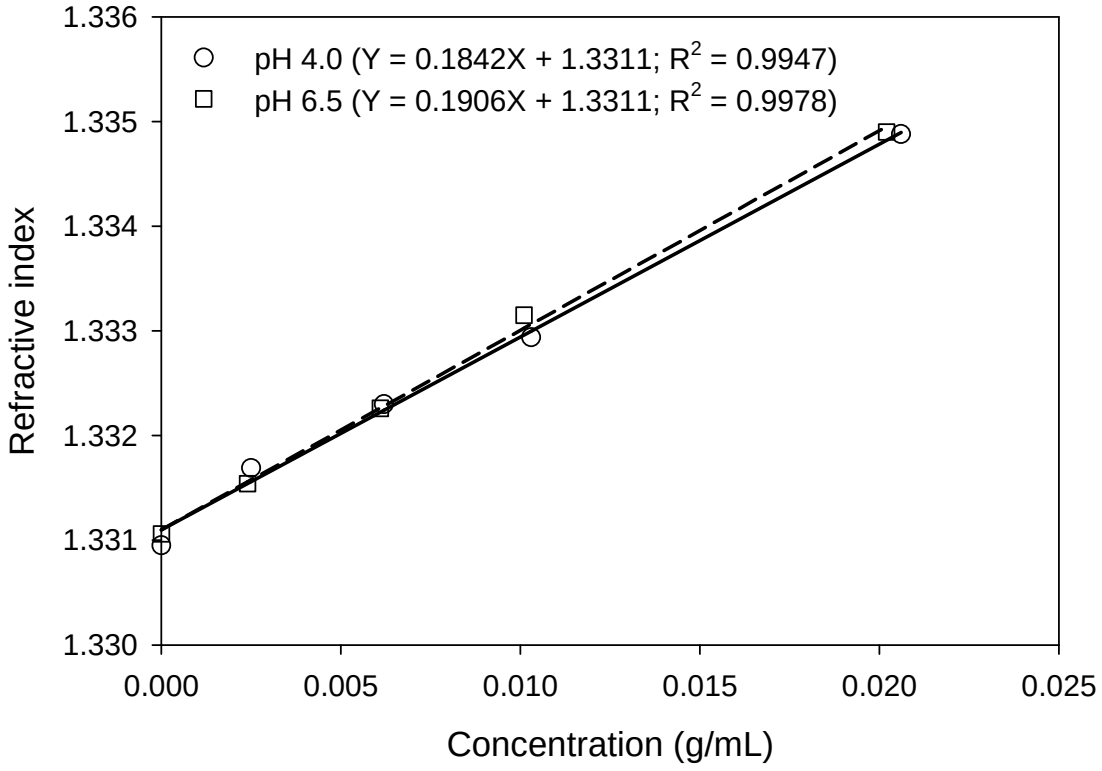

Figure IV-24. The specific refractive index (dn/dC) of daptomycin solutions at pH 4.0 (solid line) and 6.5 (short dash).

Table IV-1. The Measured Molecular Weights and Calculated Aggregation Numbers of Daptomycin at Different Concentrations in pH 4.0 and 6.5 Aqueous Solutions using Static Light Scattering

Daptomycin Conc. (mM)	**Average molecular weight (Dalton)**		**Aggregation number**	
	pH 4.0	pH 6.5	pH 4.0	pH 6.5
1.50	32,150	1,087	20	1
3.75	28,380	949	18	1
6.30	27,600	1,089	17	1
12.70	26,580	1,630	16	1

*The aggregation numbers were calculated and rounded to integer based on the daptomycin molecular weight 1620.67.

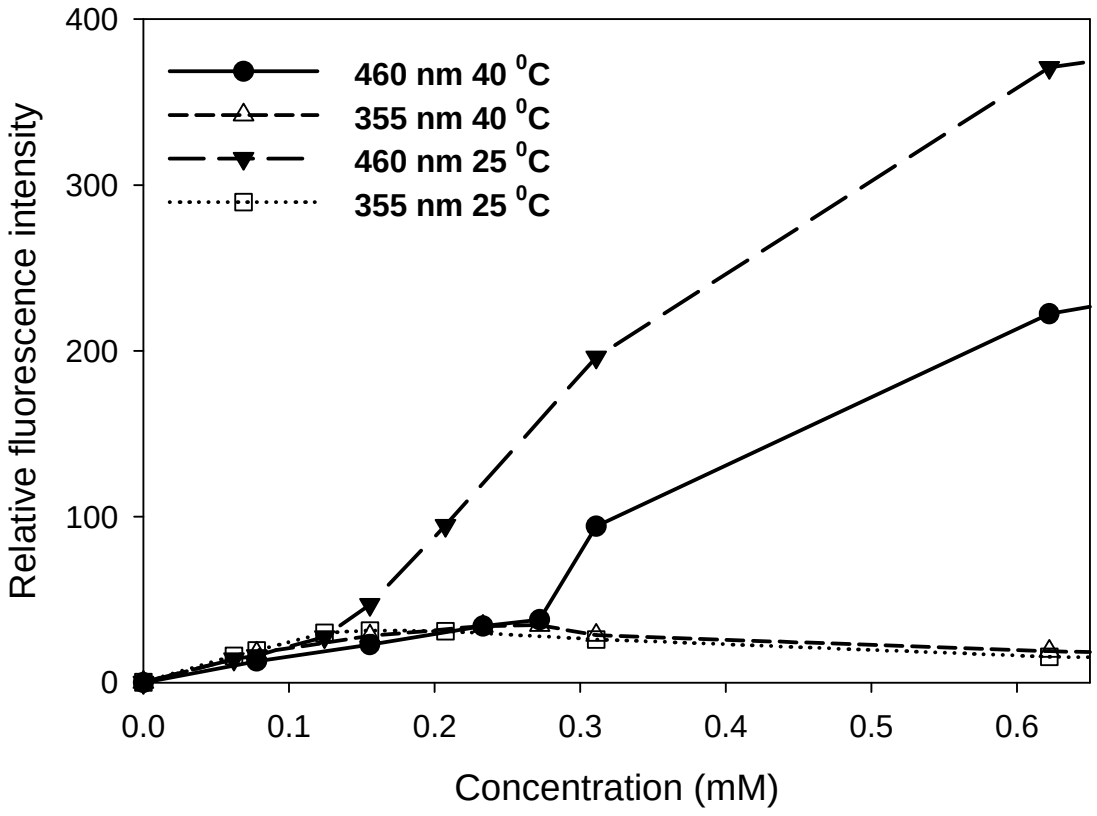

Figure IV-25. Plots of fluorescence intensities at 355 and 460 nm as a function of daptomycin concentration in pH 4.0 aqueous solutions at 25°C and 40°C. (cuvette path length 3 mm; excitation wavelength at 285 nm).

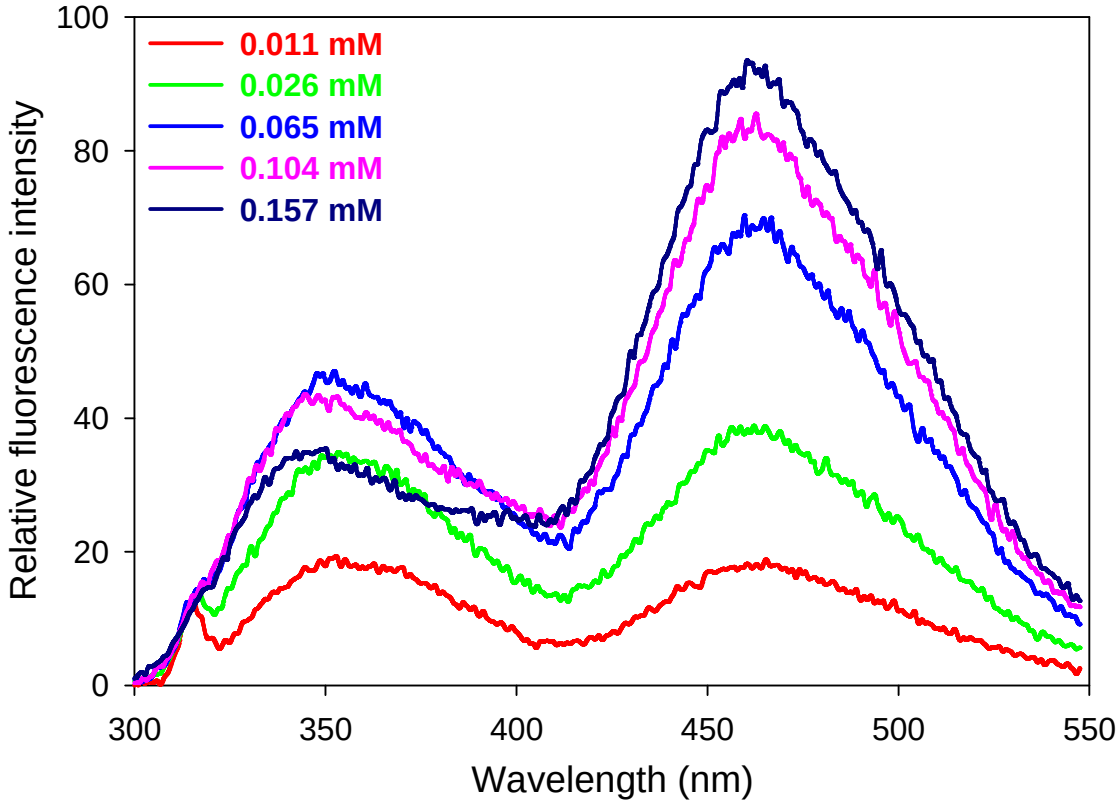

Figure IV-26. The fluorescence spectra of daptomycin at the different concentration in 1.0 mM calcium ions pH 7.4 solutions (cuvette path length 10.0 mm; excitation wavelength at 285 nm).

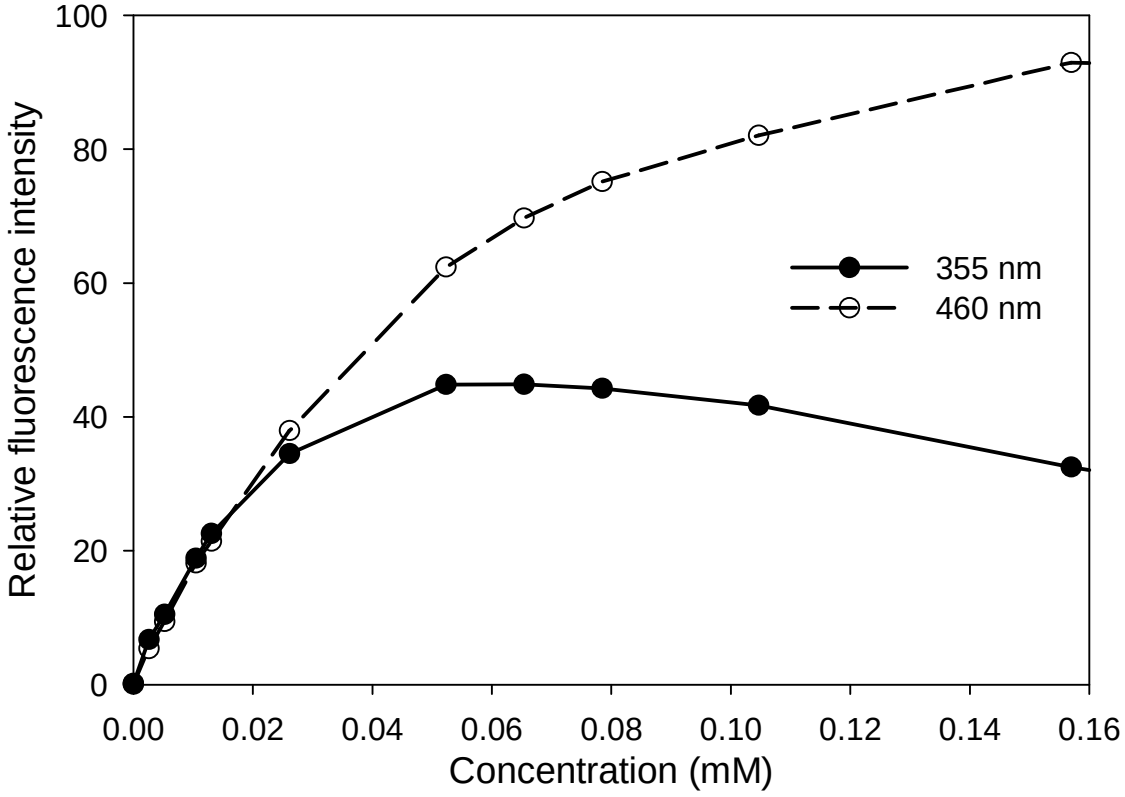

Figure IV-27. Plots of fluorescence intensities at 355 and 460 nm as a function of daptomycin concentration in 1.0 mM calcium ions pH 7.4 solutions (cuvette path length 10.0 mm; excitation wavelength at 285 nm).

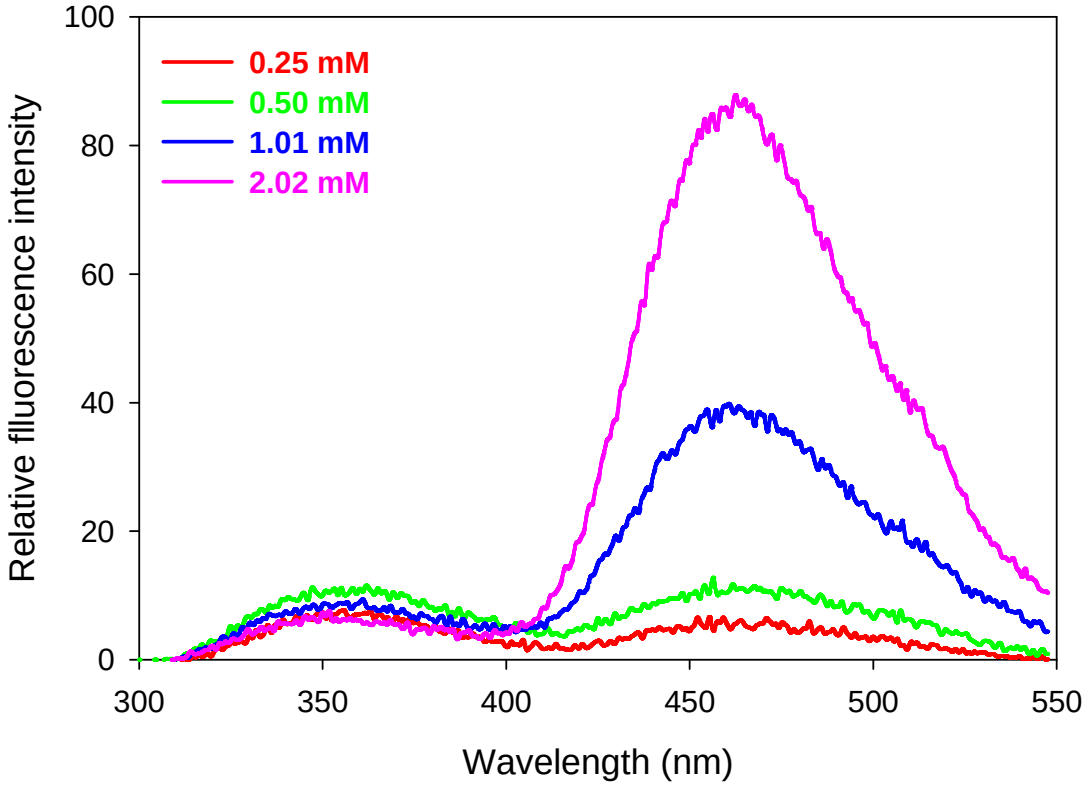

Figure IV-28. The fluorescence spectra of daptomycin at the different concentration in 10.0 mM calcium ions pH 6.5 solutions (cuvette path length 1.5 mm; excitation wavelength at 285 nm).

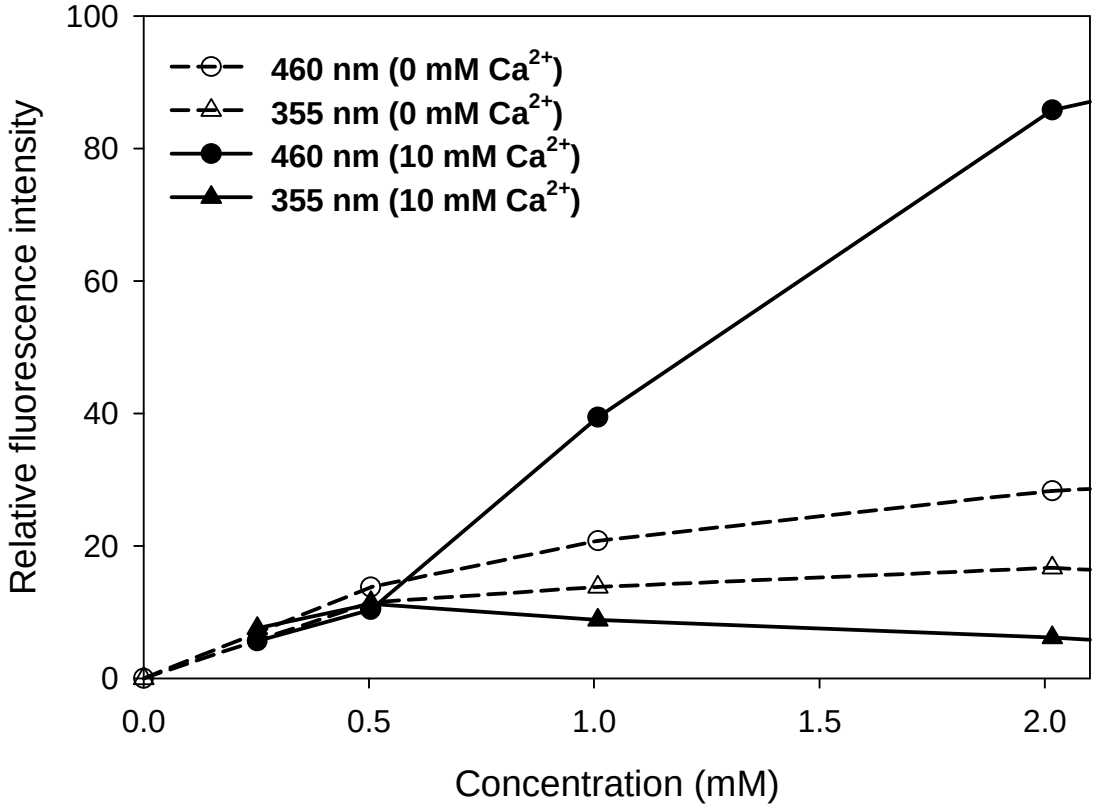

Figure IV-29. The fluorescence intensities at 355 and 460 nm of daptomycin in pH 6.5 solutions without calcium added and in 10.0 mM calcium. (cuvette path length 1.5 mm; excitation wavelength at 285 nm).

Discussion

The CAC values of daptomycin can be detected by the abrupt increase of the emission intensity at 460 nm and inflection points of the count rate plots versus daptomycin concentration by DLS measurement. The CAC values of daptomycin were 0.14 mM at pH 3.0, 0.12 mM at 4.0, and 0.20 mM at pH 2.5 and 5.0. The CAC values obtained with fluorescence spectroscopy in these pH regions agreed to those estimated using dynamic light scattering and were consistent with the changes in the resonance linewidth and intensity of proton NMR measurements.

Based on the estimated sequence-specific apparent pK_a values of daptomycin in monomeric state in Chapter II, the comparison of fraction of daptomycin ionization and pH-dependent CAC values of daptomycin is shown in Figure IV-30. There is always a positive charge in Orn-6 residue below pH 10. The abnormally low pK_a of Asp-7 (pK_a 1.0) could be caused by the formation of a salt bridge between the negatively charged Asp-7 and positively charged neighboring Orn-6. In the pH from 2 to 6, the main species of daptomycin exhibit the transitions through zwitterion ($H_4A^{\pm}$), monoanion (H_3A^-), dianion (H_2A^{2-}), and trianion (HA^{3-}) as the gradual ionization from Asp-9 (pK_a 3.85), Asp-3 (pK_a 4.15), and mGlu-12 (pK_a 4.55). The estimated CAC values of daptomycin in pH 2.5 and 5.0 were 0.20 mM greater than those in pH 3.0 (0.14 mM) and 4.0 (0.12 mM) aqueous solutions. In pH 2.5 daptomycin solutions, the main species is zwitterion ($H_4A^{\pm}$), and the net charge of daptomycin molecules is close to zero. In the pH 3.0 and 4.0 daptomycin solutions, monoanion (H_3A^-) is gradually dominant species due to the deprotonation of Asp-9, and the net charge of daptomycin molecule is one negative charge. As shown in Figure IV-31, daptomycin is composed of a 10-membered cyclic ring and a 3-member exocyclic tail. The anionic Asp-9 residues are on the one end, while the hydrophobic moieties (Trp-1 and decanoyl aliphatic tail via DAsn-2 and Asp-3 connected with Thr-4) are clustered on the other end, leading to amphipathicity in daptomycin molecules. The behavior of monoanion (H_3A^-) daptomycin is similar to ionic

surfactant and more favorable to form self-association aggregation than in zwitterions ($H_4A^{\pm}$). As shown in Figure IV-32, the pH-dependent daptomycin CAC values are closely correlated with the reciprocal of monoanionic form (H_3A^-) fraction with high R value 0.9944 (Y = -9.6296 + 104.1662X, where Y and X denote the reciprocal of monoanionic (H_3A^-) form fraction and the pH-dependent daptomycin CAC values, respectively). This suggests that the primary aggregating daptomycin species is the monoanion and that the critical aggregation concentration for this species were 0.019 mM at pH 2.5, 0.027 mM at pH 3.0, 0.040 mM at pH 4.0, and 0.016 mM at pH 5.0, respectively.

Increased fraction of dianion (H_2A^{2-}), and trianion (HA^{3-}) occurs due to the deprotonation of Asp-3 and mGlu-12. The former residue is situated near the N-terminal lipid tail and the latter is next to the aromatic residue Kyn-13 which is also in the vicinity of the N-terminus. Increased ionization of these residues would be expected to destabilize aggregates formed by hydrophobic interactions of the N-terminal lipoidal tails. Thus aggregation was associated with the presence of the monoanionic species but not observed in the presence of di- and tri-anionic species.

As the pH values of daptomycin aqueous solutions were > 5.5, the sensitive upward inflection points of emission intensity changes at 460 nm from Kyn-13 as a function of daptomycin concentration were not found at all. The noticeable daptomycin aggregates were not detected using dynamic and static light scattering, and NMR. The high quality NMR spectra were obtained at a higher daptomycin concentration up to 21 mM in pH 6.5 aqueous solution. However, as the concentration increased from 10.6 to 21.2 mM in pH 6.5 (Figure IV-20), the chemical shifts in Trp-1 residue changed from 10.02 to 9.95 ppm (N-H in indole ring) and from 7.9 to 7.7 ppm (amide proton). The aliphatic proton chemical shifts remained constant over the same concentration range. Only aromatic protons of Trp-1 and Kyn-13 were observed to exhibit concentration dependent up-field chemical shifts, which are attributed to the influence of the aromatic

ring current. It is a typical phenomenon of aromatic π-π interaction. The variations of aromatic proton chemical shifts as a function of concentration are also reported in the literature.[55-57]

In pH 6.0 and 6.5 solutions from 10 to 21 mM (Figure IV-17 and IV-18), the emission intensity at 460 nm continually increased with the increase of daptomycin concentration, while the fluorescence intensity at 355 nm from Trp-1 went down. The fluorescent emission spectral patterns of daptomycin are affected by daptomycin concentration. Both concentration-dependent fluorescence quenching and self-association aggregation could occur with increasing daptomycin concentration. The concentration quenching would reduce the fluorescence emission intensities from both Trp-1 and Kyn-13, while the self-association aggregation would increase the emission intensities from Kyn-13 at 460 nm due to FRET efficiency enhancement between Trp-1 and Kyn-13. Typically, the fluorescence intensity from Trp-1 decreases corresponding to the increasing intensities from Kyn-13 reflects more efficient FRET between the two groups. Hence, the changes of fluorescent emission spectral patterns disclose the interaction between the two aromatic residues, Trp-1 and Kyn-13. As daptomycin concentration at pH 6.5 aqueous solutions increased from 10.62 to 21.21 mM, the proton chemical shifts related to the aromatic residues Trp-1 and Kyn-13 moved to low chemical shift ppm. The changes of the fluorescent emission patterns and the amide and aromatic proton chemical shifts reflected the interaction between the aromatic residues Trp-1 and Kyn-13.

As the temperature increased from 25 ^{0}C to 40 ^{0}C, the CAC values of daptomycin in pH 4.0 solutions changed from 0.12 mM to 0.27 mM. As expected, the higher temperature favors to the dissociation of daptomycin aggregates.

In the pH 6.5 and 7.4 solutions, the effects of calcium ions on daptomycin aggregation were observed from the transitions of the fluorescence spectral patterns shown in Figure IV-26 and IV-28, the emission intensity from Kyn-13 increase with the decreasing of that from Trp-1. In 10 mM calcium ions pH 6.5 solutions, the CAC of

daptomycin in Figure IV-29 was noticeably identified at 0.50 mM from the steep increase of the fluorescence intensity at 460 nm. The increase in resonance line-widths observed in ^{1}H NMR spectra of 2 mM daptomycin in 2 mM $CaCl_2$ pH 6.70 solution was reported.[14]

Daptomycin three-dimensional structure and its biologically active conformation have been investigated with a number of recent NMR studies.[11-15] As to the aqueous conformation of daptomycin, different findings were also observed by Rotondi and Gierasch[15] compared to previous investigators (Figure I-3).[13,14] The present research may clarify the reported differences in daptomycin structures as determined by NMR studies in the absence of calcium ion. The three proposed structures of daptomycin[13-15] was regarded as the very high flexibility of daptomycin.[12] Based on our studies, daptomycin aggregation is dependent on pH and concentration. The different findings of daptomycin conformation and calcium-conjugated daptomycin conformation are possibly due to the slightly different experimental conditions, especially daptomycin concentration and sensitive pH regions. Jung et al.[14] used a 2 mM daptomycin solution at pH 6.60; as we demonstrated that daptomycin was probably in non-aggregation state at 2 mM in pH 6.60. Ball et al.[13] conducted studies using 0.8 mM solution of daptomycin at pH 5.0; Rotondi et al.[15] prepared the samples consisting of 1.9 mM daptomycin at pH 5.3. In both cases, solutions were prepared in the close pH values at pH 5.0 and 5.3, but with quite different daptomycin concentrations at 0.8 mM and 1.9 mM. Probably, daptomycin was in the aggregation state at 1.9 mM in pH 5.3. Thus, a preferred aqueous conformation for daptomycin proposed by Jung et al and Ramesh et al, in the non-aggregation state or less interaction between the two aromatic residues Trp-1 and Kyn-13, differs from that from Rotonidi et al[15] primarily by the presence or absence of clustering of hydrophobic side chains between Trp-1 and Kyn-13 (Figure I-3). A daptomycin structure in aqueous solution proposed by Rotondi et al[15] is qualitatively similar to the Ca^{2+}-bound structure reported by Jung et al.[14], which also validates the explanation.

The evaluation of daptomycin's therapeutic activity has been complicated by the influence of factors such as concentration, pH, and total or ionized calcium concentration.[58] A pH-dependent daptomycin activity was also demonstrated.[59] All these factors could affect daptomycin conformation, aggregation, and further therapeutic activity. It is understandable that the calcium ion concentration induced daptomycin conformation and aggregation is essential for daptomycin function in the physiological pH value. Many approaches have investigated the interaction between calcium ions and daptomycin.[11,14]

The factors of pH, calcium ion, and daptomycin concentrations were designed to simulate the interaction of daptomycin with calcium ion in the physiological conditions. According to daptomycin plasma concentrations ranged from 0 to 150 μg/mL[60-63] in pharmacokinetics studies and calcium ion concentration in plasma[64], daptomycin aggregation and conformation was investigated in the presence of 1.0 mM calcium ion in phosphate buffered saline solutions. As shown in Figure IV-26, the typical change of fluorescence emission patterns due to daptomycin conformation and aggregation was observed at 0.06 mM (100 μg/mL) daptomycin concentration in 1.0 mM calcium ion solution. The increased daptomycin concentration caused aggregation and conformation changes matches with its therapeutic plasma concentrations.[65-67]

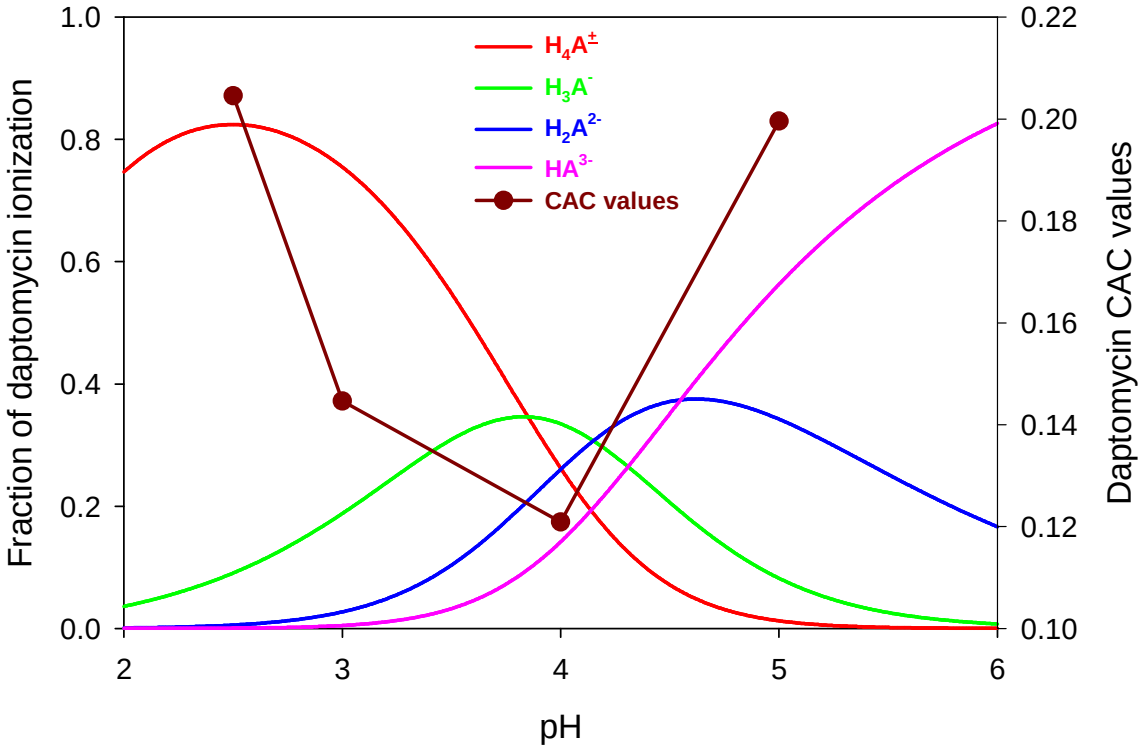

Figure IV-30. Comparison of the distribution of ionic forms of daptomycin and the estimated CAC values. Fraction of daptomycin ionization varied from zwitterion ($H_4A^{\pm}$), monoanion (H_3A^-), dianion (H_2A^{2-}), and trianion (HA^{3-}), respectively. Each solid circle point represented CAC value obtained in pH solutions from 2.5 to 5.0. The pK_a values and Hill coefficients used in this calculation are pK_{a1} = 1.01 (Asp-7), n_1 = 0.72; pK_{a2} = 1.30 (Kyn-13), n_2 = 0.88; pK_{a3} = 3.85 (Asp-9), n_3 = 0.71; pK_{a4} = 4.15 (Asp-3), n_4 = 0.73; pK_{a5} = 4.55 (mGlu-12), n_5 = 0.48; pK_{a6} = 10.7 (Orn-6), n_6 = 1.00; The calculations of pH-dependent species distribution for daptomycin are described in Appendix B.

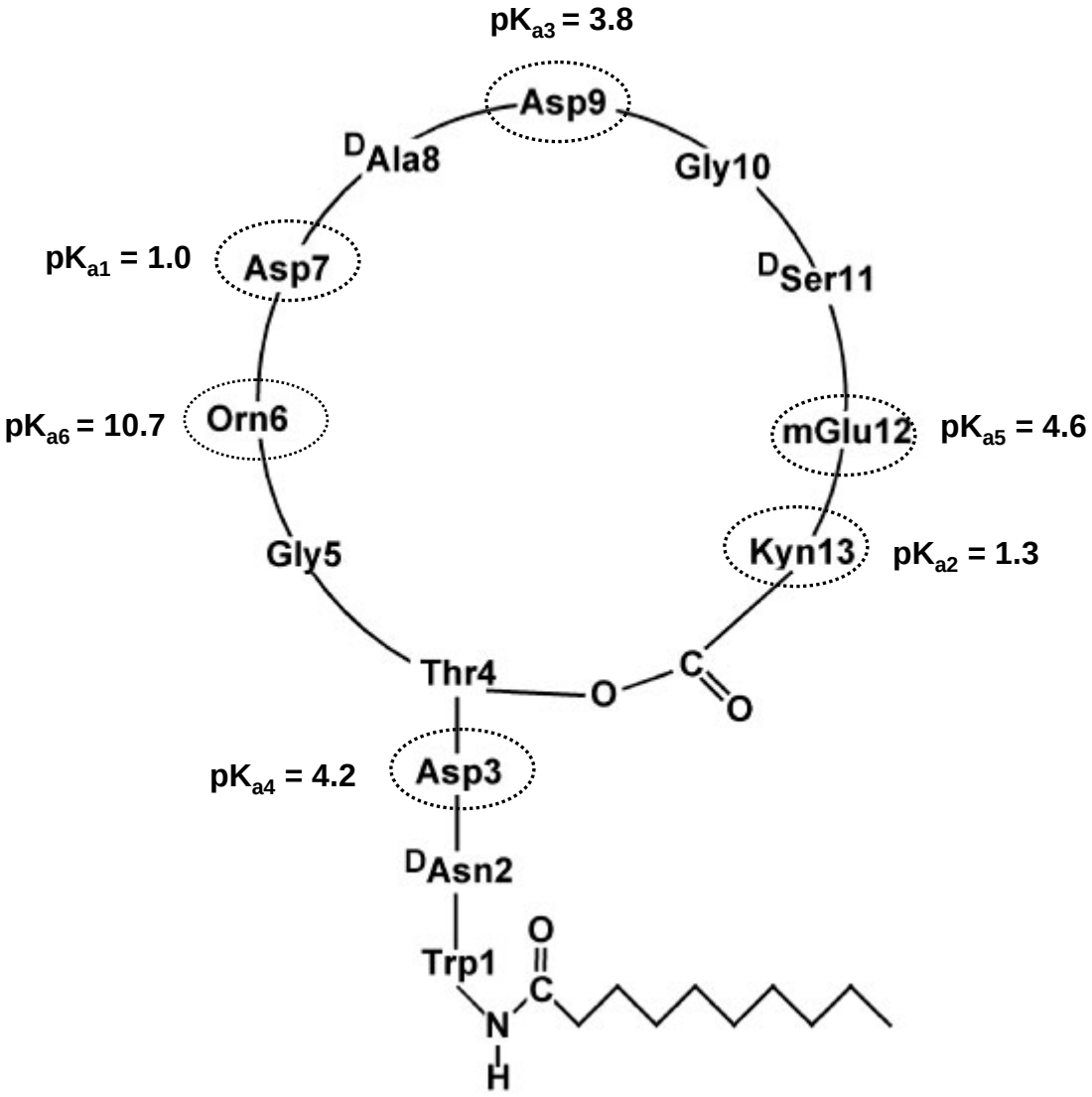

Figure IV-31. Daptomycin pK$_a$ values and molecular structure.

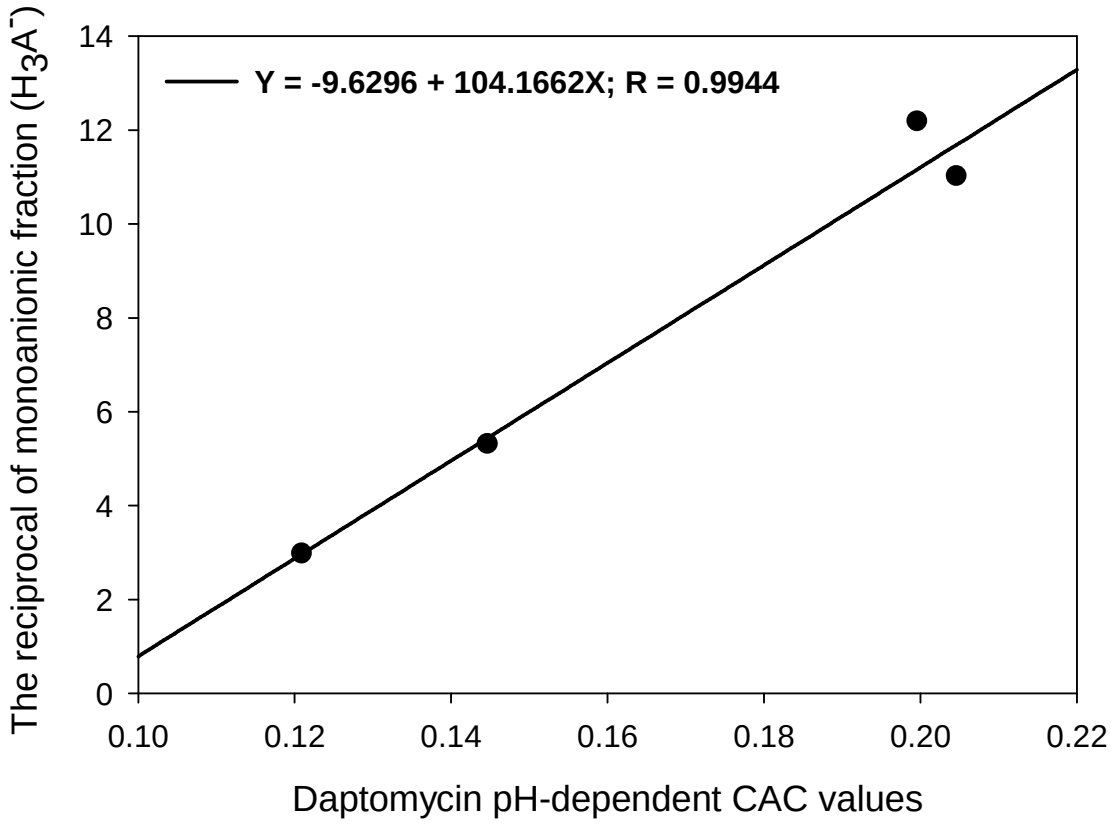

Figure IV-32. The correlation between pH-dependent daptomycin CAC values and the reciprocal of daptomycin monoanionic (H_3A^-) fraction.

CHAPTER V EFFECTS OF IONIZATION ON INTERMOLECULAR INTERACTION

Introduction

Daptomycin is a cyclic lipopeptide antibiotic with activity against multi-resistant Gram-positive organisms, such as vancomycin-resistant *enterococci* and methicillin-resistant *staphylococci*.[68-70] Initial clinical trials resulted in some treatment failure due, in part, to protein binding, rapid renal clearance, and inadequate biophase concentrations.[71-74] Daptomycin is an acidic lipopeptide with six side-chain ionizable groups (four carboxylic acids and two amines). Polyamidoamine (PAMAM) dendrimers are monodisperse branched globular macromolecules that carry a multiplicity of functional groups at their periphery.[75,76] The number of surface functional groups, molecular weight and size of dendrimers are defined by the generation number which describes the number of layers of sub-units that have been attached during synthesis.[77-79] For example, polyamidoamine dendrimers (PAMAM) in Figure V-1 are cationic polymers synthesized by a two-step iterative reaction that results in concentric generations of units around a central initiator core, having specifically controlled size, molecular mass and electrical charge.[80] This PAMAM core-shell architecture grows linearly in diameter as a function of added shells (generations), and the surface groups amplify exponentially at each generation.[77] PAMAM dendrimers have primary amine end groups on the surface and tertiary amine groups situated at the branching points within the core. Negatively charged drug molecules can be entrapped in the interior core as well as electrostatically attached to the positive amine groups on the surface.[81] Dendritic formulations were reported to prolong blood/plasma retention owing to their hydrophilicity, surface characteristics, and molecular size.[82] This type of drug-carrier system could provide a pharmacokinetic enhancement of daptomycin biophase concentrations.[83]

The interaction of the lipopeptide antibiotic daptomycin and PAMAM dendrimer has been investigated by fluorescence spectroscopy.[84] Several factors, such as pH, molecular size, and surface structure have been shown to influence the formation of dendrimeric complex.[85-87]

In this chapter, the interaction mechanism of daptomycin binding to PAMAM dendrimers is investigated based on our recent estimation of the individual ionization constants for the amino acid side chains (Chapter II), the understanding of the individual pH-dependent species distributions of daptomycin. The experimental data and binding parameter calculations were conducted by Dr. Boontarika Chanovrachote.

Materials and Methods

Materials

Daptomycin obtained from Eli Lilly Research Laboratories (Indianapolis, IN) was used as received. Sodium chloride, standard sodium hydroxide, and standard hydrochloric acid solutions were purchased from Fisher Scientific (Fair Lawn, NJ). 1,4-diaminobutane core PAMAM generation 5 (PAMAM 5) and generation 6 (PAMAM 6) in 10% methanol solutions were purchased from Sigma-Aldrich (St. Louis, MO).

Methods

Preparation of PAMAM-daptomycin complex

The methanolic solutions of PAMAM dendrimers were used to prepare aqueous stock solutions. The methanol was evaporated by purging nitrogen gas. The dendrimers were re-dissolved in double-distilled water. Daptomycin and PAMAM solutions were separately prepared at the same target pH values adjusted using 0.1 M sodium hydroxide or hydrochloric acid solutions. PAMAM 5 (0.18 μM) and daptomycin (3 μM) aqueous solutions at pH 4.0 were prepared to evaluate the fluorescence properties of PAMAM-daptomycin complex.

Fluorescence spectroscopy

Fluorescence spectra were recorded using a Perkin-Elmer LS55 luminescence spectrometer (Perkin Elmer Inc., Norwalk, CT). The excitation wavelength was 285 nm, and the emission spectra were scanned from 320 to 540 nm to observe the emission responses from both Trp-1 and Kyn-13.

Binding isotherm constructions[84]

Daptomycin-PAMAM complex binding isotherms were generated by the addition of aqueous daptomycin to PAMAM solutions using various size dendrimers (PAMAM 5 and 6). Daptomycin and PAMAM solutions were prepared separately by adjusting each solution to a target pH value using 0.1 M sodium hydroxide and/or hydrochloric acid solutions in the range of pH 3 to 9 for PAMAM 5 and pH 3.5 to 7.0 for PAMAM 6. A 3 mL aliquot of PAMAM 5 or 6 solutions was placed in a fluorescence quartz cell (10 mm path length) equipped with a magnetic stirrer. Typically 15 aliquots (5 μL) of aqueous daptomycin solutions were added incrementally using a Hamilton microliter syringe to a final daptomycin maximum concentrations in the range of 5.80 to 74.07 μM. After the addition of each aliquot, the mixtures were stirred for 3 minutes, and then the fluorescence spectra were collected. As above, the control titrations were performed by adding 5 μL aliquots of daptomycin to the same pH value aqueous solutions in the absence of dendrimers. All solutions were pH adjusted to the desire value prior to the addition, and the pH values of the titration mixtures were constant ($\leq$ 0.1 ΔpH) throughout each titration experiment.

The binding isotherms were constructed by plotting the fluorescence intensity differences (ΔF) at 460 nm in the presence and absence of dendrimers against the total daptomycin concentrations.

Estimation of the binding parameters

Briefly, a quadratic equation was derived for one-site binding model that relates in the total daptomycin concentration to fluorescence differences as described in the following equation.[84]

$$\Delta F = \frac{\Delta E}{2}\{([\text{daptomycin}]_T + K_d + R) \pm \sqrt{([\text{daptomycin}]_T + K_d + R)^2 - 4 \times R \times [\text{daptomycin}]_T}\}$$

where $[\text{daptomycin}]_T$, ΔE, K_d, and R represent the total daptomycin concentration, the difference in molar extinction coefficient between the free and bound fluorophores, the equilibrium dissociation constant, and the total number of independent binding sites, respectively.

For a two-site binding model, the following equation was derived to describe fluorescence difference titration curves in terms of the molar extinction parameters, total daptomycin concentration, and binding parameters.

$$\Delta F = \Delta E_1 \times \left(\frac{R_1 \times [\text{daptomycin}]_F}{K_{d1} + [\text{daptomycin}]_F} \right) + \Delta E_2 \times \left(\frac{R_2 \times [\text{daptomycin}]_F}{K_{d2} + [\text{daptomycin}]_F} \right)$$

where $[\text{daptomycin}]_F$, a, b, c and θ are given by the following relationships and are defined in terms of binding parameters and the total daptomycin concentration.

$$[\text{daptomycin}]_F = -\frac{a}{3} + \frac{2}{3}\sqrt{(a^2 - 3b)}\cos\frac{\theta}{3}$$

$$b = K_{d1}K_{d2} + K_{d2}R_1 + K_{d1}R_2 - (K_{d1} + K_{d2})[\text{daptomycin}]_T$$

$$c = -K_{d1}K_{d2}[\text{daptomycin}]_T$$

$$\theta = \arccos\frac{-2a^3 + 9ab - 27c}{2\sqrt{(a^2 - 3b)^3}} \qquad (0 < \theta < \pi)$$

The utility of the model equation to distinguish between the binding mechanism and estimate the binding parameters including the difference in molar extinction coefficient (ΔE) between the free and bound fluorophores, dissociation constant (K_d), and

the total number of independent binding sites (R) has been previously described.[84] The nonlinear regression analysis was used to estimate binding parameters (WinNonlin Softer Version 5.0.1, Pharsight Corporation).

Results

Fluorescence Properties of PAMAM-daptomycin Complex

Shown in Figure V-2 are the fluorescence spectra of daptomycin at 3.0 µM, PAMAM 5 at 0.18 µM, and PAMAM-daptomycin complex (a mixture of daptomycin and PAMAM 5) at pH 4.0 aqueous solutions. Daptomycin has intrinsic fluorescence emissions at 355 nm from Trp-1 and 460 nm from Kyn-13, but PAMAM dendrimer shows no fluorescence emission maxima over the wavelength range between 320 to 540 nm. The PAMAM-daptomycin complex formed by adding PAMAM to daptomycin had a fourteen-fold increase in emission intensity at 460 nm from Kyn-13 and a 50% decrease at 355 nm from Trp-1. The significant fluorescence emission enhancement at 460 nm could be the self-association aggregation of daptomycin or the interaction of daptomycin with dendrimers. The existing daptomycin concentration here was only 3.0 µM. As discussed in Chapter III and IV, the CAC values of daptomycin in the pH range of 3 to 7 were always more than 100 µM. Therefore, the fluorescence enhancements observed herein could be unequivocally attributed to daptomycin dendrimer interactions. The similar fluorescence enhancements at 460 nm from Kyn-13 have also been reported in the interaction of daptomycin and phospholipids.[42]

The fluorescence changes observed were associated with daptomycin and dendrimer interactions. Typical fluorescence intensity changes in the absence and presence of dendrimers (PAMAM 5) as a function of daptomycin concentrations in pH 5.0 aqueous solutions are depicted in Figure V-3. In the absence of dendrimer (PAMAM 5), the fluorescence intensities at 460 nm increased linearly over the range of daptomycin concentrations. Moreover, these increases were co-linear in all pH value solutions. In the

presence of PAMAM 5, the fluorescence emission intensities at 460 nm displayed a steep increase at low daptomycin concentrations and a gradual linear increase at higher concentrations.

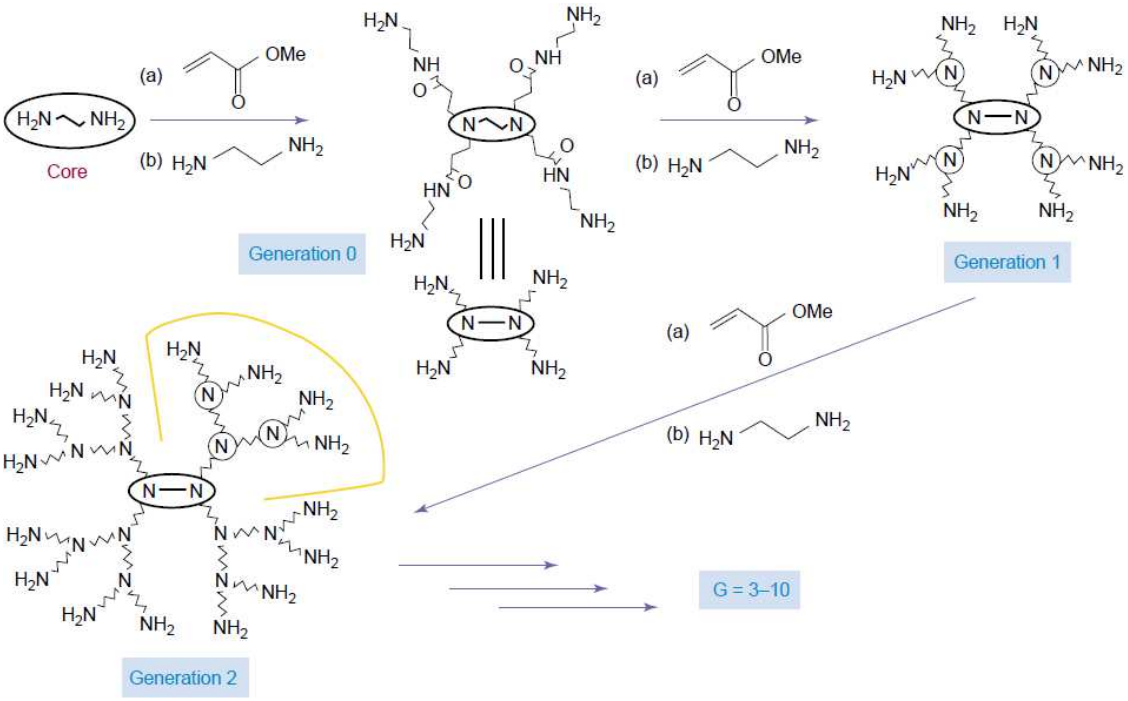

Figure V-1. Synthesis of tetra-functional polyamidoamine dendrimers PAMAM.[77]

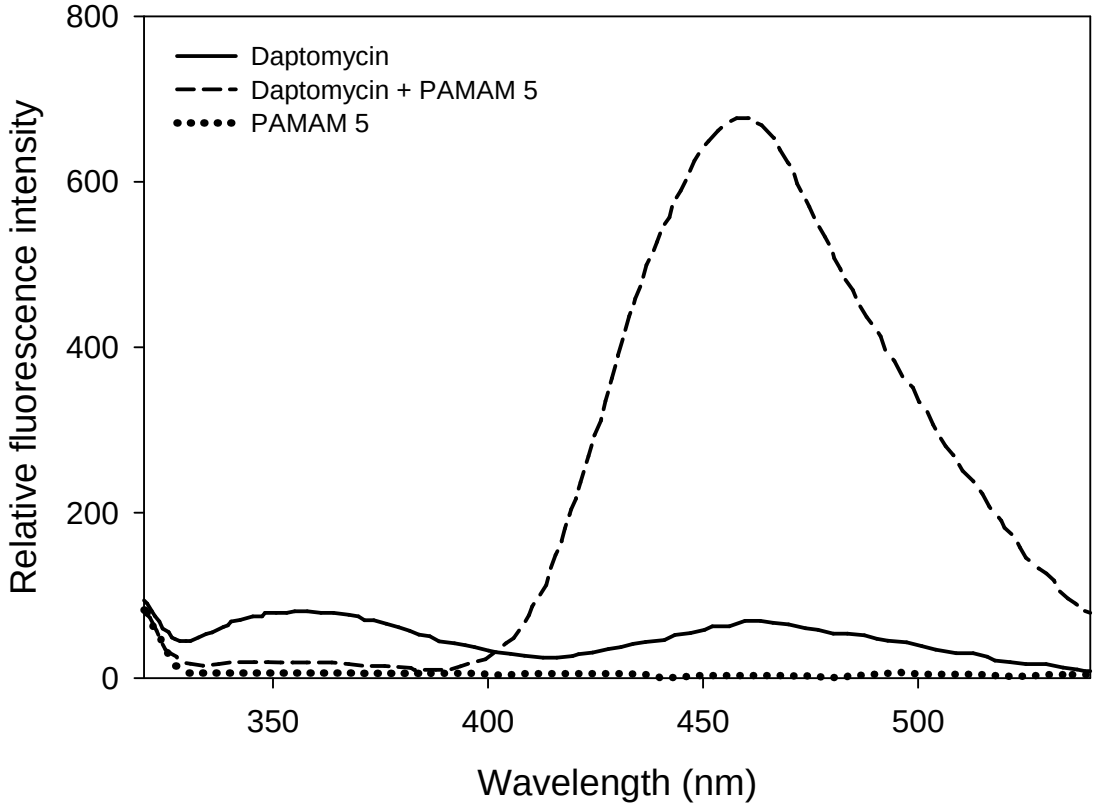

Figure V-2. The fluorescence spectra of daptomycin (3.0 µM), PAMAM 5 (0.18 µM), and a mixture of daptomycin (3.0 µM) and PAMAM 5 (0.18 µM) at pH 4.0 (cuvette path length 10 mm; excitation wavelength at 285 nm).

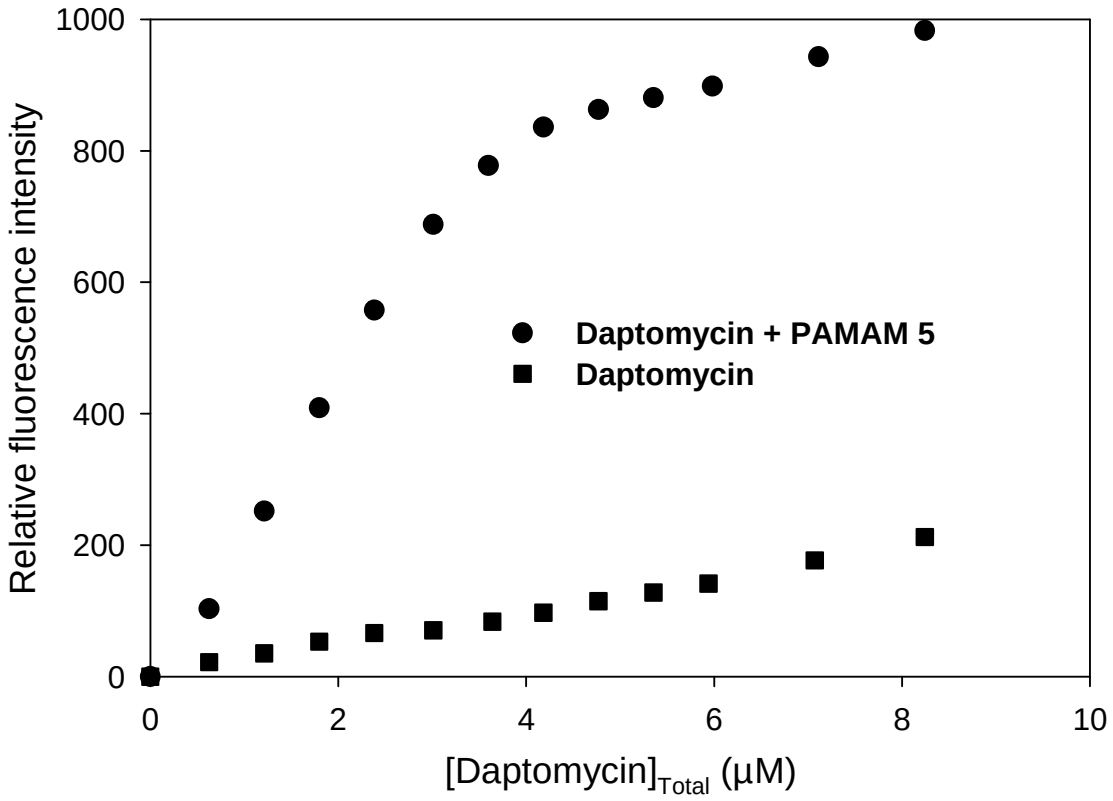

Figure V-3. The fluorescence intensities of daptomycin at 460 nm in the absence (solid square) and in the presence (solid circle) of PAMAM 5 at pH 5.0 (cuvette path length 10 mm; excitation wavelength at 285 nm).

Effects of pH and Dendrimer Size on the Binding Characteristics of Daptomycin Dendrimer Complex

The interaction between daptomycin and dendrimer is anticipated to be ionic interaction. The factors affecting the ionic states of both compounds were investigated using various size dendrimers PAMAM 5 and 6 in the pH range from 3 to 9. The generation number of dendrimers determines the size and amount of surface functional groups. The magnitude of the maximum fluorescence intensities varied with pH and necessitated using different concentrations of PAMAM and daptomycin. The binding isotherms in the different pH solutions were normalized by the substrate (PAMAM) concentrations.

In the presence of PAMAM 5 (Figure V-4), the typical binding isotherms of the normalized fluorescence differences (ΔF) from pH 3.5 to 8 showed a steep increase at low concentration and a plateau at higher concentrations of daptomycin, which were consistent with one-site binding model.[84] In addition, the magnitude of the normalized ΔF values in the ranges of pH 3.5 to 4.5 were 4 to 5 fold greater than those in the ranges of pH 5 to 8.

In the presence of PAMAM 6 (Figure V-5), the normalized fluorescence differences (ΔF) in the ranges of pH 3.5 to 5 steeply increased and attained plateau with increasing daptomycin concentrations as described in PAMAM 5, which conformed to the one-site binding model . In the pH range of 6 to 7, the isotherms were different in that the normalized ΔF values increased at low daptomycin concentration, attained a maximum value, and then gradually decreased with increasing daptomycin concentrations. This isotherm shape suggested changes in binding at higher concentrations either due to a loss in binding capacity or a second binding site that was associated with a loss in fluorescence intensity. The binding isotherms shapes varied with the pH values of the titration solutions.

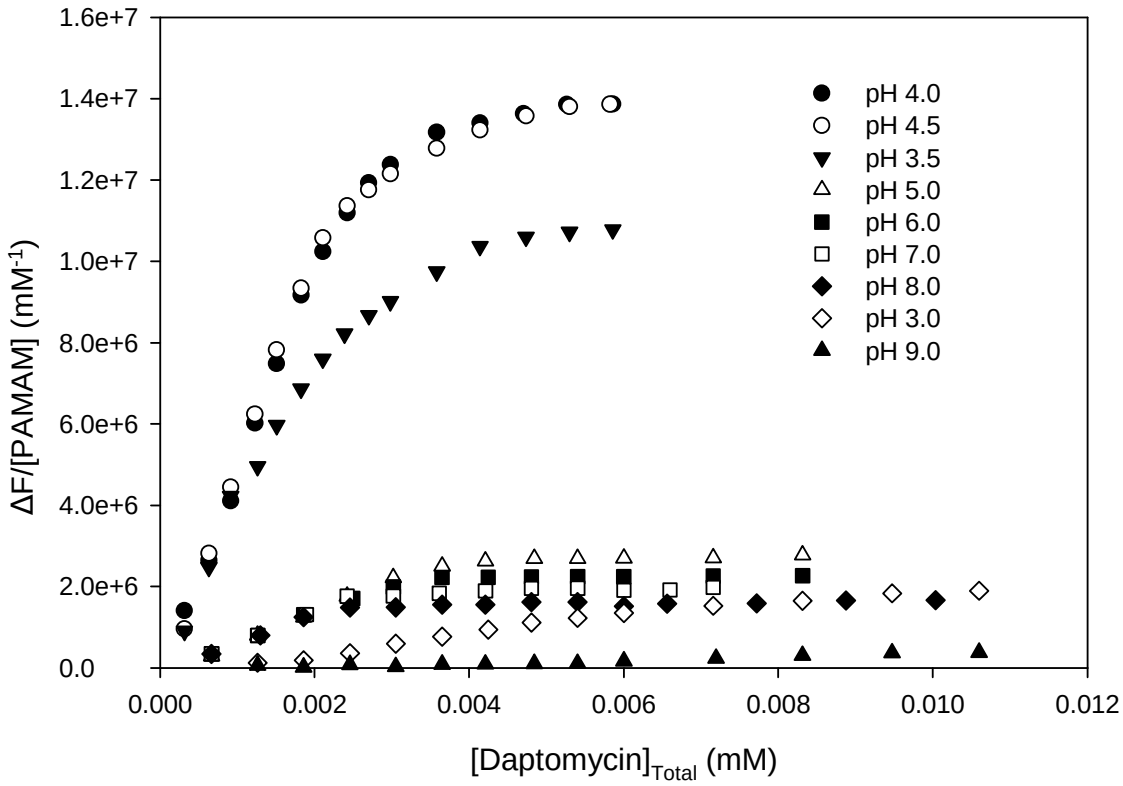

Figure V-4. The binding isotherms of the interaction between PAMAM 5 and daptomycin in the range of pH 3.0 to 9.0. The normalized ΔF values were the ratio of ΔF value to PAMAM 5 concentration.

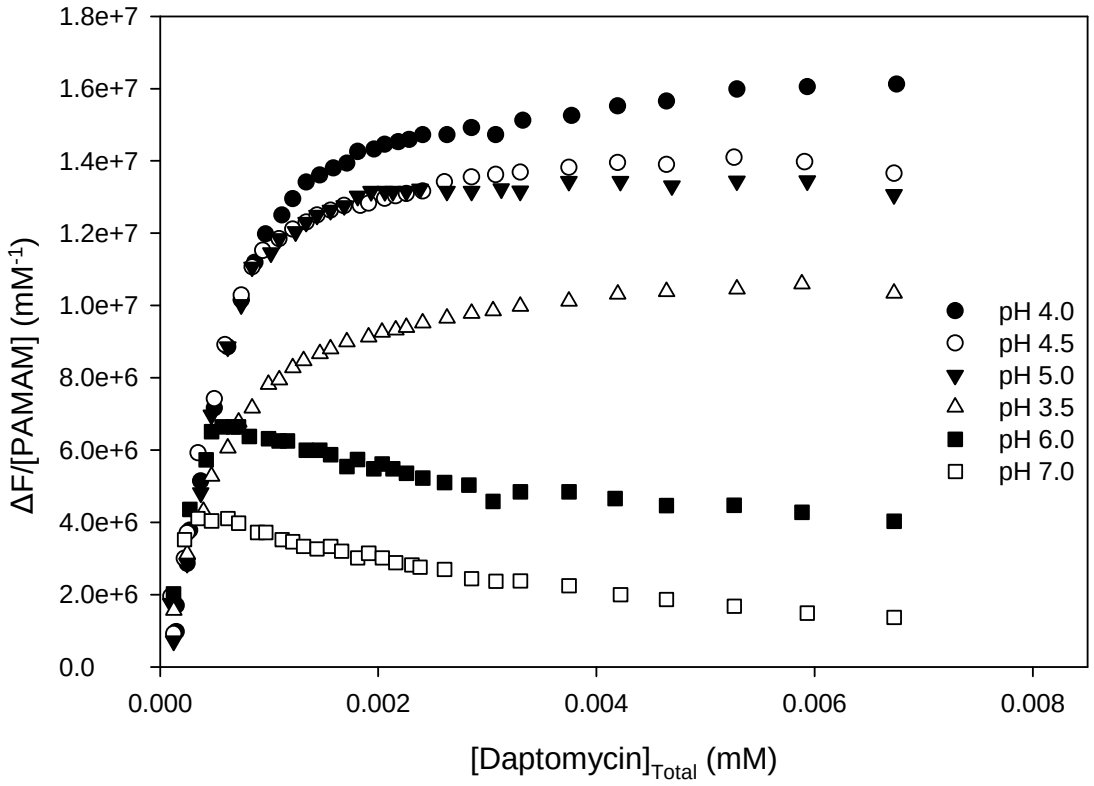

Figure V-5. The binding isotherms of the interaction between PAMAM 6 and daptomycin in the range of pH 3.5 to 7.0. The normalized ΔF values were the ratio of ΔF value to PAMAM 6 concentration.

Binding Parameters

The shapes of the isotherms were used to deduce the nature of the binding process and then to estimate the binding parameters. The binding parameter, molar extinction coefficient (ΔE), dissociation constant (K_d), and the total number independent binding sites (R), were estimated by simultaneously fitting the model equation to the binding isotherm by nonlinear regression analysis.

The molar extinction coefficient (ΔE) obtained from the fitting of the binding isotherms of PAMAM 5 titration in the pH ranges from 3.5 to 8 were not significantly different. The constant value of ΔE indicated that the interaction between daptomycin and PAMAM 5 was identical throughout the pH range of 3.5 to 8. Consequently, the ΔE value was fixed for all binding isotherms at a constant mean value of 240.1. Then, the one-site model was re-fitted to all binding isotherms with just two adjustable parameters in an attempt to attribute pH differences to the binding parameters, K_d and R. The capacity constant (n, molecules of bound daptomycin per one molecule of PAMAM dendrimer) of each individual pH range was then calculated based on the ratio of the estimated R value to the total concentration of PAMAM dendrimer. The capacity constants (n) in Figure V-6 appeared to change dramatically as function of pH, whereas the dissociation constants were not notably pH-dependent.

From the titration of PAMAM 6 experimental data in the pH ranges from 3.5 to 5, the binding interactions were consistent with one-site binding model. Two-site model were used to describe the data obtained at pH 6 and 7. The binding parameters were estimated by simultaneously fitting the model equation to the binding isotherm data using nonlinear regression analysis. The molar extinction coefficient (ΔE), the dissociation constant (K_d), and the capacity constant (n) to the one-site and two-site types of binding interactions were estimated at each pH value.

The major ionic species of daptomycin and dendrimers play an important role in the binding interactions. To understand the binding mechanism between daptomycin and

dendrimers, the comparisons of the ionization profiles of daptomycin and the capacity constants (n) of dendrimers in different pH ranges are shown in Figure V-6.

Discussion

As discussed in Chapter II, daptomycin contains six ionizable groups, four side-chain carboxylic groups (three aspartic acids, Asp-3, Asp-7, and Asp-9, and one methyl-glutamic acid, mGlu-12) and two primary amines (an aromatic amine in Kyn-13 and an aliphatic amine in Orn-6). Based on the 2D ^{1}H TOCSY NMR pH titration, the sequence specific pK_a values for Asp-7, Kyn-13, Asp-9, Asp-3, and mGlu-12 were estimated to be 1.01, 1.30, 3.85, 4.15, and 4.55, respectively. The aliphatic amine Orn-6 in daptomycin has a pK_a value of 10.7. The Orn-6 residue is always protonated at pH values below 10.[19] In the pH range of 0.8 to 3.5, major ionic species of daptomycin is a zwitterionic ($H_4A^{\pm}$) form due to the deprotonation of Asp-7 (Figure V-6). Monoanion (H_3A^-) and dianion (H_2A^{2-}) forms dominate in the pH range of 3.5 to 4.7 due to the further deprotonation of Asp-9 and Asp-3 (Figure V-6). Above pH 4.7, the trianion (HA^{3-}) is the main ionic form as mGlu-12 residue is gradually deprotonated.

PAMAM dendrimers have an outer shell of primary amines with a pK_a values in the range of 7-9 and internal, tertiary amines with pK_a values between 3 and 6.[78,88-90] PMAMA 5 has 128 primary amines and 126 tertiary amines. The numbers of primary and tertiary nitrogens in PAMAM 6 are 256 and 254, respectively.[78,91] The protonation of PAMAM dendrimers first involves protonation of primary amine groups at the outer rim of the dendrimer at high pH, while the tertiary amine groups in the dendrimer core are protonated at lower pH. The last groups to protonate at low pH are a central tertiary amines.[88]

Comparisons of daptomycin ionization profiles and the pH-dependent binding capacity parameters obtained using PAMAM 5 and 6 (Figure V-6) suggest that the primary determinants in the magnitude of the binding capacity appear to be the presence

of the monoanionic (H_3A^-) and dianionic (H_2A^{2-}) forms. In the pH range from 3.7 to 5.2, all primary amine groups are protonated, and tertiary amino groups situated in the dendrimer interior are partially protonated.[88] Thus, the major binding sites may be due to electrostatic interaction between Asp-9 and Asp-3 and cationic moieties on the dendrimer surface. The dominant species of daptomycin in pH 3.5 is in zwitterionic ($H_4A^{\pm}$) form, so the capacity constants for PAMAM 5 and 6 in pH 3.5 were less than those in pH 4.0 and 5.0.

The capacity constants greatly decreased as pH > 4.7 for PAMAM 5 and pH > 5.2 for PAMAM 6. This could be explained by the unique property of polyelectrolyte dendrimers, the pH dependence of size, charges, and structure of dendrimers.[92] Increasing the solutions from low pH (~4, primary amines protonated and tertiary amines also protonated), neutral (~7, only primary amines protonated), to high pH (~10, no protonation), the gyration radius of PAMAM 5 changes from 25 to 22 to 21 Å, respectively.[93] The numbers of total positive charges and diameter of PAMAM 6 (Figure V-7) are reported to be 405 e^+ and 7.1 nm at pH 5.5, 256 e^+ and 6.28 nm at pH 7.0, and 160 e^+ and 6.08 nm at pH 8.5, respectively.[94] Enhancing the solution pH from 5.5 to 8.5 results in a 2.7-fold decrease of dendrimer (PAMAM 6) valence.[94] As a consequence of interior electrostatic repulsions at low pH, dendrimer branches are further extended leading to an increase in dendrimer radius and surface area. Thus, the decrease in the estimated capacity constants observed for PAMAM 5 (pH >4.7) and 6 (pH>5.2) could be explained based on the combination of reduced dendrimer size, surface area, and effective positive charges due to the deprotonation of interior amines and the loss of internal electrostatic repulsion.[93]

The interaction between negative charges in Asp-3 and Asp-9 residues with positive primary amines on the surface of PAMAM 5 is consistent with the one-site binding model via throughout the pH range of 3.5 to 8. Thus, the capacity constant

decrease as a function of pH is likely due to pH-dependent changes in dendrimer properties rather than changes in daptomycin ionization.

The mono- and di-anionic forms are contributed to daptomycin binding to PAMAM 6 in the pH range of 3.5 to 5. This observation is consistent with the relationship observed for PAMAM 5. Since large dendrimers have a greater number of amines that can bind daptomycin, the overall binding constant on a per dendrimer basis increases with dendrimer generations from PAMAM 5 to 6.[95] The decrease in the estimated capacity constant observed in the pH range 5 to 7 appears to correlate to the deprotonation of the dendrimer tertiary amines (Figure V-6). This observation is more distinct for capacity constants estimated for daptomycin interactions with PAMAM 6 than PAMAM 5. The larger pH-dependent capacity constant change observed for the larger dendrimer PAMAM 6 over the range of pH values are associated with tertiary amine deprotonation. In the pH range of 6 to 7, the interaction between daptomycin with PAMAM 6 conforms to the two-site model.

For both PAMAM 5 and 6, the optimal binding occurs in the pH region 3.5 to 4.5 wherein both the external and internal dendrimer amines are protonated and daptomycin is in its monoanionic and dianionic forms. The intermolecular interaction is based on electrostatic attraction, wherein the deprotonated Asp-9 and Asp-3 of daptomycin primarily interacts with surface amine on the dendrimers.

Conclusions

The fluorescence changes of the enhanced FRET between Trp-1 and Kyn-13 were observed upon PAMAM solutions titrated with daptomycin, which are due to the alteration of daptomycin conformation. The shapes of the binding isotherms and the dependence of the estimated capacity constants on dendrimer size and solvent pH values provide meaningful insight into the interaction mechanism of daptomycin and dendrimers. By comparing the ionization profiles of daptomycin based on the estimated

individual pK_a values and Hill coefficients with the pH-dependent binding capacity, the ionized Asp-3 and Asp-9 residues of daptomycin primarily interact with PAMAM cationic surface amines.

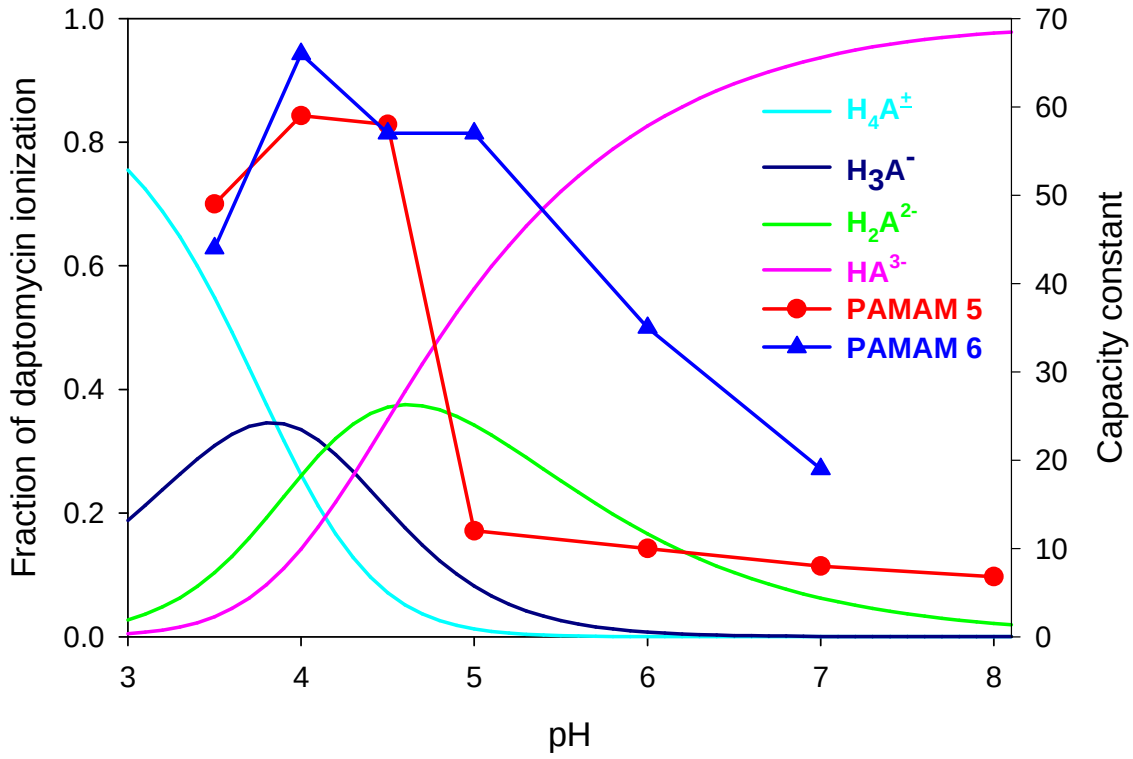

Figure V-6. Comparison of the distribution of ionic forms of daptomycin with the estimated capacity constants for its interactions with PAMAM 5 and 6. Fraction of daptomycin ionization varied from zwitterion ($H_4A^{\pm}$), anion (H_3A^-), dianion (H_2A^{2-}), and trianion (HA^{3-}), respectively. Each point represented the capacity constant (molecule of daptomycin/molecule of PAMAM) obtained from binding interaction between daptomycin and PAMAM 5 and 6 at various pH solutions.

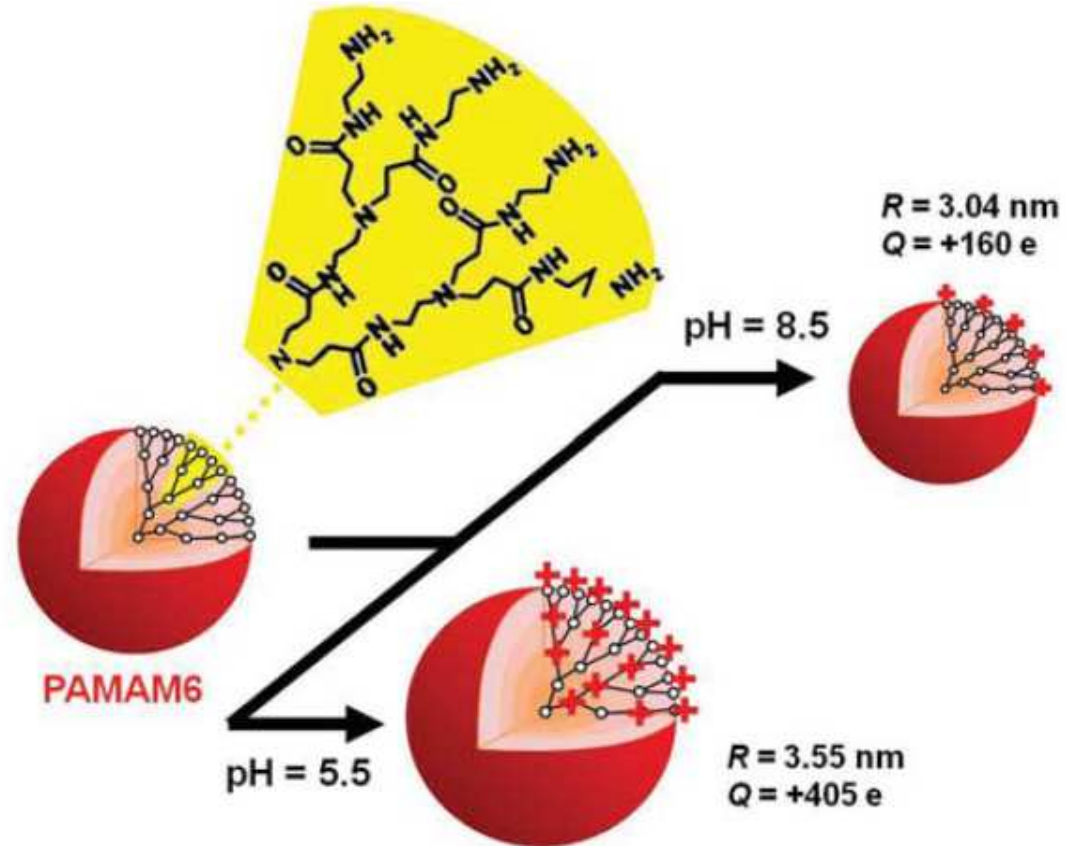

Figure V-7. Schematic representation of PAMAM 6 size and charge pH dependence.[94]

APPENDIX A. DAPTOMYCIN BJERRUM PLOT

Daptomycin contains six ionizable groups (aliphatic amine in Orn-6, aromatic amine in Kyn-13, and four carboxylic groups, Asp-3, Asp-7, Asp-9, mGlu-12). In the pH range from 3 to 7, an aliphatic amine in Orn-6 is always protonated in one positive charge. Daptomycin can be considered to be dissociable with its 4 side-chain carboxylic groups. When the four carboxylic acid side chains are completely protonated, the daptomycin is in its DH_5^+ form. There are only four titrable protons in DH_5^+ form in the potentiometric titration pH range from 3 to 7.

Note: Sodium ions (Na^+) are introduced by the deliberated addition sodium hydroxide (NaOH) to adjust pH to 7 to ensure complete dissociation prior to titration. Chloride ions (Cl^-) originate from the titrant (HCl).

Derivation of dissociation of daptomycin (DH_5^+)

Charge balance:

$$[H^+] + [Na^+] + [DH_5^+] = [OH^-] + [Cl^-] + [DH_3^-] + 2[DH_2^{2-}] + 3[DH^{3-}] \quad (1)$$

Total daptomycin $[DH_5^+]_{Total}$:

$$[DH_5^+] + [DH_4^{\pm}] + [DH_3^-] + [DH_2^{2-}] + [DH^{3-}] = [DH_5^+]_{Total} \quad (2)$$

Rearranging Equation (1) gives

$$[DH_5^+] - [DH_3^-] - 2[DH_2^{2-}] - 3[DH^{3-}] = [OH^-] + [Cl^-] - [H^+] - [Na^+] \quad (3)$$

Multiplying equation (2) by 3 and adding it to Equation (3) gives

$$4[DH_5^+] + 3[DH_4^{\pm}] + 2[DH_3^-] + [DH_2^{2-}] = 3[DH_5^+]_{Total} + [OH^-] + [Cl^-] - [H^+] - [Na^+] \quad (4)$$

Total bound hydrogen ions (H^+) is:

$$4[DH_5^+] + 3[DH_4^{\pm}] + 2[DH_3^-] + [DH_2^{2-}] = 3[DH_5^+]_{Total} + [OH^-] + [Cl^-] - [H^+] - [Na^+] \quad (5)$$

Dividing Equation (4) by $[DH_5^+]_{Total}$ (Equation (2)) gives

n_H = (Total moles of bound hydrogen ions, H^+)/(Total moles of weak acid daptomycin)

$$=4[DH_5^+] + 3[DH_3] + 2[DH_3^-] + [DH_2^{2-}] / \{[DH_5^+] + [DH_4^{\pm}] + [DH_3^-] + [DH_2^{2-}] + [DH^{3-}]\}$$

$$=3[DH_5^+]_{Total} + [OH^-] + [Cl^-] - [H^+] - [Na^+]/\{[DH_5^+] + [DH_4^{\pm}] + [DH_3^-] + [DH_2^{2-}] + [DH^{3-}]\}$$

$= 3 + \{[OH^-] + [Cl^-] - [H^+] - [Na^+]\} / [DH_5^+]_{Total}$

$= 3 - \{[H^+] - [OH^-] + [Na^+] - [Cl^-]\} / [DH_5^+]_{Total}$ (6)

Titrant: C_A HCl (C_A = 1.0 M)

Initial Volume: V_0

Added Volume: V

Total Volume: V_0 +V

n_H = (moles of bound H^+)/(total moles of daptomycin)

$=\{4[DH_5^+] + 3[DH_3] + 2[DH_3^-] + [DH_2^{2-}]\}/\{[DH_5^+] + [DH_3] + [DH_3^-] + [DH_2^{2-}] + [DH^{3-}]\}$

$n_H = 3 - \{[H^+] - [OH^-] + [Na^+] - [Cl^-]\}/ [[DH_5^+]_{Total}$

$= 3 - \{ 10^{-pH} - 10^{pH - pKw} + [Na^+] - [Cl^-]\} / [DH_5^+]_{Total}$

$[H^+] = 10^{-pH}$

$[OH^-] = 10^{pH - pKw}$

$[Na^+] = C_bV_b/(V_0 + V)$ (calculated by accurately adding NaOH moles to adjust pH before acidic titration)

$[Cl^-] = C_A*V/(V_0 + V)$ (calculated by accurately adding the volume (V) of standard titrant HCl concentration, C_A)

$[DH_5^+]_{Total}$ (C_M) = Accurate weight of daptomycin added (mg)/1620.67 (MW)/($V+V_0$) (mL)

APPENDIX B. CALCULATIONS OF pH-DEPENDENT SPECIES DISTRIBUTION FOR DAPTOMYCIN

pK_a values and Hill coefficients (n) of the ionizable groups of daptomycin:

pK_{a1} = 1.01 (Asp-7); $K_{a1} = 10^{-1.01}$; n_1 = 0.72;

pK_{a2} = 1.30 (Kyn-13); $K_{a2} = 10^{-1.30}$; n_2 = 0.88;

pK_{a3} = 3.85 (Asp-9); $K_{a3} = 10^{-3.85}$; n_3 = 0.71;

pK_{a4} = 4.15 (Asp-3); $K_{a4} = 10^{-4.15}$; n_4 = 0.73

pK_{a5} = 4.55 (mGlu-12); $K_{a5} = 10^{-4.55}$; n_5 = 0.48

pK_{a6} = 10.7 (Orn-6); $K_{a6} = 10^{-10.7}$; n_6 = 1.00*

* The Hill coefficients value of Orn-6 (n_6) was not obtained using TOCSY NMR and is assumed to be 1.00.

The six ionizable residues in daptomycin are considered to be in the completely protonated and deprotonated states.

Species: H_6A^{2+}, H_5A^{+}, $H_4A^{\pm}$, H_3A^{-}, H_2A^{2-}, HA^{3-}, A^{4-};

Polyprotic (polybasic) acids dissociate in multiple steps which are characterized by the consecutive dissociation constants K_1, K_2, … K_n ($K_1 > K_2$, … K_n).

Fractions of ionic species (α_n):

$C_{H6A} = [H_6A^{2+}] + [H_5A^{+}] + [H_4A^{\pm}] + [H_3A^{-}] + [HA^{2-}] + [HA^{3-}] + [A^{4-}]$

$\alpha_0 = [H_6A^{2+}] / C_{H6A}$

$\alpha_1 = [H_5A^{+}] / C_{H6A}$

$\alpha_2 = [H_4A^{\pm}] / C_{H6A}$

$\alpha_3 = [H_3A^{-}] / C_{H6A}$

$\alpha_4 = [H_2A^{2-}] / C_{H6A}$

$\alpha_5 = [HA^{3-}] / C_{H6A}$

$\alpha_6 = [A^{4-}] / C_{H6A}$

Denominator:

$$D = [H^+]^6 + K_1[H^+]^5 + K_1K_2[H^+]^4 + K_1K_2K_3[H^+]^3 + K_1K_2K_3K_4[H^+]^2 + K_1K_2K_3K_4K_5[H^+] + K_1K_2K_3K_4\,K_5K_6$$

$$\alpha_0 = [H^+]^6 / D;$$

$$\alpha_1 = K_1[H^+]^5 / D;$$

$$\alpha_2 = K_1K_2[H^+]^4 / D;$$

$$\alpha_3 = K_1K_2K_3[H^+]^3 / D;$$

$$\alpha_4 = K_1K_2K_3K_4[H^+]^2 / D;$$

$$\alpha_5 = K_1K_2K_3K_4K_5[H^+] / D;$$

$$\alpha_6 = K_1K_2K_3K_4\,K_5K_6 / D;$$

Fractions of ionic species calculated with the measured Hill coefficients:

Denominator:

$$D = [H^+]^{(n1+n2+n3+n4+n5+n6)} + K_1^{n1}[H^+]^{(n2+n3+n4+n5+n6)} + K_1^{n1}K_2^{n2}[H^+]^{(n3+n4+n5+n6)} + K_1^{n1}K_2^{n2}K_3^{n3}[H^+]^{(n4+n5+n6)} + K_1^{n1}K_2^{n2}K_3^{n3}K_4^{n4}[H^+]^{(n5+n6)} + K_1^{n1}K_2^{n2}K_3^{n3}K_4^{n4}K_5^{n5}[H^+]^{n6} + K_1^{n1}K_2^{n2}K_3^{n3}K_4^{n4}K_5^{n5}K_6^{n6}$$

$$\alpha_0 = [H^+]^{(n1+n2+n3+n4+n5+n6)} / D;$$

$$\alpha_1 = K_1^{n1}[H^+]^{(n2+n3+n4+n5+n6)} / D;$$

$$\alpha_2 = K_1^{n1}K_2^{n2}[H^+]^{(n3+n4+n5+n6)} / D;$$

$$\alpha_3 = K_1^{n1}K_2^{n2}K_3^{n3}[H^+]^{(n4+n5+n6)} / D;$$

$$\alpha_4 = K_1^{n1}K_2^{n2}K_3^{n3}K_4^{n4}[H^+]^{(n5+n6)} / D;$$

$$\alpha_5 = K_1^{n1}K_2^{n2}K_3^{n3}K_4^{n4}K_5^{n5}[H^+]^{(n6)} / D;$$

$$\alpha_6 = K_1^{n1}K_2^{n2}K_3^{n3}K_4^{n4}K_5^{n5}K_6^{n6} / D;$$

REFERENCES

1. Philo JS, Arakawa T 2009. Mechanisms of protein aggregation. Curr Pharm Biotechnol 10(4):348-351.

2. Debono M, Abbott B, Molloy R, Fukuda D, Hunt A, Daupert V, Counter F, Ott J, Carrell C, Howard L, Boeck L, Hamill R 1988. Enzymatic and chemical modifications of lipopeptide antibiotic A21978C: the synthesis and evaluation of daptomycin (LY146032). J Antibiot 41(8):1093-1105.

3. Tally FP, DeBruin MF 2000. Development of daptomycin for Gram-positive infections. J Antimicrob Chemother 46(4):523-526.

4. Enoch DA, Bygott JM, Daly M-L, Karas JA 2007. Daptomycin. J Infection 55(3):205-213.

5. Raja A, LaBonte J, Lebbos J, Kirkpatrick P 2003. Daptomycin. Nat Rev Drug Discov 2(12):943-944.

6. Tenover FC 2006. Mechanisms of antimicrobial resistance in bacteria. Am J Med 119(6A):S3-S10.

7. Silverman JA, Perlmutter NG, Shapiro HM 2003. Correlation of daptomycin bactericidal activity and membrane depolarization in *Staphylococcus aureus*. Antimicrob Agents Chemother 47(8):2538-2544.

8. Steenbergen JN, Alder J, Thorne GM, Tally FP 2005. Daptomycin: a lipopeptide antibiotic for the treatment of serious Gram-positive infections. J Antimicrob Chemother 55(3):283-288.

9. Straus SK, Hancock REW 2006. Mode of action of the new antibiotic for Gram-positive pathogens daptomycin: Comparison with cationic antimicrobial peptides and lipopeptides. Biochim Biophys Acta - Biomembr 1758(9):1215-1223.

10. Eliopoulos GM. 2008. Antimicrobial Resistance in the Enterococcus. 2nd ed., New York: CRC Press. p 264.

11. Ho SW, Jung D, Calhoun JR, Lear JD, Okon M, Scott WRP, Hancock REW, Straus SK 2008. Effect of divalent cations on the structure of the antibiotic daptomycin. Eur Biophys J 37(4):421-433.

12. Scott WRP, Baek S-B, Jung D, Hancock REW, Straus SK 2007. NMR structural studies of the antibiotic lipopeptide daptomycin in DHPC micelles. Biochim Biophys Acta - Biomembr 1768(12):3116-3126.

13. Ball L-J, Goult CM, Donarski JA, Micklefield J, Ramesh V 2004. NMR structure determination and calcium binding effects of lipopeptide antibiotic daptomycin. Org Biomol Chem 2(13):1872-1878.

14. Jung D, Rozek A, Okon M, Hancock REW 2004. Structural transitions as determinants of the action of the calcium-dependent antibiotic daptomycin. Chem & Biol 11(7):949-957.

15. Rotondi KS, Gierasch LM 2005. A well-defined amphipathic conformation for the calcium-free cyclic lipopeptide antibiotic, daptomycin, in aqueous solution. Biopolymers 80(2-3):374-385.

16. Clark AT, Smith K, Muhandiram R, Edmondson SP, Shriver JW 2007. Carboxyl pK_a values, ion pairs, hydrogen bonding, and the pH-dependence of folding the hyperthermophile proteins Sac7d and Sso7d. J Mol Biol 372(4):992-1008.

17. Huyghues-Despointes BMP, Thurlkill RL, Daily MD, Schell D, Briggs JM, Antosiewicz JM, Pace CN, Scholtz JM 2003. pK_a values of histidine residues in ribonuclease Sa: Effect of salt and net charge. J Mol Biol 325(5):1093-1105.

18. Kirsch LE, Molloy RM, Debono M, Baker P, Farid KZ 1989. Kinetics of the aspartyl transpeptidation of daptomycin, a novel lipopeptide antibiotic. Pharm Res 6(5):387-393.

19. Muangsiri W. 2000. The Kinetics of the Alkaline Degradation of Daptomycin. ed., Iowa City: University of Iowa. p 25-30.

20. Keeler J. 2010. 8 Two-dimensional NMR. Understanding NMR Spectroscopy, 2nd ed., Hoboken, NJ: John Wiley & Sons. p 183-226.

21. Claridge TDW. 2009. Correlations through the Chemical Bond I: Homonuclear Shift Correlation. In Claridge TDW, editor High-Resolution NMR Techniques in Organic Chemistry, 2nd ed., New York: Elsevier. p p129-188.

22. Avdeef A 2001. Physicochemical profiling (solubility, permeability and charge state). Curr Top Med Chem 1:277-351.

23. Avdeef A. 2003. Charge State. In Avdeef A, editor Absorption and Drug Development: Solubility, Permeability, and Charge State, 1st ed., Hoboken, New Jersey: Wiley Interscience. p 22-41.

24. Kraft A 2003. The determination of the pK_a of multiprotic, weak acids by analyzing potentiometric acid-base titration data with difference plots. J Chem Educ 80(5):554-559.

25. Delaglio F, Grzesiek S, Vuister GW, Zhu G, Pfeifer J, Bax A 1995. NMRPipe: A multidimensional spectral processing system based on UNIX pipes. J Biomol NMR 6(3):277-293.

26. Johnson BA, Blevins RA 1994. NMR View: A computer program for the visualization and analysis of NMR data. J Biomol NMR 4(5):603-614.

27. Albert A, Serjeant EP. 1984. Determination of Ionization Constants by Spectrophotometry. The Determination of Ionization Constants: A Laboratory Manual, 3rd ed., New York: Chapman and Hall. p 70-73.

28. Markley JL 1975. Observation of histidine residues in proteins by nuclear magnetic resonance spectroscopy. Acc Chem Res 8(2):70-80.

29. Quijada J, López G, Versace R, Ramírez L, Tasayco ML 2007. On the NMR analysis of pK_a values in the unfolded state of proteins by extrapolation to zero denaturant. Biophys Chem 129(2-3):242-250.

30. Albert A, Serjeant EP. 1984. Determination of Ionization Constants by Spectrophotometry. The Determination of Ionization Constants: A Laboratory Manual, 3rd ed., New York: Chapman and Hall. p 24-25.

31. Cistola DP, Hamilton JA, Jackson D, Small DM 1988. Ionization and phase behavior of fatty acids in water: application of the Gibbs phase rule. Biochem 27(6):1881-1888.

32. Tang C, Smith AM, Collins RF, Ulijn RV, Saiani A 2009. Fmoc-diphenylalanine self-assembly mechanism induces apparent pK_a shifts. Langmuir 25(16):9447-9453.

33. Qiu J, Kirsch LE. 2007. Evaluation of lipopeptide aggregation (Daptomycin) using light scattering, fluorescence, and NMR spectroscopy. 2007 AAPS Annual Meeting and Exposition, ed.

34. Qiu J, Kirsch LE. 2008. The role of aggregation on the ionization, hydrolytic degradation, and intermolecular interactions of daptomycin. 2008 AAPS Annual Meeting and Exposition, ed.

35. Balón M, Carmona MC, Muñoz MA, Hidalgo J 1989. The acid-base properties of pyrrole and its benzologs indole and carbazole. A reexamination from the excess acidity method. Tetrahedron 45(23):7501-7504.

36. Bartik K, Redfield C, Dobson CM 1994. Measurement of the individual pK_a values of acidic residues of Hen and Turkey lysozymes by Two-Dimensional ^1H NMR. Biophys J 66(4):1180-1184.

37. Joshi MD, Hedberg A, McIntosh LP 1997. Complete measurement of the pK_a values of the carboxyl and imidazole groups in *Bacillus circulans* xylanase. Protein Sci 6(12):2667-2670.

38. Kelly RN, Schulman SG. 1985. Proton Transfer Kinetics of Electronically Excited Acids and Bases. In Schulman SG, editor Molecular Luminescence Spectroscopy Methods and Applications: Part 2, 1st ed., New York: John Wiley & Sons. p 461-471.

39. Grimsley GR, Scholtz JM, Pace CN 2009. A summary of the measured pK_a values of the ionizable groups in folded proteins. Protein Sci 18(1):247-251.

40. Wang W 1999. Instability, stabilization, and formulation of liquid protein pharmaceuticals. Int J Pharm 185(2):129-188.

41. Wang W 2005. Protein aggregation and its inhibition in biopharmaceutics. Int J Pharm 289(1-2):1-30.

42. Lakey JH, Ptak M 1988. Fluorescence indicates a calcium-dependent interaction between the lipopeptide antibiotic LY146032 and phospholipid membranes. Biochem 27(13):4639-4645.

43. Muangsiri W, Kirsch LE 2001. The kinetics of the alkaline degradation of daptomycin. J Pharm Sci 90(8):1066-1075.

44. Garidel P, Kebbel F 2010. Protein therapeutics and aggregates characterized by photon correlation spectroscopy. BioProcess Inter 8(3):38-46.

45. Hawe A, Sutter M, Jiskoot W 2008. Extrinsic fluorescent dyes as tools for protein characterization. Pharm Res 25(7):1487-1499.

46. Lakowicz JR. 1999. Energy Transfer. In Lakowicz JR, editor Principles of Fluorescence Spectroscopy, 2nd ed., New York: Kluwer Academic/Plenum Publishers. p 367-388.

47. Grunewald J, Kopp F, Mahlert C, Linne U, Sieber SA, Marahiel MA 2005. Fluorescence resonance energy transfer as a probe of peptide cyclization catalyzed by nonribosomal thioesterase domains. Chem Biol 12(8):873-881.

48. Villari V, Micali N 2008. Light scattering as spectroscopic tool for the study of disperse systems useful in pharmaceutical sciences. J Pharm Sci 97(5):1703-1730.

49. Muraih JK, Harris J, Taylor SD, Palmer M 2012. Characterization of daptomycin oligomerization with perylene excimer fluorescence: Stoichiometric binding of phosphatidylglycerol triggers oligomer formation. Biochim Biophys Acta 1818(3):673-678.

50. He F, Phan DH, Hogan S, Bailey R, Becker GW, Narhi LO, Razinkov VI 2010. Detection of IgG aggregation by a high throughput method based on extrinsic fluorescence. J Pharm Sci 99(6):2598-2608.

51. Mahler H-C, Friess W, Grauschopf U, Kiese S 2009. Protein aggregation: Pathways, induction factors and analysis. J Pharm Sci 98(9):2909-2934.

52. Riek R, Pervushin K, Wüthrich K 2000. TROSY and CRINEPT: NMR with large molecular and supramolecular structures in solution. Trends Biochem Sci 25(10):462-468.

53. Hitscherich CJ, Aseyev V, Wiencek J, Loll PJ 2001. Effects of PEG on detergent micelles: implications for the crystallization of integral membrane proteins. Acta Crystallogr D Biol Crystallogr 57(2):454-459.

54. Podzimek S. 2011. Light Scattering. Light Scattering, Size Exclusion Chromatography and Asymmetric Flow Field Flow Fractionation, 1st ed., Hoboken, New Jersey: John Wiley & Sons, Inc. p 37-98.

55. Mitra A, Seaton PJ, Ali Assarpour R, Williamson T 1998. Unprecedented concentration dependent chemical shift variation in ^{1}H-NMR studies: A caveat in the investigations of molecular recognition and structure elucidation. Tetrahedron 54(51):15489-15498.

56. Shetty AS, Zhang J, Moore JS 1996. Aromatic π-stacking in solution as revealed through the aggregation of phenylacetylene macrocycles. J Am Chem Soc 118(5):1019-1027.

57. Veselkov AN, Dymant LN, Kulikov ÉL 1985. Investigation of aggregation of acridine orange dye molecules by means of proton magnetic resonance. J Struct Chem 26(3):354-357.

58. Lamp KC, Rybak MJ 1993. Teicoplanin and daptomycin bactericidal activities in the presence of albumin or serum under controlled conditions of pH and ionized calcium. Antimicrob Agents Chemother 37(3):605-609.

59. Lamp KC, Rybak MJ, Bailey EM, Kaatz GW 1992. In vitro pharmacodynamic effects of concentration, pH, and growth-phase on serum bactericidal activities of daptomycin and vancomycin. Antimicrob Agents Chemother 36(12):2709-2714.

60. Dvorchik BH, Brazier D, DeBruin MF, Arbeit RD 2003. Daptomycin pharmacokinetics and safety following administration of escalating doses once daily to healthy subjects. Antimicrob Agents Chemother 47(4):1318-1323.

61. Benvenuto M, Benziger DP, Yankelev S, Vigliani G 2006. Pharmacokinetics and tolerability of daptomycin at doses up to 12 milligrams per kilogram of body weight once daily in healthy volunteers. Antimicrob Agents Chemother 50(10):3245-3249.

62. Bahte SK, Bertram A, Burkhardt O, Martens-Lobenhoffer J, Goedecke V, Bode-Böger SM, Hiss M, Kielstein JT 2010. Therapeutic serum concentrations of daptomycin after intraperitoneal administration in a patient with peritoneal dialysis-associated peritonitis. J Antimicrob Chemother 65(6):1312-1314.

63. Goedecke VA, Clajus C, Burkhardt O, Martens-Lobenhoffer J, Bode-Böger SM, Kielstein JT, Hiss M 2009. Pharmacokinetics and dialysate levels of daptomycin given intravenously in a peritoneal dialysis patient. Scand J Infect Dis 41(2):155-157.

64. Larsson L, Öhman S 1978. Serum ionized calcium and corrected total calcium in borderline hyperparathyroidism. Clin Chem 24(11):1962-1965.

65. Wenisch JM, Meyer B, Fuhrmann V, Saria K, Zuba C, Dittrich P, Thalhammer F 2011. Multiple-dose pharmacokinetics of daptomycin during continuous venovenous haemodiafiltration. J Antimicrob Chemother:1-7.

66. Vilay AM, Grio M, DePestel DD, Sowinski KM, Gao L, Heung M, Salama NN, Mueller BA 2011. Daptomycin pharmacokinetics in critically ill patients receiving continuous venovenous hemodialysis. Crit Care Med 39(1):19-25.

67. Khadzhynov D, Slowinski T, Lieker I, Spies C, Puhlmann B, König T, Uhrig A, Eggers K, Neumayer H, Traunmüller F, Joukhadar C, Peters H 2011. Plasma pharmacokinetics of daptomycin in critically ill patients with renal failure and undergoing CVVHD. Int J Clin Pharmacol Ther 49(11):656-665.

68. Akins RL, Rybak MJ 2001. Bactericidal activities of two daptomycin regimens against clinical strains of glycopeptide intermediate-resistant *Staphylococcus aureus,* vancomycin-resistant *Enterococcus faecium,* and methicillin-resistant *Staphylococcus aureus* isolates in an In Vitro pharmacodynamic model with simulated endocardial vegetations. Antimicrob Agents Chemother 45(2):454-459.

69. Rybak MJ, Hershberger E, Moldovan T, Grucz RG 2000. In vitro activities of daptomycin, vancomycin, linezolid, and quinupristin-dalfopristin against *Staphylococci and Enterococci*, including vancomycin- intermediate and -resistant strains. Antimicrob Agents Chemother 44(4):1062-1066.

70. Snydman DR, Jacobus NV, McDermott LA, Lonks JR, Boyce JM 2000. Comparative in vitro activities of daptomycin and vancomycin against resistant Gram-positive pathogens. Antimicrob Agents Chemother 44(12):3447-3450.

71. Bergeron MG 1986. Tissue penetration of antibiotics. Clin Biochem 19(2):90-100.

72. Garrison MW, Vance-Bryan K, Larson TA, Toscano JP, Rotschafer JC 1990. Assessment of effects of protein binding on daptomycin and vancomycin killing of *Staphylococcus aureus* by using an in vitro pharmacodynamic model. Antimicrob Agents Chemother 34(10):1925-1931.

73. Lee BL, Sachdeva M, Chambers HF 1991. Effect of protein binding of daptomycin on MIC and antibacterial activity. Antimicrob Agents Chemother 35(12):2505-2508.

74. Rybak MJ, Bailey EM, Lamp KC, Kaatz GW 1992. Pharmacokinetics and bactericidal rates of daptomycin and vancomycin in intravenous drug abusers being treated for gram-positive endocarditis and bacteremia. Antimicrob Agents Chemother 36(5):1109-1114.

75. Fréchet JMJ 2003. Dendrimers and other dendritic macromolecules: From building blocks to functional assemblies in nanoscience and nanotechnology. J Polym Sci A: Polym Chem 41(23):3713-3725.

76. Tomalia DA, Baker H, Dewald J, Hall M, Kallos G, Martin S, Roeck J, Ryder J, Smith P 1985. A new class of polymer: Starburst -dendritic macromolecules. Polym J 17(1):117-132.

77. Esfand R, Tomalia DA 2001. Poly(amidoamine) (PAMAM) dendrimers: From biomimicry to drug delivery and biomedical applications. Drug Discovery Today 6(8):427-436.

78. Tomalia DA, Naylor AM, Goddard WA 1990. Starburst dendrimers: Molecular-level control of size, shape, surface chemistry, topology, and flexibility from atoms to macroscopic matter. Angew Chem Int Ed Engl 29(2):138-175.

79. Caminade A-M, Laurent R, Majoral J-P 2005. Characterization of dendrimers. Adv Drug Deliv Rev 57(15):2130-2146.

80. Klajnert B, Bryszewska M 2001. Dendrimers: Properties and applications. Acta Biochim Pol 48(1):199-208.

81. Cheng Y, Xu Z, Ma M, Xu T 2008. Dendrimers as drug carriers: applications in different routes of drug administration. J Pharm Sci 97(1):123-143.

82. Bos GW, Kanellos T, Crommelin DJA, Hennink WE, Howard CR 2004. Cationic polymers that enhance the performance of HbsAg DNA in vivo. Vaccine 23(4):460-469.

83. Muangsiri W, Kirsch LE 2006. The protein-binding and drug release properties of macromolecular conjugates containing daptomycin and dextran. Int J Pharm 315(1-2):30-43.

84. Chanvorachote B, Nimmannit U, Muangsiri W, Kirsch L 2009. An evaluation of a fluorometric method for determining binding parameters of drug–carrier complexes using mathematical models based on total drug concentration. J Fluoresc 19(4):747-753.

85. Klajnert B, Stanislawska L, Bryszewska M, Palecz B 2003. Interactions between PAMAM dendrimers and bovine serum albumin. Biochim Biophys Acta - Proteins & Proteomics 1648(1-2):115-126.

86. Leisner D, Imae T 2003. Interpolyelectrolyte complex and coacervate formation of poly(glutamic acid) with a dendrimer studied by light scattering and SAXS. J Phys Chem B 107(32):8078-8087.

87. Shcharbin D, Klajnert B, Bryszewska M 2005. The effect of PAMAM dendrimers on human and bovine serum albumin at different pH and NaCl concentrations. J Biomater Sci Polym Ed 16(9):1081-1093.

88. Cakara D, Kleimann J, Borkovec M 2003. Microscopic protonation equilibria of poly(amidoamine) dendrimers from macroscopic titrations. Macromolecules 36(11):4201-4207.

89. Diallo MS, Christie S, Swaminathan P, Balogh L, Shi X, Um W, Papelis C, Goddard WA, Johnson JH 2004. Dendritic chelating agents. 1. Cu(II) binding to ethylene diamine core poly(amidoamine) dendrimers in aqueous solutions. Langmuir 20(7):2640-2651.

90. Niu Y, Sun L, Crooks RM 2003. Determination of the intrinsic proton binding constants for poly(amidoamine) dendrimers via potentiometric pH titration. Macromolecules 36(15):5725-5731.

91. Maiti PK, Cağin T, Wang G, Goddard WA 2004. Structure of PAMAM dendrimers: Generations 1 through 11. Macromolecules 37(16):6236-6254.

92. Maiti PK, Bagchi B 2009. Diffusion of flexible, charged, nanoscopic molecules in solution: size and pH dependence for PAMAM dendrimer. J Chem Phys 131(21):214901-214907.

93. Maiti PK, Cağin T, Lin S-T, Goddard WA 2005. Effect of solvent and pH on the structure of PAMAM dendrimers. Macromolecules 38(3):979-991.

94. Dootz R, Toma AC, Pfohl T 2011. PAMAM 6 dendrimers and DNA: pH dependent "beads-on-a-string" behavior revealed by small angle X-ray scattering. Soft Matter 7(18):8343-8351.

95. Kleinman MH, Flory JH, Tomalia DA, Turro NJ 2000. Effect of protonation and PAMAM dendrimer size on the complexation and dynamic mobility of 2-naphthol. J Phys Chem B 104(48):11472-11479.